Università Politecnica delle Marche, Ancona

Dipartimento di Scienze Agrarie, Alimentari e Ambientali

Corso di Dottorato (D.M.45/2013) - XXXV ciclo

Final Thesis

PhD Student:
Ing. Stefano Chiappini (1095450)

Research title:

Precision agriculture by proximal and remote sensing: from the 3D modelling and tree metrics computation to the analysis of rural landscape

Tutor:
Prof. Andrea Galli – D3A

Co-tutors:
Prof.ssa Eva Savina Malinverni – DICEA

Content

Abstract

Precision agriculture PA is a new concept adopted worldwide. Precision farming methods use large amounts of data and information to improve agricultural resource use and crop quality. In essence, PA is the science of improving agriculture sustainability by assisting farmers' decisions using high-tech sensors and analytical tools. The main PA technology solutions available today belong to remote and proximal sensing fields. Among them, Lidar (light detection and ranging) and stereoscopic vision systems are used for the three-dimensional modelling of plant elements (3D models, point clouds, meshes, etc.). Regarding the latter, most studies are in forestry, while the use of 3D modelling systems has a broad scope for study and application in permanent crops. As we will see in the following paragraphs, the doctoral work focused on agricultural systems for olive cultivation. Above all because focusing on the olive sector has a twofold significance. On the one hand, it allows us to test the potential of PA in a crucial sector from the production point of view of permanent crops. On the other, to test the seminal contribution of PA from the ecological and landscape point of view. This approach of the work allows us to seek to have an impact in the promising field of farming technological innovation. Therefore, the PhD project focuses on three main lines of research. The first line of research aims to demonstrate the high accuracy of metric data extracted from single tree tests by model reconstruction starting from point clouds sampled through a Mobile Laser Scanner Lidar (MLS) device. The second line of research focuses on the Mobile Laser Scanner survey of tree structures in specialised olive groves by applying different tree classification and canopy mashing algorithms to derive the volume of individual canopies with high accuracy. The analysis is conducted by comparing the volumes obtained from the MLS survey with two ground truths or primitives (toroidal and paraboloid shapes). The third line of research focused on landscape analysis inside a case study in central Italy (PDO Cartoceto). The landscape analysis is conducted by adopting different approaches of diachronic analysis of land use changes and landscape metrics. The analysis uses a robust multi-temporal dataset (orthophoto maps, historical maps, aerial images, etc.) to reconstruct the land use for five periods over more than 70 years in a GIS environment. The dataset allowed for identifying the different types of olive grove cropping patterns within the investigated area. Further, the landscape transformations have been analysed by measuring a pool of landscape metrics (diversity, entropy, shape, frequency, etc.) to provide a clear view of the dynamics of change that occurred in those areas. The overall results achieved in the development of these three lines of research appear very satisfactory. They, therefore, represent a significant stimulus for both individual olive growers and the associative structures that manage the local olive sector, particularly the Cartoceto DOP extra virgin olive oil production consortium, to introduce innovative practices based on the use of advanced digital technologies in the agricultural sector.

Riassunto

L'agricoltura di precisione (AP) rappresenta un nuovo modo di impiegare la tecnologia digitale per rendere l'agricoltura più efficiente e produttiva utilizzando dati accurati. Le principali soluzioni tecnologiche di PA oggi disponibili appartengono ai campi del telerilevamento e del rilevamento prossimale. Tra queste, l'uso dei sistemi Lidar (light detection and ranging) e di visione stereoscopica sono utilizzati per la modellazione tridimensionale degli elementi vegetali (modelli 3D, point clouds, mesh, etc.). In merito a quest'ultimo aspetto la maggior parte degli studi è in ambito forestale, mentre l'utilizzo dei sistemi modellazione 3D presenta ampi spazi di studio e applicazione nel settore delle colture permanenti. Come vedremo in successivamente, il lavoro di dottorato si è concentrato su sistemi agricoli per la coltivazione dell'olivo. In particolare perché concentrarsi sul settore olivicolo ci permette di testare le potenzialità della PA in un settore cruciale non solo dal punto di vista produttivo delle culture permanenti, ma anche ecologico e paesaggistico. Questo approccio del lavoro ci permette di avere impatto in un promettente campo di innovazione tecnologica. Pertanto, il progetto di dottorato si concentra su tre linee di ricerca principali. La prima linea di ricerca mira a dimostrare l'elevata accuratezza dei dati metrici estratti da test su singoli alberi mediante ricostruzione del modello a partire da nuvole di punti campionati attraverso un dispositivo Mobile Laser Scanner Lidar (MLS). La seconda linea di ricerca si concentra sul rilevamento con Laser Scanner Mobile delle strutture arboree in oliveti specializzati. Applicando diversi algoritmi di classificazione degli alberi e di mashing delle chiome per derivare il volume di singole chiome con elevata precisione. L'analisi è condotta confrontando i volumi ottenuti dal rilievo MLS con due verità a terra o primitive (forme toroidali e paraboloidi).

La terza e linea di ricerca si è concentrata sull'analisi del paesaggio all'interno in un caso di studio in centro Italia (DOP Cartoceto). L'analisi del paesaggio è condotta adottando diversi approcci di analisi diacronica dei cambiamenti

di uso del suolo e metriche del paesaggio. Per l'analisi è stato necessario costruire un robusto dataset multi temporale (ortofoto aeree, carte storiche, etc.). In particolare è stato possibile ricostruire lo stato di uso del suolo per cinque periodi nell'arco di oltre 70 anni, in ambiente GIS, individuando le diverse tipologie di modelli colturali di oliveto all'interno del territorio indagato. Successivamente è stato possibile misurare un pool di metriche del paesaggio (diversità, entropia, forma, frequenza, etc.) per analizzare le trasformazioni del paesaggio fornendo una chiara visione delle dinamiche di cambiamento avvenute in quelle aree. I risultati complessivi conseguiti nello sviluppo di queste tre linee di ricerca appaiono molto soddisfacenti. Essi rappresentano quindi un significativo stimolo sia per i singoli olivicoltori sia per le strutture associative che gestiscono il comparto olivicolo locale, in particolare il consorzio di produzione dell'olio extravergine di oliva di Cartoceto DOP, per introdurre pratiche innovative fondate sull'utilizzo di tecnologie digitali avanzate all'interno di questo importante comparto agricolo.

1. Introduction to the research subject

At the cutting edge of technological innovation, smart farming technologies claim the potential to feed a growing global population with less, but much more precise, use of inputs, a compelling narrative in an era of climate change, shrinking resources, and mounting agricultural pollution [1]. The new digitalized model of farming, interchangeably called 'precision farming' (PF) or 'precision agriculture' (PA), promises to increase efficiency and production through the use of data-driven precise or 'smart' inputs [2]–[4]. According to ground-breaking researchers, precision agriculture is the science of improving crop yields and assisting management decisions using high-technology sensors and analysis tools. This translates to what is often defined as the "4 R" strategy: doing the right thing, at the right place, at the right time, and in the right manner [5].

PA is a new concept adopted worldwide to increase production, reduce labour time, and ensure the effective management of fertilizers and irrigation processes. It uses a large amount of data and information to improve the use of agricultural resources, yields, and the quality of crops [6]. It requires a considerable amount of information about the crop condition or crop health in the growing season at high spatial resolution. Independently of the data source, PA's most crucial objective is to support farmers in managing their businesses [7].

In order to manage crop yields and make wise use of farming resources, it is crucial to quickly improve the accuracy of agricultural growth monitoring and its health assessment [8]. Implementing remote sensing (RS) or proximal sensing (PS) is one way to overcome these obstacles.

RS platforms, such as satellites, airborne and unmanned aerial vehicles (UAVs), are equipped with a variety of sensors that can provide valuable information on crop growth and health, including ultrasound [9], digital photographs [9], laser sensors [10], [11], stereoscopical images [12], light sensors [13], [14], high-resolution radar images [15], and high-resolution X-ray computed tomography [16]. Even though the same sensor can be used on PS platforms, the information obtained may differ significantly.

Light detection and ranging (LiDAR) and stereoscopic vision systems are probably the most promising techniques for obtaining 3D images and maps of canopies or single trees [17]. LiDAR is an active system that emits pulses whose return to the sensor after being reflected by an "object" on the Earth's surface is measured by calculating the elapsed time between the emission of the energy pulse and its return [18]. From this information, a point cloud with X, Y and Z coordinates is obtained that corresponds to the impacts of the initial pulse energy on the objects, thus making it possible to digitally reconstruct the tree structure with high accuracy [19], [20].

The rapid development of acquisition systems able to collect 3D point clouds, allowed the automation of forest inventory procedures. Several platforms have been developed to reduce the time and cost of traditional measurements held with optical or electronic instruments and to improve their precision and accuracy [21], [22]. LiDAR techniques are boosting ecological and forest research, and researchers in various fields began to apply it for modelling analysis [23]. Terrestrial Laser Scanner (TLS) is a ground-based LiDAR scanning system able to offer data to analyse, improving significantly Above-Ground Biomass (AGB) estimation [24]. The 3D models derived by Terrestrial Laser Scanning application are treated as ground truth validation of forest biomass models [25], [26]. From these data is possible to extract and storing different metric data, such as diameter at breast height (DBH) [27], [28], individual tree height (H) [29], [30], steam volume [31]–[33], AGB [25], [34] and branch architecture [35]. Unfortunately, due to the static nature of TLS, it requires multiple scanning stations to ensure the effective detection of the trees. This task is time-consuming and requires significant manpower [36]. The most important problems are the effects of the occlusion by trunks, crown and the understory vegetation [37]–[39]. The limitation listed on TLS have boosted researchers to move up technologies able to produce 3D point clouds in a ready to use manner.

A solution is given by mobile laser scanner (MLS) [40]. These systems combine a laser scanner with an inertial measurement unit (IMU), exploiting the so called SLAM (Simultaneous Localization and Mapping). The accuracy of measurements mainly depends on the synchronization of these components. Moreover, thanks to the moving platform, the occlusion effect is reduced [37]. MLS applications are divided in two categories: handheld laser scanning (HMLS) and backpack personal laser scanning (BMLS). Early scientific publications with MLS date back 2013, and the first system prototype was large in size and weighed approximately 30 kg, which limited its operability and mobility [41]. More recent out-of-the-shelves products are lighter and more compact MLS systems, easily handeld by a single operator even in a challenging scenario. Several studies evaluate the accuracy of these different scanning systems in forestry settings. Comparative studies between TLS and MLS revealed that MLS got more accuracy than TLS rate [38], and took less time to collect the data. The use of TLS requires multiple scanning bases

to ensure the effective detection of the trees, and the most significant problems are the effects of shade or concealment by trees [37], [42]. Conversely, some studies on the quality of the point cloud obtained by MLS report a problem in the model due to noise [37] or errors in fitting the geometric shapes [43]. In order to achieve high accuracy, several factors must be taken into account, such as a small research plot, the best environmental conditions, the instrument used and the visibility of the surrounding environment during real-time mapping [44].

From a search on the Scopus website (www.scopus.com), we looked for the trend of publications of indexed articles containing the keywords "LIDAR" and "forest". The overall trend (Figure 1) of the 5611 searched articles from 1982 to 2023 (January) that met the study criteria is shown in figure 1, remarkably the number of published articles increased every year.

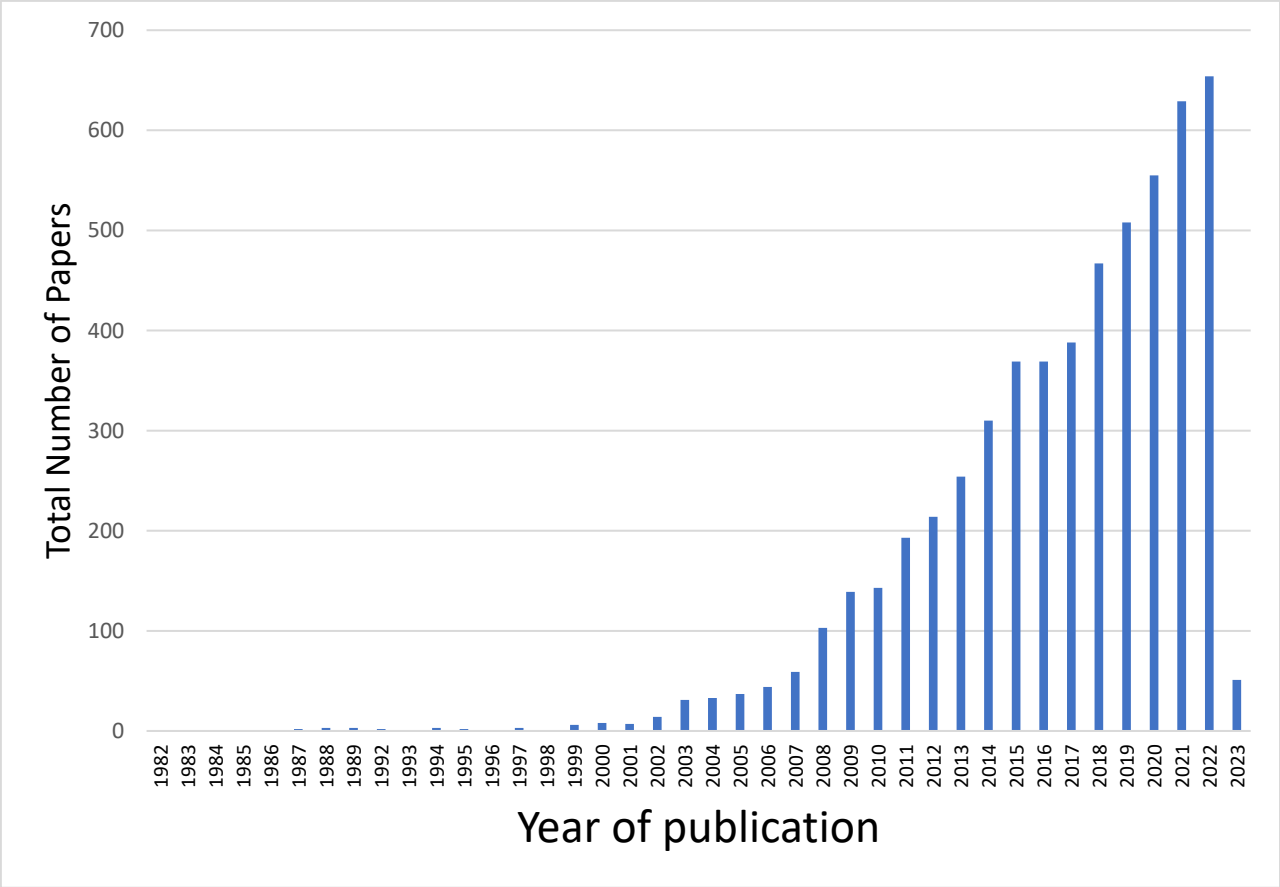

Fig. 1 Number of relevant articles for the two keywords (LIDAR and Forest).

However, 3D models obtained from LiDAR surveys can also be helpful in permanent crop cultivation [45], [46], applying procedures similar to those used in forested areas, thus obtaining much information on the amount of biomass [47], growth activity [48], productivity [49], water consumption [50] and health status [51] from canopy characterization. Using the crop, also permanent crop, and lidar keywords on the search engine in Scopus, the system provides 636 documents. But the results were too dispersive, so the survey focused on some keywords identified by the system such as orchards, tree, fruit, providing us with only 334 papers published in scientific journals. Figure 2 shows the trend of articles published over the period of 1998 to 2023 (January). It is significant that there have been more publications since 2019. This demonstrates that the 3D study of tree crops farming is a young field of study, where researchers are concentrating on putting various methodologies into use and verifying them.

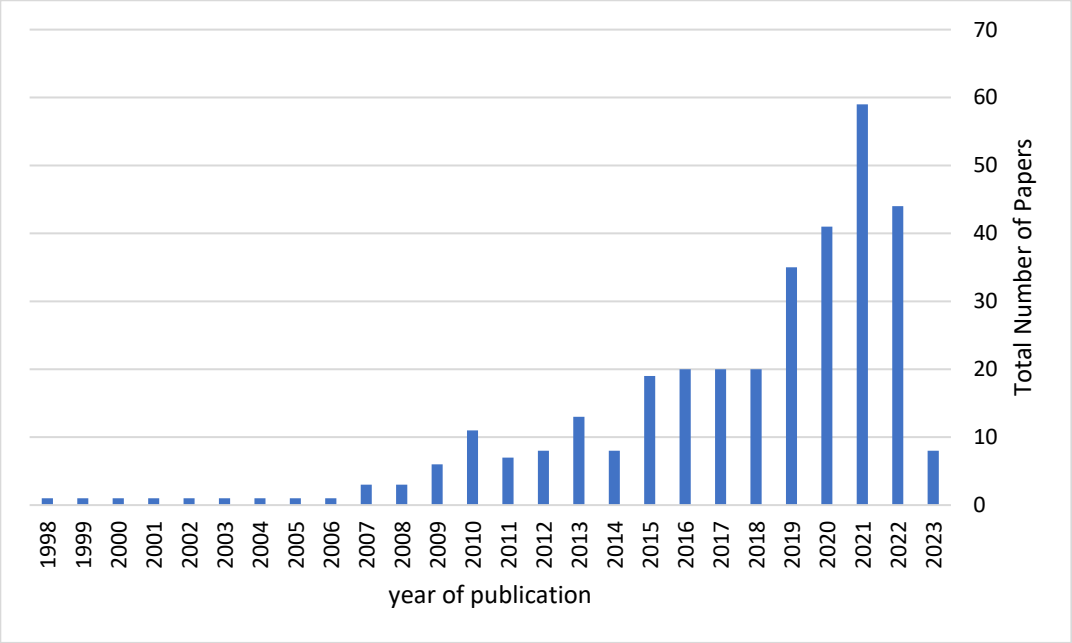

Fig. 2 Number of relevant articles for each keyword (LIDAR,Crop, Orchard, Tree and Fruits).

Among the most widespread crop cultivations in the world, it may include the agricultural areas dedicated to olive tree cultivation, particularly for extra virgin olive oil (EVOO) production [52]. These surfaces have seen a significant increase in recent years [53]. Additionally, it has been noted that cultivation methods are constantly changing, creating new difficulties in maintaining olive farms' economic and environmental sustainability [54]. Today, olive trees are cultivated in about 40 countries, covering a global area of about 10.5 million hectares [52]. Olive trees are almost entirely cultivated (over 98 per cent) in the Mediterranean area, where olive orchards have always been traditional grows and a characteristic component of landscapes in rural and peri-urban areas [55]. Italy ranks as the world's second-largest Extra Virgin Olive Oil producer, between Spain and Greece, with a production in 2021 of 328 thousand tons [56]. Today olive orchards play a crucial role not only at the ecological and landscape level, but also as a promising field of technological and economic innovation to be performed by implementing the new strategies of PA. In Italy, for example, the olive grown sector is still based on traditional olive orchards, mainly with a low-medium density of trees, thus managed by traditional techniques of cultivation showing a shallow level of applied technological tools. Therefore, is out of any doubt that this sector claims a radical shock of innovation. Considering the world olive orchard system, it is possible to divide it into three forms of cultivation: traditional olive cultivation, which consists of both isolated olive trees and olive rows mixed with crops. Sequentially, there are different types of "modern" models of olive tree cultivation: specialized olive growing, high-intensity olive growing and super-intensive olive growing [57], [58]. It is also worth noting that, in recent years, home gardens of smaller size than traditional olive groves have grown in popularity as a trend for hobby olive growing, where production is for self-consumption and encourages a kind of rural revival [59]. These four significant classes are deeply different in terms of cultivation techniques. They require appropriate and very different agronomic choices for the success of cultivation. Furthermore, the expansion of the most intensive olive growing has unavoidably contributed to landscape degradation, posing challenges to biodiversity conservation and prompting farmers to abandon traditional field management techniques [60].

In order to prevent the loss of rural landscapes threatened by unregulated choices of planners and climate change issues, it is necessary to characterize and monitor the landscape from every point of view over time, allowing for an enhancement of the relationship with local people and the maintenance of ecosystem services. Since 1992, the Geographical Indication (GI) Scheme has been launched at the EU level to support more sustainable and profitable agricultural systems, the preservation of traditional local culture and the planning of rural landscapes [61], [62]. Experts in territorial marketing have praised the GIs as the best option for representing the sustainability of high-quality food products based on sustainable production and landscape [63]. However, certifying the geographical origin of food products can also help rural communities to earn money [64]. At the same time, successful GI intensification brings the risk of compromising environmental benefits [65], [66]. More and more researchers have posed the need to implement new methodologies for the preservation and

enhancement of both the cultural and natural heritage of rural landscapes [67], [68]. In some way, this motivation has prompted at the European level the formulation of the European Landscape Convention (ELC) [51], which commits the signatory States (Art. 6, paragraph C) [51] to analyse the characteristics of their landscapes and the mechanisms of their dynamics by monitoring all changes in the landscape.
The most widely used approaches to conduct this type of analysis are provided by geographic information systems (GIS), landscape metrics, and remote sensing [69]–[72]. Land use maps are generally obtained by digitising historical maps [56], incorporating historical statistics and old maps [73], aerial photographs [74] or satellite images [75]. However, the field of studying landscape dynamics is huge, and many techniques and methodologies are deferring from each other [76]. Large data volume collection from different sources is necessary to monitor landscape transformations and protect nature [77] through sound landscape planning policies, strategies and actions [78], [79].

As a consequence, these outcomes can influence the formulation of guidelines and policies to address future growth of territories as well as to put ecosystem functioning into practice in implementing protection actions [80]. The European Commission has recently promoted a policy for the sustainable development of rural areas through various instruments [81]. For instance, Farm to Fork, one of the key strategies included in the EU's Green Deal vision [82], aims to make the agri-food sector more sustainable regarding people's health and nature protection [83]. To boost this transition of food systems, the EU is committed to reforming the Common Agricultural Policy (CAP).

Actually, current conditions in the rural landscape require constant improvement of methods for controlling and assessing the environmental consequences of urbanisation and the impact of man-made factors. It is necessary to create new operational tools and valid methods for monitoring and forecasting the environmental conditions of cities and rural settings to propose measures of anthropogenic impact reduction [84].

For instance, landscape metrics [85], [86] [85, 86] help the researchers to quantify the spatial properties of patches, classes, or landscape mosaics over the time, thus becoming the best way to compare the state of different landscapes and different land uses.

[85], [86]Geographic Information Systems (GIS) are the most widely used informatic tool to process spatial datasets of different origins for landscape metrics computing, such as historical maps or historical statistical databases. Additionally, many tools can be integrated into GIS platforms, e.g. Remote Sensing, by collecting, storing, processing and analysing different remotely sensed data, documenting information and saving both time and resources too[87].

Figure 3 shows the trend of articles published over the period of 1977 to 2022 (until January) using the keywords "Rural Landscape" and "Land Use", which also contain the following sub-keywords; "Land Use Change", "Agricultural Land", "Landscape Change" and "Rural Area". It is significant that there have been more publications since 2011 by reaching a peak in 2019. This demonstrates that the field of landscape transformation research, which aims to evaluate changes in land use and land cover and their impacts on the functionality of ecological systems, is still a challeng for researchers. This because it is difficult to develop a clear methodology for quantifying landscape diversity. A lot of researchers pointed out two crucial factors to be considered when analysing landscapes: the first is based on the personal perception of operators which do a qualitative assessment of the landscape, essentially. Conversely, the second is founded on the actual identification of tangible features within the landscape that are unrelated to the observer's perception point of view[88].

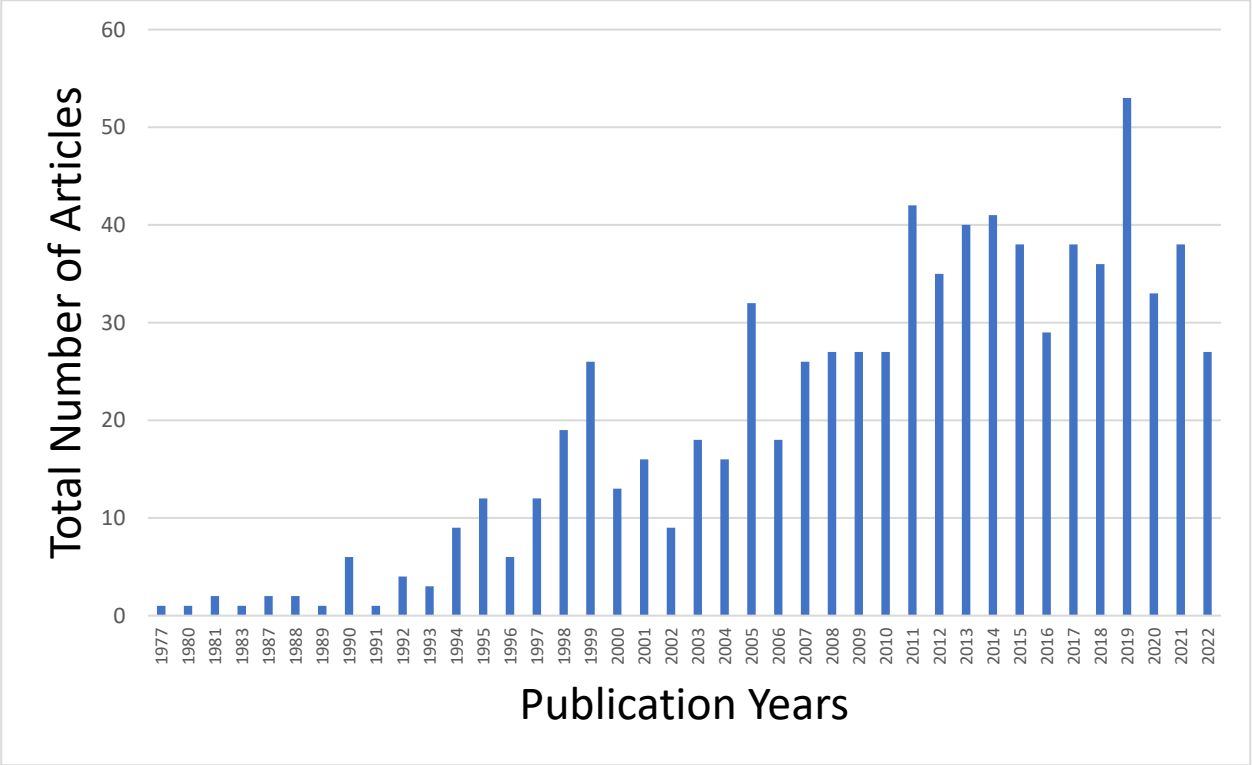

Fig. 3 Number of relevant articles for each keyword (Rural Landscape and Land use).

Fig. 1 shows how, starting in the late 1990s, Lidar technology emerged as a valid alternative to both Remote Sensing and manual inventory, which often included destructive evidence in forest environments [89] . According to Liang et al. [90] the Lidar device is one: "a survey technique for collecting a three-dimensional (3-D) cloud of reflective objects...".

This technology allows forestry professionals to collect more accurate data even at the level of a single tree [91]. Conventional LIDAR systems used in forestry, such as aerial laser scanning (ALS) and terrestrial laser scanner (TLS), have some limitations [30], [92]. ALS data are often characterized by a relatively low point density, have sensor calibration problems and require numerous field reference data [91], [93], [94]. The static TLS, on the other hand, provides high-precision data but is limited by the laser beam occlusion effect in the single-scanning measurement approach [95] [95].

Recently, mobile laser scanning devices (MLS) have emerged as an ideal solution for forest inventory surveys thanks to simultaneous localization and mapping technology (SLAM) and their ease of portability [91]. Thanks to SLAM, MLS devices are able to greater precision without the need for a GNSS signal that is challenging under the dense canopy [37]. Additional survey objectives are not required for registration. Compared to TLS, the user can walk freely within the forest landscape with the MLS device, both in portable mode and mounted on a backpack. Thus, the 3D data of the attributes of each individual tree is collected continuously without the effect of occlusion, at a reduced cost and time [96]. The data is then pre-processed and tree attributes (e.g. DBH, number of trees) can be estimated with sufficient accuracy using commercial software packages. However, for large datasets, post-processing efforts can be complicated and require a lot of time for manual use [96] [97], [98]. Ryding et al. [99] were the first to use MLS for a relief in a forest in the UK. since then MLS applications have increased progressively in forestry [100], [101]. Currently, MLS-based forestry research mainly focuses on combining MLS data with different types of data sources [102];; increasing mapping accuracy [103], [104] and data processing automation [97], [105]. The applications of MLS have also extended to the cultivation of permanent crop types, using Lidar devices mounted on irrorators or commercial tractors that can easily pass between the rows of trees. As described by Sefien et al. (2023) [106] this led to a strong boost in the use of the Mobile Laser Scanner for the precision management of the fruit plant and to improve the productive efficiency and quality of the fruits through a morphological-based management strategy to characterize the apples. In general, the MLS for this sector is mainly used for estimating the volumes of the plants [107], [108], the estimation of the leaf cover [109], [110] and also for the detection of individual fruits [111], [112], following the strategies of the Precision agriculture.

Finally, the study of rural landscape includes the analysis of its ecological diversity that has unfortunately seen a decline in scientific interest in recent years, as shown in Fig. 3. The rural landscape represents an important historical element that best represents the cultural identity of local communities as it contributes to the preservation of not only cultural but also ecological diversity [113]–[116].

However, the rapid socio-economic changes that have affected European countries since the 1950s have radically transformed most of the traditional rural landscapes. It has witnessed the transition from medium-sized agricultural models to large agricultural areas specialized in monoculture or converted into urban areas [117].

Consequently, it is important to preserve the traditional characteristics of the remaining agricultural activity and adopt a sustainable approach [118]. Before proceeding with rural landscape planning, it is necessary to apply methods of technical and spatial analysis on land use [119], which can be used, for example, for the continuous monitoring of landscaping metrics and comparable indices over time [119] [120]. In addition, it is important to consider appropriate models to assess the impact of anthropological choices and external factors, such as climate change, on different scales of landscape. This has been widely demonstrated by several studies [121]–[124].

1.1 Research objectives

Throughout my doctoral studies, I engaged in research activities that explored innovation potentials of digital technologies in agriculture. In this context, I focused in the olive growing sector. The reason for my choice is inherent to the fact that despite advancements in technology, the Italian olive growing sector continues to depend heavily on traditional cultivation techniques and orchards, limiting the integration of technological tools. According to many autors, over coming this gap is mandatory to get to an actual penetration of precision agriculture (PA) in the sector, allowing for improving yields and assisting the management decisions by using high-technology sensors and analysis tools. From this point of view, one of the most important application aspects concerns the ability to quickly and accurately reconstruct the structure and volume of olive trees.

Consequently, the first research objective has addressed to verify the efficiency and reliability of the different Lidar instruments available today for the 3D reconstruction of arboreal vegetation. Considering some limitations highlighted by many researchers for TLS tools, we turned to MLS tools which allows to comparable results in terms of accuracy, while they may result convenient in order to reduce the time spent for performing the survey and the post processing phase of point cloud registration. In particular, Mobile Laser Scanner (MLS) efficiency and accuracy have been compared, in combination with Simultaneous Localisation and Mapping (SLAM) technology and traditional field survey for computing key forest dendrometric variables like stem diameter at breast height (DBH), individual tree height (H), crown base height (CBH) and branch-free stem volume (VOL). This first step of the PhD research has been developed in forestry environment as it was an ideal arena to evaluate Light detection and ranging (LiDAR) performance because these techniques are boosting ecological and forest research, and researchers in various fields began to apply them widely.

The second step of PhD research activity has addressed the implementation of MLS tools in the olive groves environment, with the aim to perform reconstruction of structural and volume of olive trees more quicky and more accurate as possible. A mobile laser scanner (MLS) survey was conducted on a specialised olive orchards for 3D data analysis. Following the survey, metric data such as tree height and canopy size were manually extracted to calculate canopy volume by associating them with the primitive toroid and paraboloid shapes. The purpose is to determine the accuracy of results by applying different meshing algorithms to replace manual work completely, and to assess whether each tree needs pruning or not, saving time and costs as the PA approach requires.

However, to manage not a single olive grove but an entire olive growing area it is necessary to know and monitor the distribution of the different types of olive grove within a territory, because they have very different performances both in terms of production and in terms of environmental contribution. For these reasons the last step of the PhD research has been dedicated to investigate the transformations affected the olive groves sector within the study area of Cartoceto. This territory belongs to a well-known Geographical Indication (GI) area acknowledged for the production of extra virgin olive oil from the year 2004. Being a central components of rural landscape from millennials, the olive growing of the study area has crossed several transformations. From the traditional olive groves mixed with crops to the contemporary intensive olive orchards, probably projected to become the high intensity new typologies in the near future. Main goals of this study was applying GIS tools to analyse landscape changes within the study area by processing a multitemporal set of multi-source georeferenced data that allows to produce several Land Use Maps covering the last 64 years. Furthermore, with the aim to identify and interpretate the most significant dynamics of change and their impact on landscape patterns a specific set of landscape metrics has been computed.

2. State of the art

This chapter provides an extensive overview of the state-of-the-art technologies used during my PhD. More in depth, the importance of Proximal Sensing and Mobile Laser Scanner for the three-dimensional representation of natural elements is described in the paragraph 2.1. Meanwhile, the paragraph 2.2 explores the potential of remote sensing

for mapping land use through aerial imagery. Finally, Paragraph 2.3 shows some scientific research published in recent years covering the technologies used in the different case studies.

2.1 Mobile Laser Scanning Systems for modelling single trees or canopies

In recent years, one of the technologies most commonly used by Precision Farming experts has been the Mobile Laser Scanner (MLS). During the PhD research, various modes of mobile Lidar use emerged, requiring a definition of the different platforms, as clarified in paragraph 2.1.1. Meanwhile, the paragraph 2.1.2 describes the essential sensors and algorithms for a device to be defined as a Mobile Mapping Systems (MMS).

2.1.1 Mobile Laser Scanning - MLS

MMS is a mobile platform that can be either aerial or terrestrial, in which measurement systems and sensors are integrated for the acquisition of geo-referenced metric data. Hence, MMS is an integration of three main hardware components: optical sensors, navigation/positioning sensors and a control unit [125]. This technology, if combined with a Light Detection and Ranging (LiDAR) unit, can be referred as Mobile Laser Scanner (MLS) which is a widely used acronym in recent literature. This approach has the great advantage to be time efficient if compared with the other survey's methods. In this case, the laser scanners have been placed on moving platforms in order to obtain multiple scan positions with artificial targets for high detection rates and avoiding, as much as possible, shadowing effect and non-detection areas. It is a further technology improvement which combines a moving sensor with position estimation to obtain continuous registration and unlimited viewing angles [126]. For what concerns the quality of the data obtained with the MLS surveys, it depends on the devices used but it generally reaches a centimetric accuracy and a resolution that is related to the data acquisition speed and the distance of the detected objects [105]. The MLS are usually categorised according to the mobile platform used. According to the recent literature reviewed, the mobile terrestrial platforms can be split in human-based, wheel-based, boat-based and sledge-based. With the term 'human-based' it is referred to platforms carried by human beings and, normally, they are mentioned as Personal/Portable Laser Scanner (PLS) or Wearable Laser Scanner (WLS). There are few differences between PLS and WLS: the first is usually referred to systems that can be carried manually by the operator (such as a hand-held laser scanner) while the second usually means small devices which can be worn by the operator, like scanners in a backpack. The 'wheel-based' platforms can be referred to as trolleys, vehicles on rails, motorbikes, bikes and vehicles. The latter include road vehicle, All-terrain Vehicle (ATV) and Unmanned Ground Vehicle (UGV). Very often UGV coincide with ATV, as they are used where people cannot access easily so a remote-controlled vehicle (in literature may be referred simply as 'robot') able to overcome difficult terrains. The 'boat-based' and the 'sledge-based' platforms are used only in certain domains or conditions, where there is the necessity to use such kinds of platforms [127], [128]. Sometimes, the acronym 'Boat Mobile Mapping System (BoMMS)' is used to denote mobile mapping systems mounted on boats, regardless the boat size. Dealing with airborne mobile systems, in literature they are mainly referred as Airbone Laser Scanner (ALS), but it is possible to find even 'Aerial Laser Scanner' and 'Aircraft Laser Scanner' and the main difference is due to the laser units equipped, which have different range in the data acquisition. Even in this case, the acronyms UAV and UAS (respectively Unmanned Aerial Vehicle and Unmanned Aircraft System) can be found in literature and they are both referred to the ALS systems. Prior to the scanners installed on mobile platforms, lasers were used on fixed platforms and these systems were named Terrestrial Laser Scanners (TLS). Technological innovation has expanded the use of such stationary laser units which, when bundled with localization and mapping systems, can become mobile laser units and in literature are directly termed either MLS or mobile-TLS [41]. As mentioned above, a typical MLS system has the capacity to localize and map itself thanks to both the Global Navigation Satellite System (GNSS) receiver and the Inertial Measurement Unit (IMU).

2.1.2 Improvement of MLS

The improvement of navigation systems has contributed to the development of MLS, which allow to acquire the surrounding environment in a rapid and efficient way through data localization, with sensors able to perform in all weather conditions [129]. Commercial MLS are equipped with multiple sensors for the navigation system consisting of GNSS (Global Navigation Satellite System) and IMU (Inertial Measurement Unit). These two components can ensure the correct geo-referenced positioning for the three-dimensional laser scanning data [41]. GNSS refers to a group of satellites which provide space signals, delivering positioning and timing information to the GNSS receivers. The latter, subsequently, use these data to establish the position [130]. Inertial measurement units have acquired a remarkable level of popularity in recent years as a low-cost way to measure motion. An IMU can measure both linear accelerations (three-axis accelerometer) and spin rates (three-axis gyroscope), which can be numerically integrated

to provide three-dimensional position and orientation of an object. In combination with the position data, IMU allows to transform the point data obtained by the MLS local frame into the ground-centric-ground-fixed system. Hence, all points are projected into a common framework and any non-compensated error from the IMU will have a direct effect on the geometrical quality of the point cloud [131] The level of accuracy of the GNSS/IMU navigation system is related to the signal detection quality of the GNSS, especially if it is composed by low-cost sensors [132]. To increase location accuracy and remove MLS errors in GNSS-denied environments, previous developers have made significant improvements on data-driven [133] and model-driven techniques. Data-driven methods may be directly used to fix point clouds data starting from ground truths and using multiple available correction algorithms. On the other hand, model-driven approaches set up mathematical models for the MLS systems and analyse the error factors to calibrate the biases [129]. Furthermore, Simultaneous Localization and Mapping (SLAM) algorithms have been investigated in robotics in the past years. SLAM algorithms generate a map of an unfamiliar environment and, in the meantime, it locates the mobile platform. The SLAM system requires a closed loop survey to improve the final precision. Different studies stated that each scan should start and end at a fixed point to ensure a closed loop and locate properly the data collected in the unknown environment, registering the whole points cloud obtained without the GNSS signal [105], [134]. To localize positions with SLAM, it is possible to apply two major strategies: absolute positioning with feature-matching and relative positioning with scan-matching. The first strategy matches feature detected (such as lines, corners, circles, etc.) with a generated feature map which allows to recognize the position. In the second strategy, two or more scan points frames are matched together by various algorithms to obtain the movement done by the MLS. Therefore, the SLAM algorithm performs better when applied indoors, with regular and repetitive features, while it has been shown to perform poorly when applied outdoors due to the complex and irregular features detected by the laser scanner. These irregularities create abrupt movements or difficulties to detect the whole area, increasing the computation payload and the complexity of the algorithm design [135]. The combination between the GNSS/IMU navigation system and SLAM will successfully reduce navigation drift whenever the GNSS signal is not clear and will provide absolute navigation information, which are not provided by the SLAM algorithms [129].

2.2 Remote sensing and mapping to land use change detection

Since the development of remote sensing and Geographical Information System (GIS) techniques, mapping land use and land cover has offered a practical and specific method to improve the selection of areas within a region that are intended to be agricultural, urban, and/or industrial zones. This method aims to improve the efficiency of the allocation of resources. This approach of mapping has offered a helpful and precise manner to accomplish that goal [136]. It was feasible to analyze the changes in land cover in a shorter length of time, at a cheaper cost, and with more precision as a result of the use of remotely sensed data. This was made possible by the utilization of satellite imagery [137] or multi-modals data with high-resolution aerial [138]. This was made feasible with the use of GIS, which offered an appropriate platform for the review, modification, and retrieval of data [139]. There has been a shift toward more regular and consistent monitoring and modeling of patterns of land use and land cover as a result of the introduction of satellite images with a high spatial resolution as well as more improved technology for image processing and geographic information systems. This shift was brought about by the combination of these two factors. The procedure of revising land use and cover maps has made substantial use of remote sensing, which has been recognized as one of the most important applications of remote sensing in recent years [140]. When it comes to the investigation of changes that occur on a worldwide scale, remote sensing, and more specifically satellite remote sensing, plays a very significant part. Because it can give synoptic as well as recurring observations of the global land surface at varied spectral, spatial and temporal resolutions, remote sensing is advantageous [141]–[143]. Large-scale mapping of land change based on remote sensing data has made significant strides in recent years thanks to several factors. These factors include the proliferation of earth observation satellites [144], [145], the implementation of free and open data policies [146]–[148], and the development of analysis-ready data formats [142], [149], [150]. The remote sensing community has lately undergone a paradigm shift, moving away from the practice of detecting change at two different points in time and instead focusing on the monitoring and tracking of change throughout time. This transition has occurred, with the use of dense time-series data becoming more common as a result of the ability to recover new land-use information. This information includes subtle changes in ecosystem health and condition as well as long-term patterns in plant production [151]. Additionally, it is now possible to monitor information regarding land change in a manner that is very close to real time [152]–[156]. This significantly boosts the usefulness of this information to those who are responsible for resource management and policymaking. In addition to this, we have witnessed a meteoric rise in the number of land change characterisation algorithms [149], the majority of which are focused on the "from-to" information, which refers to the information regarding the land cover and/or land use both before and after the change [157], [158]. It is vital to highlight that "land cover," which refers to the physical qualities

at the surface of the Earth, and "land use," which refers to the social, economic, and cultural use of land, are not the same thing at all. The distinction between the two cannot be overstated [159]. Despite this, the terms "land cover" and "land use" are usually bundled together in remote sensing products. Additionally, "land cover" is typically used as a substitute for comprehending "land use." Agricultural land and land that has been developed are two examples [160]. Because the data obtained through remote sensing provide information on land cover as opposed to information on land use, many researchers have focused on the driving forces that cause changes in land cover and on creating predictive models of future landscape conditions [161]. The user doesn't need to wait for two clear remote sensing photographs before these time-series-based algorithms may provide change detection results, and they are also capable of doing so more rapidly. The field of remote sensing has progressed from utilizing pictures that were taken decades apart [162], [163] to utilizing pictures that were obtained annually [164], [165], and is now progressing all the way to near-real-time change detection [151], [152], [154], [156], [165], [166]. This is especially the case in light of the recent successful launches of Sentinel-2 A/B [167], Landsat 9 [168], and the hundreds of orbiting CubeSats [169]. All of these satellites have the potential to provide sub weekly or even daily land surface observations at medium to high spatial resolutions [170], [171].

In addition to satellite images, Europe's Copernicus Land Monitoring Service (CLMS) offers a number of Earth observation products for use in environmental terrestrial applications. The European Environment Agency (EEA) and the European Commission DG Joint Research Centre collaborate to provide this service (JRC). The CORINE Land Cover (CLC) project is the oldest of the three; it began in 1985 and proposes a land cover inventory [13]. These datasets are extensive, encompassing the whole continent, but have rather low levels of geographic precision (scale 1:100,000, Minimum Mapping Units 25 ha)[172]. The use of CLC for an accurate LULC is limited due to a lack of adequate spatial information [173]. Because the smallest mapping unit is greater than the bulk of the discontinuous patches, this data source is untrustworthy when it comes to surveying urban areas, particularly urban dispersion. To enhance the CLC data, the CLMS has produced products known as High Resolution Layers (HLR). These HLR products give data on specific land cover characteristics such as imperviousness, forests, grassland, water and wetness, and tiny woody features [174], [175]. These datasets are produced from satellite imagery that use a variety of sensors in tandem (optical and radar data). With the exception of the Small Woody Feature and Forest Products categories, which are generated from data with a better exact resolution of 10 meters, the reference year is 2015, and the spatial resolution is 20 meters.

Satellite survey databases are a relatively new technology that offers the benefit of collecting totally uniform and comparable data for wide geographical expansions. The use of fairly large Minimum Mapping Units (MMU) on the other hand limits the degree of fineness and detail in the data and leads to excessive simplifications and approximations. All class sizes with a fragmented or parcelled distribution (e.g., impermeable or urbanised areas of less than or close to the minimum mapping unit are not surveyed) and linear areas are often underestimated (such as transport infrastructure). The presence of many land uses/coverages within each survey unit is also underrepresented: in reality, the concept of predominant use is applied, implying that distinct land use/coverage classes are homogenous within each minimal survey unit. The use of a hybrid categorization system, in which classifications correspond to land cover but also include components of use, is likewise undesirable. As is well known, use and land cover provide distinct geographical information. Cover characterizes the soil based on what is really present on its surface (bio-physical evidence), whereas usage characterizes the resources based on the purpose for which they are used by man (socio-economic functions). From a technical-operational standpoint, it is clear that while coverage data may be effectively captured by aerial or satellite acquisition, use information can only be marginally recorded.

Because of the use of a mixed categorization method (use and coverage) and the low resolution of CLC (connected to the nominal scale and minimum mapping unit), this data source is not suited for fine scale analysis, but it might be useful for comparisons between various European nations.

There are databases created using sampling techniques as an alternative to cartographic methodologies based on the analysis and categorization of satellite pictures (generally gridded or stratified). Using in-situ monitoring campaigns and/or on-screen photo interpretations of high-definition aerial or satellite pictures, the sampling methods used to choose regions and sites are evaluated.

In Italy, the Istituto Superiore per la Protezione e la Ricerca Ambientale (ISPRA)[176] in collaboration with the System of Regional and Provincial Agencies for Environmental Protection, has developed a mixed-type survey methodology that integrates local data derived from photo-interpretation of sample points with high-resolution remote sensing data, with particular reference to the soil consumption monitoring network [176], [177]. In addition to the ISPRA monitoring network, which is the only one dedicated specifically to soil consumption, there are several

databases in Italy produced by point and aerial sampling, which have the advantage of high precision and statistical reliability but, because they are aimed at specific knowledge needs, focus on specific themes and use resolutions, time intervals, and classification systems that are not always suitable for monitoring soil consumption. The Ministry of the Environment and Protection of Land and Sea (MATTM), for example, conducts the IUTI (Italian Land Use Inventory) survey to monitor changes in forest cover and land use in Italy, with a particular focus on information useful for the National Register of Forest Carbon Sinks, which was established in 2007. The Ministry of Agricultural, Food, and Forestry Policies (MiPAAF) also compiles a dataset by point sampling (55,000 points, almost entirely agricultural), which, after an initial photo-interpretation phase (on the POPOLUS matrix), is verified in the field and classified using a two-level hierarchical system with 86 classes, 59 of which are especially detailed for agricultural areas (only 10 for artificial areas). For thorough analyses that can be used for planning purposes, large- and medium-scale technical cartography created by photo-interpretation of aero-photogrammetric images and direct surveying is required. This category includes topographic maps, regional technical maps, regional land use maps, municipal cadastres, and so on.

2.3 Examples of application domains

Following are listed a number of case studies that demonstrate the effectiveness and reliability of the technology employed during this research period.

Bauwens et al. (2016) [178] compared the results from two different survey modes in forestry for estimating different metric data. From hand held mobile laser scanner (HMLS) and from Terrestrial laser scanner (TLS). The latter was employed with two approaches, either single scan (SS) or multi scan (MS). From the analyses of the entire cross section at 1.3 m height which was scanned on 91% of the trees (DBH > 10 cm) surveyed with the HMLS, this resulted in the best results for DBH estimates (bias of -0.08 cm and RMSE of 1.11 cm), compared to no fully - scanned trees for SS and 42% of trees fully scanned for MS.

Hartley et al. (2022) [179] applied the mobile laser scanner (MLS) to derive phenotypic measurements from mature *Pinus radiata* by walking under the canopy. Additionally, MLS data were co-registered with above-canopy UAV laser scanner (ULS) data and imported to a pipeline that segments individual trees from the point cloud before extracting tree-level metrics. MLS-derived tree metrics were compared to field measurements and metrics derived from ULS alone. Their pipeline was able to segment individual trees with a success rate of 90.3%. They also observed strong agreement between field measurements and MLS-derived DBH (R2 = 0.99, RMSE = 5.4%) and stem volume (R2 = 0.99, RMSE = 10.16%). One of the main results of this study was that MLS data acquired from below the canopy were able to derive canopy heights with a level of accuracy comparable to that of a high-end ULS scanner (R2 = 0.94, RMSE = 3.02%), negating the need to acquire above-the-canopy data to obtain accurate canopy height models.

Liu et al. (2021) [180] obtained a point cloud data for *Citrus grandis var. Longanyou* by means of hand-held 3D Lidar MLS with the aim of facilitating canopy management of this species. After calculating canopy height and width, canopy reconstruction and volume calculation were realized using six approaches: by a manual method and using five algorithms based on point clouds (convex hull (CH); convex hull by slices (CHBS); voxel-based (VB); alpha-shape (AS); alpha-shape by slices (ASBS)). From the results of the showed that the CH algorithm had the shortest run time, while the R2 values of volume CH, VB, AS, and VASBS algorithms were above 0.87. The volume with the highest accuracy was obtained from the ASBS algorithm, and the CH algorithm had the shortest computation time.

Osgouei et al. (2022)[181] have determined the historical LULC changes using multi-modal geospatial data, which are the cadastral maps produced in 1858, monochrome aerial photographs obtained in 1955, and multi-spectral WorldView-3 satellite images of 2020. The authors propose methods to facilitate the preparation of historical datasets for the LULC change detection and present an object-oriented joint classification scheme for multi-source datasets to accurately map the spatio-temporal changes on two different town Aksu and Kestel, in the Bursa region, Turkey. The classification scheme is based on Corine Land Cover nomenclature exploiting both codes and names from that one. The statistical analysis of LULC changes between 1858 and 2020 shows that Kestel had more land changes than Aksu. Forest and semi-natural areas decreased from 48% in 1858 to 18% in 2020 at Kestel. Agriculture declined from 49% in 1858 to 16% in 2020. Meanwhile, Aksu's LULC changed slightly. Heterogeneous agricultural areas increased from 12% in 1858 to 28% in 2020. In the other hand, the artificial areas increased in both Kestel and Aksu town. In the earlier the LULC is passed from 2% in 1858 to 66% in 2020, and in the latter only marginally from 0.62% in 1858 to 3.66% in 2020.

Modica et al. (2012) [80] have presented the spatio-temporal analysis of urban–rural gradient was performed to investigate LULC transformations and dynamics that occurred over the period 1955-2006 in the municipality of Serra San Bruno (Calabria, Italy), an area particularly representative of the Mediterranean mountainous landscape. Photointerpretation of aerial photographs was conducted by the same operator for all the years investigated (1955, 1983, 1994 and 2006) at a fixed scale of 1 :1000 –1 : 1500 (minimum mapping unit 0.2 ha). Leading agricultural areas decreased from 41.19 percent in 1955 to 20.98 percent in 2006 as a result of increased silvicultural operations, a continuing upward trend in agricultural abandonment, and the subsequent colonization of these regions by shrub and herbaceous vegetation (Shrub).

Barwicka et al. (2021)[182] did a more detailed study of how the landscape has changed in the Puchaczów commune. They used landscape metrics to look at how the mining industry is changing the rural landscape and what is causing those changes. The cartographic material available in this research consisted of a scaled tactical topographic map valid in the years 1937–2020, a scaled topographic map showing the state of the area from the 1960s to the 1970s, a level 2 vector map valid for the years 1990-2000, and an orthophoto map (geoportal) presenting the state in 2020. It is worth noting the from 1937–2020 there was a decrease in the area occupied by agricultural land, meadows and pastures. The values in percentage of land cover are as following: agricultural land is passed from 50,16% to 37,05%, while meadows and pastures from 26,47% to 20,57%.
The researchers have pointed out the case of the industrial area accounts for slightly more than 2% of the land cover. However, because of the pollution it causes, it has a significant impact on the commune's landscape. To mitigate its impact, a buffer zone comprised of forestal complexes and meadows and pastures was established in the central part.

Picuno et al. (2019) [183] have presented the findings of a multi-temporal analysis of the natural evolution of the rural landscape. Using landscape metrics and spatial analysis tools, it was discovered that the rural landscape evolved naturally without any human intervention during the time period studied, and the changes that occurred on the rural landscape were quantified. The starting dataset considered are maps from four different time steps (years 1875, 1955, 1988, and 2013). At the end of the manual procedure of land class recognition, the rasters were converted into vector maps using the CLC at level 1. The analysis of net change for each time lap reveals a significant decrease in forest area, with a percentage change from 73.0% in 1875 to 47.1% in 2013. While arable land increased significantly, from 20,7 acres in 1875 to 20,9 acres in 2013, Other analysis are carried out such as cross tabulation matrix and calculate of Shannon’s Diversity Index to understand the naturalness, of the landscape diversity and on the visual quality of the rural landscape.

3. Experimental activities

The research activities developed during my PhD period have dealt with different technological and methodological tools that have been used to address the different case studies that are shown as follow. We begin by describing our work of proximal sensing using Mobile Laser scanning, both in forestry and in specialised olive orchards, which allowed us to

collect detailed ground data accurately and quickly. Next, we focus on land use/land cover (LU/LC) transformations over a period of 64 years within the study area of Cartoceto territory. In particular, we have explored the driving forces that led to transform agricultural landscape. In a few words, through my research activities I tried to provide a comprehensive and detailed contribution to analyse some important issues affecting contemporary agricultural sector and landscape, emphasising the importance of adopting an interdisciplinary approach for understanding the complexity of the environmental and social problems we are facing. In addition, the research that will be described in Sections 3.1 and 4.1 has already been published, while Section 5.1 is going to be sent to a specialised Journal, thus what reported here mustn't be considered like published.

Comparing Mobile Laser Scanner and manual measurements for dendrometric variables estimation in black pine

doi.org/10.1016/j.compag.2022.107069

Chiappini S., Pierdicca R., Malandra F., Tonelli E., Malinverni E.S., Urbinati C. and Vitali A.

3.1.1 Introduction

The accurate measurement of forest stand features is not only a scientific value per se but a fundamental step in silvicultural management and forest planning. There is an increasing need for accurate and fast forest field inventories, due also to the growing demand for the assessment of the multiple ecosystem services [184]. Besides the widespread use, in the last decades, of techniques in forest inventories, the operational surveys still require manual measurements of field plots[185]. Diameter at breast height (DBH), individual tree height (H) and crown base height (CBH) are the tree parameters most frequently measured in the field. Although traditional field measurements are as yet broadly practised, they present some bottlenecks being time consuming and limited in their spatial extent [178].

Current forestry management practices, can benefit from different surveying approaches: Terrestrial Laser Scanning (TLS), Airborne Laser Scanning (ALS), Mobile Laser Scanning (MLS) and Personal Laser Scanning (PLS, a subcategory of MLS). DBH, H, CBH and other tree variables can be estimated using either the ALS system[186]–[188], the TLS survey [189], [190] or the MLS technology [191], [192]. In this scenario, the increasing consciousness and the availability of technological innovations have made possible a stronger bond between geomatic and forestry disciplines. Forest inventory at different scales and levels of detail plays a key role for the management choices and the geomatic techniques can increase the automation level during the field measurements [193]. Indeed, over the last decades, technological development in data collection and computational processes have opened up new fields of research, also in forest data analysis, using remote and proximal sensing approaches [194]. Then, the forestry point cloud data analysis and management can be conducted using different softwares, as argued by several studies in the literature: CloudCompare [195], FUSION/LDT [196], [197], LiDAR 360 [91], [186], "3D Forest" [198], Computree [104], MATLAB [199], [200], Python [201], [202], R packages such as "lidR" [203], [204], "TreeLS" [205], [206]) and "rLiDAR" [207].

The rapid development of acquisition systems able to collect 3D point clouds, allowed the automation of forest inventory procedures. Several platforms have been developed to reduce time and cost of traditional measurements held with optical or electronic instruments and to improve their precision and accuracy [21], [208](Luoma et al., 2017, Wang et al., 2019). Light detection and ranging (LiDAR) techniques is boosting ecological and forest research, and researchers in various fields began to apply it for modelling analysis [23](Zhou et al., 2019). TLS is a ground based LiDAR scanning system able to offer data to analyze, improving significantly Above-Ground Biomass (AGB) estimation [24](Stovall et al., 2017). The 3D model derived by TLS application are treated as ground truth validation of forest biomass models [25], [209]. From these data is possible to extract and storing different metric data, such as DBH [27], [28], H [29], [30], stem volume [31]–[33], AGB [25], [34] and branch architecture [35]. Unfortunately, due to the static nature of TLS, it requires multiple scanning stations to ensure the effective detection of the trees. This task is time-consuming and requires manpower [36]. The most significant problems are the effects of the

occlusion by trunks, crown and the understory vegetation [38], [39], [178]. The limitation listed on TLS have boosted researchers to move up technologies able to produce 3D point clouds in a ready to use manner.

A solution is given by mobile laser scanner (MLS) [210]. These systems combine a laser scanner with an inertial measurement unit (IMU), exploiting the so called SLAM (Simultaneous Localization and Mapping). The accuracy of measurements mainly depends by the synchronization of these components. Moreover, thanks to the moving platform, the occlusion effect is reduced [178]. MLS applications are divided in two categories: handheld laser scanning (HMLS) and backpack personal laser scanning (BMLS). Early scientific publications with MLS date back 2013, and the first system prototype was large in size and weighed approximately 30 kg, which limited its operability and mobility [211]. More recent out-of-the-shelves products are lighter and more compact than more complex MLS systems, and can be easily held by a single operator even in challenging scenario. Several studies evaluate the accuracy of these different scanning systems in forestry settings. Comparative studies between TLS and MLS revealed that MLS got more accuracy than TLS rate [38], and took less time to collect the data. The use of TLS requires multiple scanning bases to ensure the effective detection of the trees, and the most significant problems are the effects of shade or concealment by trees [178], [212]. Conversely, some studies on the quality of the point cloud obtained by MLS report a problem in the model due to noise [178] or errors in fitting the geometric shapes[43]. In order to achieve high accuracy, several factors must be taken into account, such as a small research plot, the best environmental conditions, the instrument used and visibility of the surrounding environment during real-time mapping [44].

Given the above-mentioned aspects and in line with the recent literature, in this study we tested the applicability of MLS technology to measure individual tree parameters in a black pine (*Pinus nigra Arn*.) plantation. Specifically, we first compared three methodologies of MLS point cloud processing to obtain DBH, H, CBH and brach-free stem VOL on standing trees and estimated their accuracy. Then, we compared the best MLS-derived and traditional manual-measured values with the ground truth data collected from selected felled trees. From the experiments, we hypothesized that DBH estimation could be affected by less error than total height and crown base height, due to the limitation of crown shielding.

3.1.2 Study area

The study area is included in the "Cesane Regional Forest" (43°42'N 12°45'E), a large forest area of approximately 1500 ha located on the homonymous mountain system in the norther part of the Marche region in Central Italy. The orographic system is ranging from 200 to 600 m a.s.l. featuring smooth hills and some steep slopes, with an extended top plateau. The forest became state owned a century ago to be restored with reafforestation after intensive agro-pastoral exploitation causing extended slope erosion. Forest plantation, often along man-made stone terraces, started in the early 1900s but continued especially after World War II using mainly a very resilient conifer species such as *Pinus nigra var. nigra*, well adapted even to bare rocky soils. Pine is by far the dominant species (Fig. 4) with a mean stand density equal to 800 n/ha, but manna ash (*Fraxinus ornus L.*) was also frequently planted along the rows. In addition we found a very sporadic occurrence of downy oak (*Quercus pubescens Willd*., 1805), sycamore maple (*Acer pseudoplatanus L*., 1753) and European smoke tree (*Cotinus coggygria Scop.*) that have probably entered naturally in the forest area.

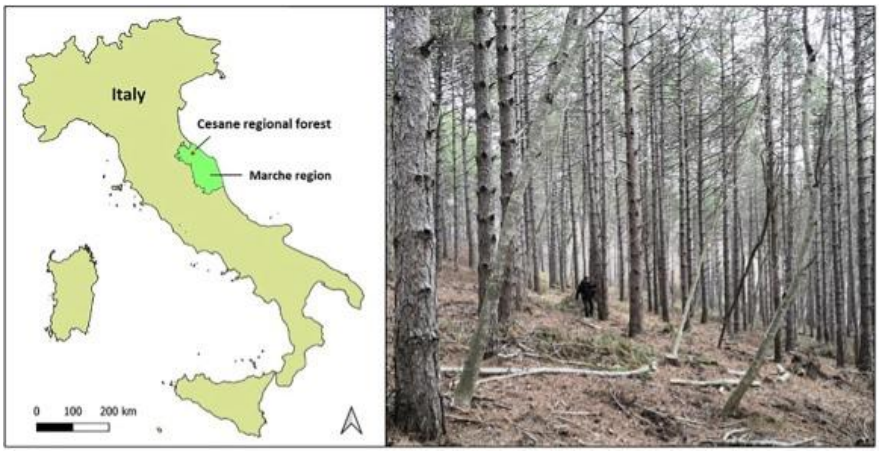

Fig. 4 The location of the study area (left) and a view of the black pine plantation (right).

3.1.3 Methodology

The survey was conducted in early February 2020 to reduce the occlusion effect caused by deciduous species of the understory, with a Mobile Mapping System device Kaarta Stencil 2 [213]. This instrumentation is equipped with a LiDAR Velodyne VLP-16 sensor mounted on top of an aluminum platform, an IMU (Internal MEMS) and an internal processor (Intel-7) for real-time localization and mapping. This instrument scans the environment around the device, quickly and automatically, in 'handheld' mode. It is a light weight (1730 grams) device, with battery life of around 2 h and internal 1 Tb SSD memory. It provides a very dense point detection (300000 maximum number of points to read from the logged up to 10 Hz). The LiDAR has a beam (= 903 nm) with 16 laser profiles and a vertical field of view of +15° to −15°, while the horizontal view is 360°. The scanning path was performed considering the following issues: i) avoiding occlusions among trees, maximizing the best coverage for the trees; ii) reducing the drift error, which may occur in repetitive environments where the alignment is harder; iii) avoiding the noise in the point cloud data. For the above-mentioned reasons, we adopted the following settings (Table 1).

Table 1 Kaarta Stencil 2 parameters setting used for field survey.

Parameters	Value (m)
VoxelSize	0.4
registrationRadius	100
cornerVoxelSize	0.2
surfVoxelSize	0.4
surroundVoxelSize	0.6
blindRadius	1.0

The scan survey covered approximately 0.5 ha of the forest stand and it was conducted walking through the forest plantation rows. The study area was surveyed in 75 min collecting 276 millions of points with a registration radius value of 100 meters (5a). During the MLS survey, it also has been possible to view the operations carried out by the tracker camera on an external monitor. Concluded these steps, the system created and currently dated a folder with files describing the configuration settings, 3D cloud characteristics and trajectory estimation. Since the Kaarta is not equipped with an internal GNSS, it has been necessary to manually perform the georeferencing post-process of the point cloud using CloudCompare tools [214]. We then collected the coordinates (x,y) of three Ground Control Points

(GCPs) with a HiPer VR Topcon GNSS antenna2 in the centre of three reflective targets placed on the ground at a considerable distance, projected in the WGS 84-UTM33N coordinate reference system.

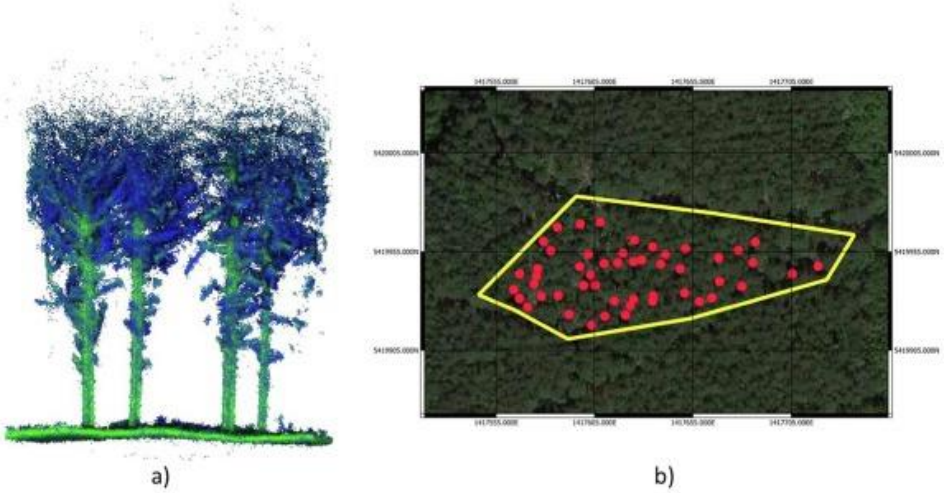

Fig. 5 a) an example of the tree point cloud view by Kaarta Stencil 2; b) distribution of the 50 selected trees (red dots) within the yellow boundary of the forest plot.

Within the MLS scanned area, we selected 50 pines of representative tree diameter and height within the pine stand (Fig. 2b). We first traditionally measured the 50 standing trees: DBH with a dendrometric caliper, H and CBH (the height from the tree stem base up to the first living tree branch) with a Haglöf Hypsometer (Vertext III). We also registered the relative tree positions measuring with sub-metric precision their horizontal distance and azimuth with a TruPulse 360B rangefinder (Laser Technology Inc.) from five GCP recorded with the HiPer VR Topcon GNSS receiver. The DBH of the selected trees ranged from 13.5 to 37.0 cm, with a mean and median value of 24.9 cm and 25.3 cm respectively.

In a second step, the selected 50 trees were cut down in September 2020 after authorization from the regional authority. We measured the stems total length (equal to the tree height) of felled trees with a measuring tape and the length from the stem base to the first living branch (corresponding to CBH). Stem diameter was measured at the stem base, at 1.30 m (corresponding to DBH) and at the median line of every 1 m long virtual sections from the base to the tapering diameter of 7 cm. The branch-free stem height was determined by visual interpretation of the stem profile, until a mean cut off height of 8 m. The branch-free volume (VOL) of single felled stems was computed applying the Heyer's formula (Eq. 1):

$$V = S_1 + S_2 + S_3 + \cdots S_{n-1} + S_n \quad (1)$$

where V is the volume up to 8 meters above the ground and S_1, S_2, S_{n-1} are the transversal surface areas of each 1 m long log. We assumed that collected measures on felled trees were error free and we used them as reference data for the comparison with traditional measurements and with remote sensed records.

For better comprehension, we outlined the data processing workflow in Figure 6.

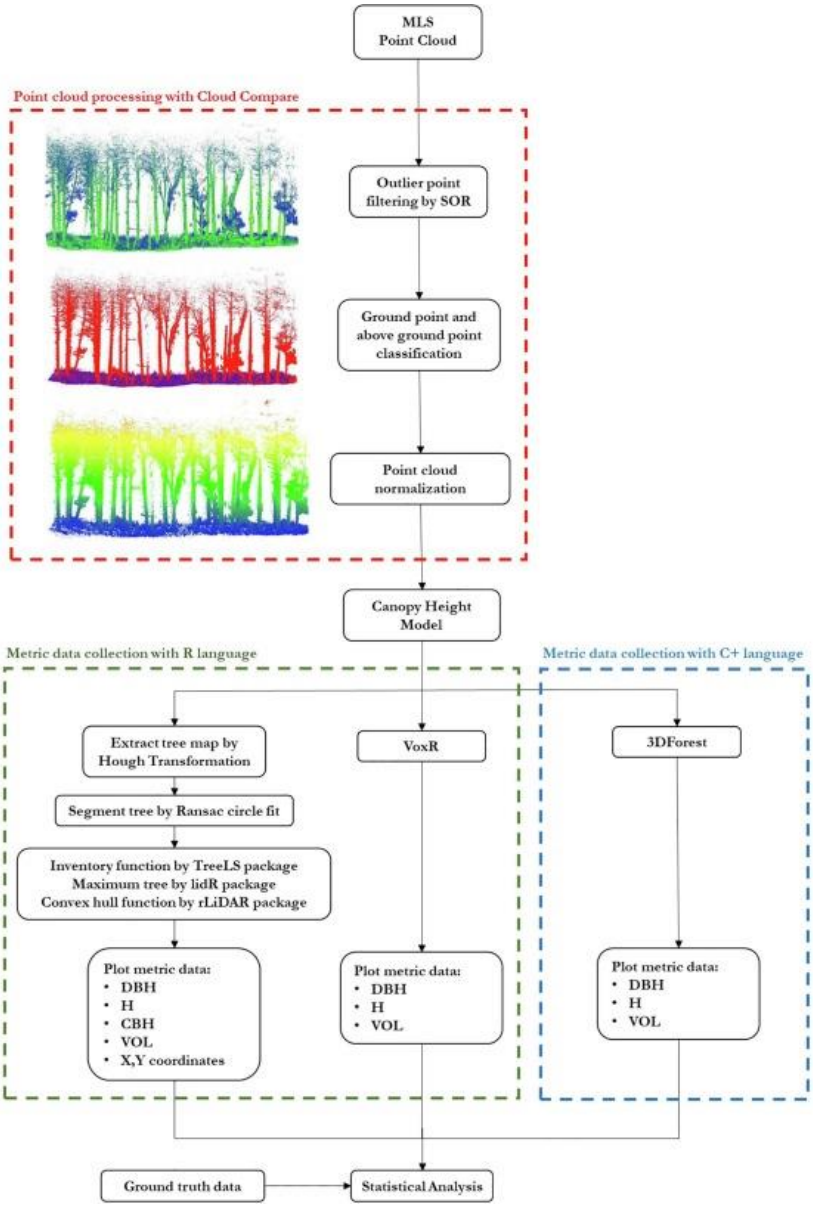

Fig. 6 Research Workflow (Diameter at breast heigh (DBH), individual tree height (H), crown base height (CBH), branch-free stem volume(VOL), barycentric coordinates (X,Y)).

We analyzed the points cloud by developing a semi-automatic approach for the extraction of metric data. The first phase concerns importing and visualising the raw data in CloudCompare [195]; then, we filtered the raw cloud by removing unnecessary detected areas to make its management easier. After having delimited the test area, we performed data filtering using the "Statistical outlier remover" SOR function [215] which allows to discard outliers and noise points produced on the trunks surface during the acquisition phase. Then, we carried out the classification between the ground and above ground points, using the Cloth Simulation Filter (CSF). CSF filters the terrain points, ensuring significant time savings and accurate reliability of the final data. The values adopted to set the parameters, optimized after several tests, were 0.3 m cloth resolution and 0.6 m distance threshold, with a maximum of 50 iterations for the analysed sample. Since some portions of the trunk were classified as ground points (Fig. 7) it required further filtering using the "Features Geometric" tool which classifies all point verticality concerning the nearest neighbours point, based on the local orientation and curvature of the stem point cloud [216]. For this project, "TreeLS" package [189] was used to segment the whole point cloud forest and to get a point cloud for each individual tree, which calculates the vertical area and enables visual detection of surfaces that extend perpendicularly to the ground. After normalizing the points cloud, we automatically extracted a set of metric data belonging to each of the 50 felled pines for statistical evaluation. We manually matched the coordinates of the extracted trees with those

collected in the field with the laser rangefinder, both data were registered in the same reference system (WGS84-UTM33N).

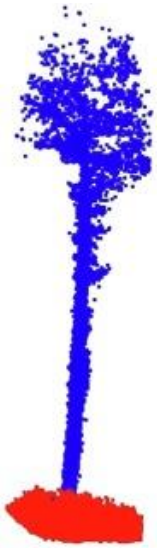

Fig. 7 The individual output from Cloth Simulated Filter (CFS) algorithm. The ground points are red and off-ground points blue.

For this scope, we analysed several data extraction methodologies. More in deep, for the detection of forest metrics we exploited the "3D Forest" open source application [198], "VoxR" package and the combination of "TreeLS-rLiDAR-lidr" packages inside R language [217]. Afterward, we compared these methods with ground truth data. The first method is "3D Forest" application, based on the C++ language and widely used to analyze points clouds from Terrestrial Laser Scanning. This is based on clustering points according to their relative distance, minimum number, corner and distance between centroids of each cluster [214]. This application is suitable for processing trees with simple crown structure, reason why it has severely limited the extraction of further data. In fact, the irregular crown shape and dense foliage limited a correct investigation, such as the segmentation and volume of branches, leading to discordant results. Therefore in this case we calculated DBH, H and branch-free stem VOL (Fig. 8a). The tool allows the extraction of two different DBH, the first Randomized Hough transformation (RHT) according to the circle detected in the point analysis, whereas the second one, based on Least Square Regression, with an algebraic estimate of the geometry calculation of the detected circle [218]. Next, we defined H as the calculation of the maximum distance between the two points along the Z axis. Finally, we computed the branch-free stem volume using the Convex hull algorithm. At the end of this procedure, a denoising operation was used to filter out those points not belonging to the trees. Noise reduction and cleaning operations are included in CloudCompare. The second test consisted on running the "VoxR" package [219], a library written with the R language [217] which is based on a voxelization algorithm that has allowed the classification of points in a regular three-dimensional grid of voxels [220]. The file, imported in.txt format, was subjected to metric analysis, using the "tree_metrics" function and setting the voxel size as 0.05 m; DBH, H and VOL values were extracted (cylinder), such as diameter, height, and volume (Fig. 8b). This function makes the metric data extraction easy and intuitive. The third method tested is a set of R-packages allowing the extraction of the whole metric data. TreeLS [189] permits the users to customize the parameters according to the tree characteristics and the points clouds, using algorithms with various functions. The most important one allows the stem mapping through the automatic detection of individual trunk points. We carried out the correct identification of the trunk's points, separating it from the branches and leaves by means of the Hough transformation and consequently exploiting the RANSAC algorithm [189]. The latter subdivides the cloud into several subsets, providing the inventory of each calculated geometric primitive (cylinder) (Fig. 8c), such as diameter, height, and volume. The last step generates a series of geometric primitives of cylindrical shape along the vertical axis of the trunk. Before being reconstructed by using the geometrical primitive, in particular the circular cylinders [221], the stem point cloud tree was sliced into three subclasses. This necessary because of stem tapering as also addressed by Panagiotidis and Abdollahnejad [33]. The slicing step has carried out along the z-axis from up to the maximum height of 8 metres for each investigated tree. We calculated a cylinder primitive geometrical by Ransanc

algorithm. It was filtered on vertical point cloud slice with high accuracy. Thus, the output a high details and accuracy concerning the metric data, such as DBH, H and branch-free stem volume.

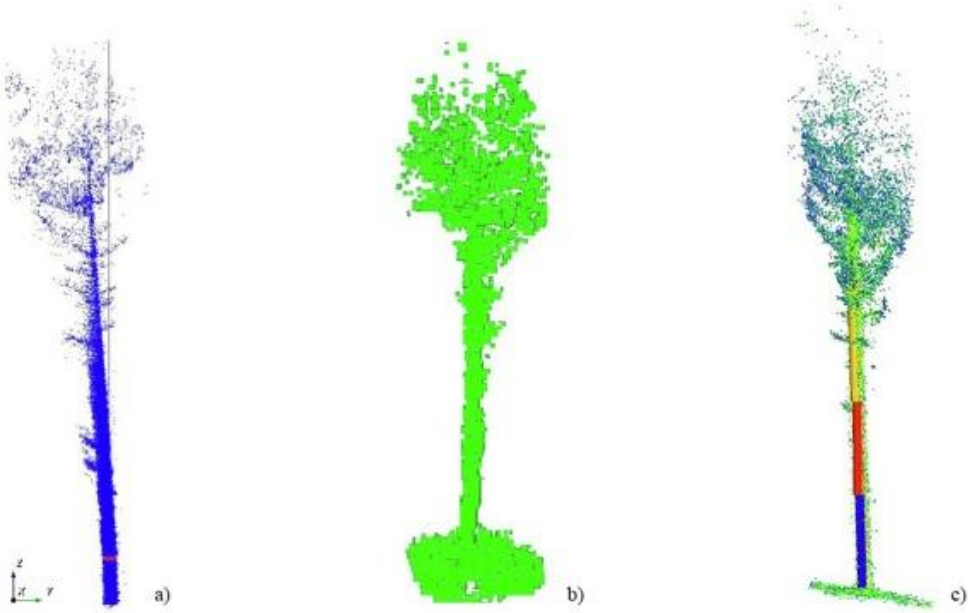

Fig. 8 DBH extraction phases: a) DBH and Tree Height data extracted by 3D Forest; b) Voxelisation by "VoxR" package; c) Reconstruction of the geometrical primitives with RANSAC on the points classified as stem.

This choice derived from LiDAR data provided an incomplete representation of the trunk surface, due to physical obstacles (fallen trees, shrubs or saplings) or shaded areas. In particular, denoising operations tend to poorly filter out even heterogeneous or unshaded portions of point clouds, compromising the correct data analysis. An interpolation of the two diameter values closest to the breast height (1.30 m) allowed to calculate each stem DBH. Furthermore, in this set, the barycentric coordinates of each point cloud tree and the DBH were extracted. Again, using the inventory data, we achieved the volumes of the cylinders, estimating them up to a height of 8 m above the ground. The maximum height was then extracted using the lidR package [222]. Finally, the "rLiDAR" package [223] was used for the calculation of the CBH. This package is able to divide and group the 3D model points into a series

of subsets using the “k-means” algorithm, filtering this search along the z-axis. Thereby, for each subset was computed “Convex Hull” algorithm which had facilitated the distinction of the crown from the trunk (Fig. 9).

Fig. 9 CBH estimated by Convex Hull function.

We evaluated the bias and root-mean-square error (RMSE) of selected variables (DBH, H) comparing first the results gained with the three different algorithms (“3D Forest”, “VoxR” and the combination of “TreeLS-lidr-rLiDAR” packages) with ground-truth measures on felled trees; then, comparing traditional field surveys and the best MLS method with ground truth (adding CBH). We used the following equations:

$$bias = \sum_{i=1}^{N} \frac{x_i - x_{i,ref}}{N} \qquad [2]$$

$$RMSE = \sqrt{\sum_{i=1}^{N} \frac{(x_i - x_{i,ref})^2}{N}} \qquad [3]$$

where N is the number of felled trees, refers to the estimates achieved with the algorithms and with traditional survey, and refers to the corresponding ground truth value. Additionally, we used the following definitions for the relative bias and RMSE:

$$bias\ \% = \frac{bias}{x_{ref}}\ x\ 100\ \% \qquad [4]$$

$$RMSE\ \% = \frac{RMSE}{x_{ref}}\ x\ 100\ \% \qquad [5]$$

Where xref is the mean of the reference values. For the comparison among the three MLS methods with ground truth measurement, we also evaluated the bias and RMSE for stem volume extraction up to 8 meters above the ground. We fitted regression lines of DBH and H values distribution derived by laser survey, traditional field operation and ground truth assessment data. Finally, we plotted all parameters distribution using boxplot charts and tested the differences of means using paired two-sided t-test with 95% of confidence level ($\alpha = 0.05$).

3.1.4 Results

Exploiting the object 3D reconstruction, we obtained the score with most accuracy, with the identification of the closest geometric primitive of its original shape. With this first analysis we wanted to discard the less accurate method for a better comparison in the following step. The best accuracy is reached with the "TreeLs-lidR-rLiDAR" packages combination (Table 2), through the Hough transformation. We then performed a stem modelling with the RANSAC algorithm, which allowed the more accurate estimation. The use of MLS has produced zones with low density and high noise point clouds (Fig. 10).

Table 2. Comparison of DBH (diameter at breast height), H (tree height) and VOL (branch-free stem volume up to 8 meters) measures collected from the 50 felled trees and parameters estimated by different algorithms. In brackets standard deviation is reported for felled trees measures and percentage values for bias and RMSE.

Table 2 Comparison of DBH (diameter at breast height), H (tree height) and VOL (branch-free stem volume up to 8 meters) measures collected from the 50 felled trees and parameters estimated by different algorithms. In brackets standard deviation is reported for felled trees measures and percentage values for bias and RMSE.

	DBH (σ) [cm]		**H (σ) [m]**		**VOL (σ) [m3]**	
FELLED	24.7 (5.2)		17.1 (1.2)		11.2 (1.5)	
Platform	Bias (%)	RMSE (%)	Bias (%)	RMSE (%)	Bias (%)	RMSE (%)
3D Forest	0.9 (3.8)	4.1 (16.3)	−2.4 (−14.4)	3.1 (18.3)	0.0 (−11.5)	0.1 (31.7)
VoxR	2.6 (10.4)	6.8 (27.0)	−1.7 (−9.9)	2.4)14.0)	0.0 (−11.1)	0.1 (39.6)
TreeLS-lidr-rLiDAR	0.0 (0.0)	2.7 (10.8)	−1.5 (−8.6)	2.4 (13.9)	0.0 (−4.1)	0.0 (12.4)

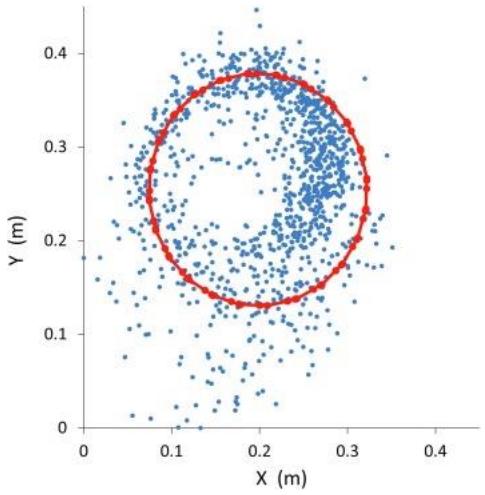

Fig. 10 DBH points extracted and plotted on a 2D graph. Red dots are the ones used to interpolate with a suitable circle, while blue dots are the discarded ones.

Bias and RMSE values of traditional field sampling compared to ground truth measurements are very low for DBH: 0.8% (0.2 cm) and 5% (1.1 cm) respectively (see Table 3). Similar gaps occur in tree sub-samples with DBH below and above 25 cm (RMSE of 0.8 cm and 1.3 cm respectively). Manual measured tree height was slightly underestimated compared to the ground truth (% bias = −0.7 and % RMSE = 10.2) as well as in trees sub-sample with heights below 17.5 m (bias % = −1.3 and RMSE % = 11.2) (Table 3). Diversely, the RMSE of H estimates of trees higher than 17.5 m indicated a minor overestimation (1.6 m and 8.9%) compared to the ground truth. CBH showed a bias of 0.1 m (0.6%) and a higher RMSE (15.8%) (Table 3).

Table 3 Tree variables values reached with traditional manual measurements on standing trees (TRAD) and from cut down trees (FELLED). Abs: absolute values; %: percent values.

Variable	N	Mean (σ)		Bias		RMSE	
		TRAD	FELLED	Abs	%	Abs	%
DBH [cm]	50	24.9 (5.4)	24.7 (5.2)	0.2	0.8	1.1	4.5
H [m]	50	17.0 (2.1)	17.1 (1.2)	−0.1	−0.7	1.7	10.2
CBH [m]	50	11.2 (1.4)	11.2 (1.5)	0.1	0.6	1.8	15.8
DBH ⩽25 [cm]	25	20.7 (3.4)	20.6 (3.4)	0.1	0.4	0.8	4.1
DBH >25 [cm]	25	29.2 (3.4)	28.9 (3.1)	0.3	1.1	1.3	4.6
H ⩽17.5 [m]	28	16.1 (2.0)	16.3 (1.0)	−0.2	−1.3	1.8	11.2
H >17.5 [m]	22	18.1 (1.8)	18.1 (0.5)	0.0	0.0	1.6	8.9
CBH ⩽17.5 [m]	28	11.2 (1.4)	11.1 (1.9)	0.1	0.7	1.9	17.5
CBH >17.5 [m]	22	11.2 (1.3)	11.2 (1.0)	0.05	0.5	1.5	13.2

Comparing MLS values with ground truth measurements (Table 4), the bias of DBH estimates was equal to 0 for both absolute and percent values and the RMSE 10.8% (2.7 cm). For DBH sub-groups, we found opposite estimates: positive for DBH below 25 cm (0.8 cm and 4.1%) and negative for DBH above 25 cm (-0.8 cm and −2.8%); % RMSE was equal for both classes (10.6%). H and CBH measured with MLS were underestimated compared to the ground truth (bias of −8.6% for H and −13.3% for CBH) but CBH estimate had the highest percent RMSE value (19.5%). Splitting the analysis by H classes (below and above 17.5 m), both SLAM measures confirmed an overall underestimation compared to the ground truth (bias % of −7.6 for H below 17.5 m and −9.8 for H above 17.5 m). Branch-free stem volume (up to 8 meters) values showed a bias and a RMSE of −4.1% (−0.01m3) and 12.4% (0.04 m3) respectively.

Table 4 Tree parameters values measured with SLAM (MLS) and on the ground (FELLED). Abs: absolute values; %: percent values

Variable	N	Mean (σ)		Bias		RMSE	
		MLS	FELLED	Abs	%	Abs	%
DBH [cm]	50	24.7 (5.1)	24.7 (5.2)	0.01	0.04	2.7	10.8
H [m]	50	15.6 (1.7)	17.1 (1.2)	−1.48	−8.64	2.4	13.9
CBH [m]	50	9.7 (1.1)	11.2 (1.5)	−1.48	−13.3	2.2	19.5
VOL [m3]	50	0.31 (0.1)	0.32 (0.1)	−0.01	−4.1	0.04	12.4
DBH ⩽25 [cm]	25	21.4 (3.3)	20.6 (3.4)	0.8	4.1	2.2	10.6
DBH >25 [cm]	25	28.0 (4.3)	28.9 (3.1)	−0.8	−2.8	3.1	10.6
H ⩽17.5 [m]	28	15.1 (1.7)	16.3 (1.0)	−1.2	−7.6	2.4	14.7
H >17.5 [m]	22	16.3 (1.6)	18.1 (0.5)	−1.8	−9.8	2.3	12.9
CBH ⩽17.5 [m]	28	9.4 (1.2)	11.1 (1.9)	−1.7	−15.5	2.5	22.4
CBH >17.5 [m]	22	10.0 (1.0)	11.2 (1.0)	−1.2	−10.4	1.7	14.9

Fig. 11a shows the overestimation of smaller DBH values and the underestimation of greater values (red line) using MLS. The comparison of tree height (Fig. 11b) reveals the same pattern of underestimation of MLS data for the

highest trees. We did not detect statistical differences in mean DBH (= 0.05) between the two estimation methods (MLS and TRAD) compared to the direct measurement on felled trees (Fig. 12a), but we found them in mean H (MLS vs FELLED) both for the whole sample (15.6 m vs 17.1 m respectively) and splitting it by H classes (15.1 m vs 16.3 m for H 17.5 m and 16.3 m vs 18.1 m for H 17.5 m) (Fig. 12b). We also detected significant statistical differences in comparison of mean CBH (9.7 m for MLS vs 11.2 m for felled trees) and for stem volume (0.31 m3for MLS vs 0.32 m3for felled trees) (Fig. 13).

a)

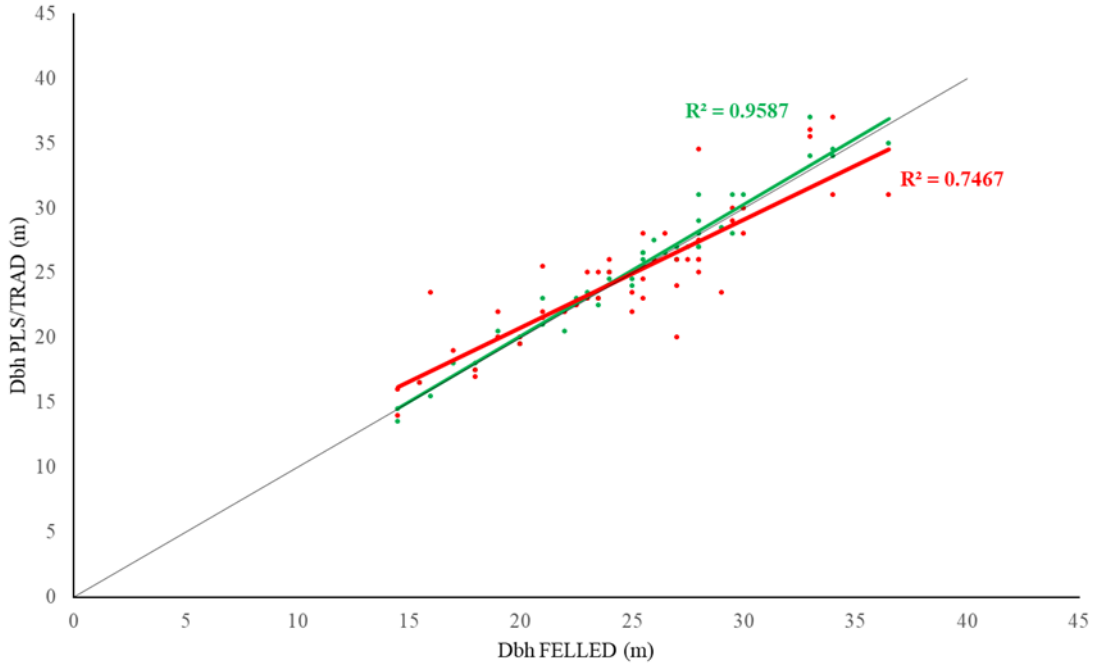

b)

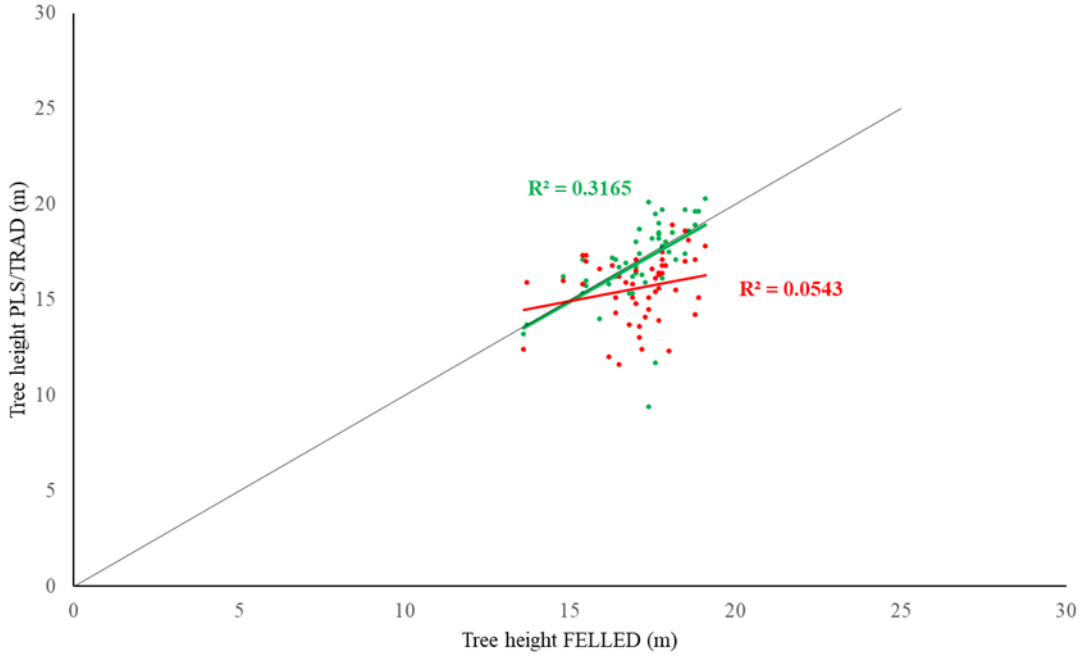

Fig. 11 Regression analysis between DBH (a) and H (b) values derived by laser survey (MLS, red dots), traditional field operation (TRAD, green dots) and ground truth assessment data (FELLED).

a)

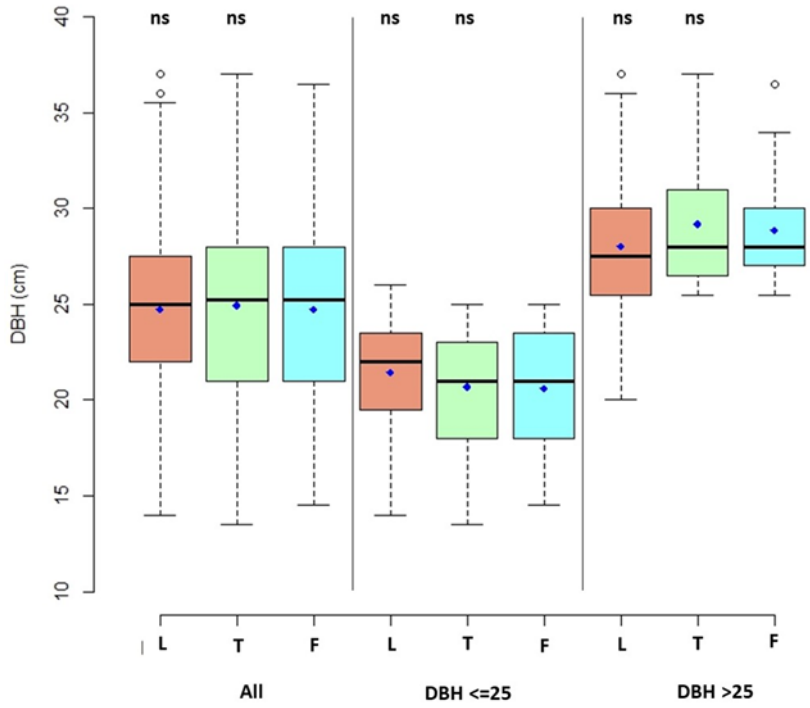

b)

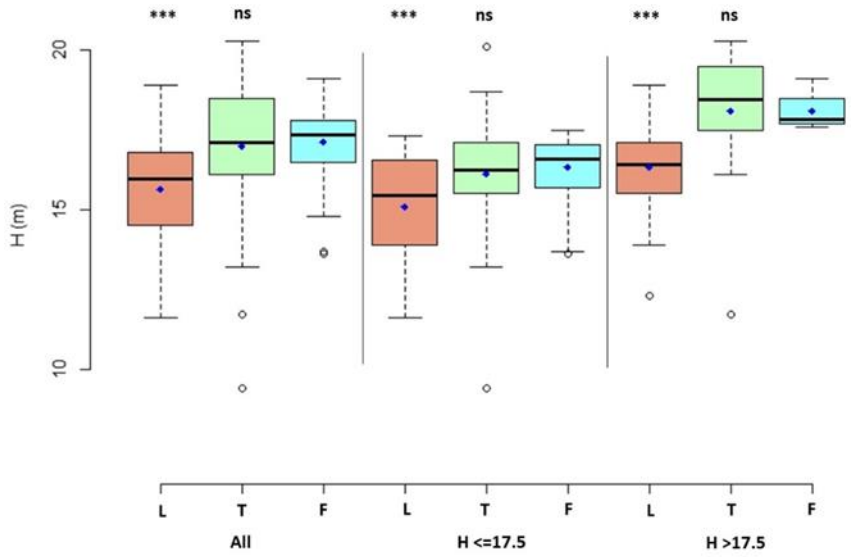

*Fig. 12 Boxplots of the DBH distribution (a) and tree height H (b) from MLS (L - red), Traditional (T - green) and FELLED trees measurement (F - blue) for the whole sample (All) and sub-samples (DBH below/above 25 cm and H below/above 17.5 m). Horizontal bold lines are medians, blue dots are the means. Whiskers are minimum and maximum values and circles are outliers. Significance of differences in DBH and H between MLS, TRAD and FELLED are marked by "ns" (not significant, p-value > 0.1) or "***" (p-value < 0.001) tested with paired two-sided Student's t-Test.*

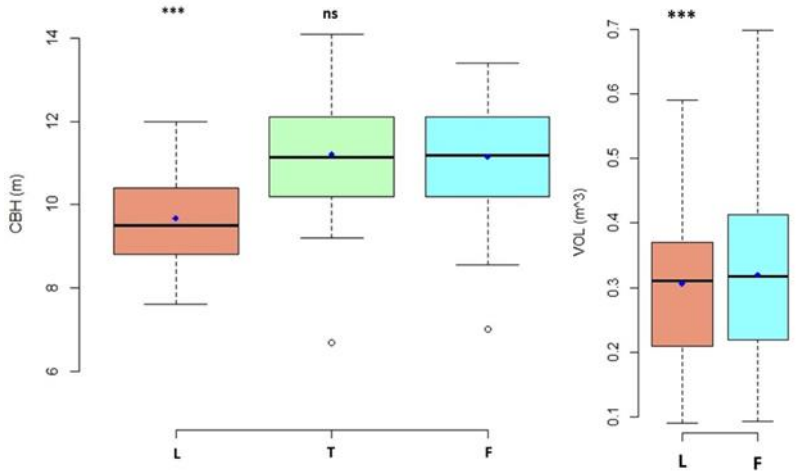

*Fig. 13 Boxplots showing the CBH distribution (a) the volume distribution (b) of the tree stems from SLAM laser technology (L - red), traditional (T - green) and field direct measurement of felled trees (F - blue), across the whole sample (n = 50). Horizontal bold lines are medians, blue dots are means. Whiskers are minimum and maximum values and circles are outliers. * = p value < 0.05, ** = p value < 0.01, *** = p value < 0.001; ns, not significant (paired and "two-sided" Student's t-Test for laser and traditional measures with the ground truth).*

3.1.5 Discussion

Forest structure and yield measurements are essential not only for computing timber productivity but also for calibrating any kind of multi-functional forest management (e.g. biodiversity conservation, carbon sequestration and other ecosystem services). Nonetheless, accurate forestry measurements are not straightforward due to forests complexity and to the characteristics of the traditional instruments used in forest field measurements (e.g., calipers and clinometers). They are easy to use but they require several operational steps, becoming time consuming, laborious and expensive when repeated in inventory survey [224]. MLS can provide very fast data collection of large areas, reducing the efforts for surface area and the measurement error. Holopainen et al. [39] compared the accuracy and the efficiency of TLS, ALS and MLS systems on 438 trees in an urban forest area in Finland. The study proves that TLS and MLS outperform ALS for the parameters detection, as the canopy effect hampers the achievement of trustful results. Vatandaşlar and Zeybek [225] evaluated the efficiency and reliable of Zeb-Revo lidar (HMLS) by GeoSlam company compared to manual field measurements, considered as ground truth, in a forest stand (79 ha) in Turkey. They reported that DBH RMSE was 2.41% and bias 0.56%, while the timber volume showed a high deviation (21,5%), compared with allometric values. Bauwens et al. [178] compared TLS with a handheld MLS. These two different systems, compared with the traditional field DBH measurements, provided similar results with a bias < −0.2 cm and a RSME < 1.5 cm. The DBH detection was determined with an accuracy of 3 cm scoring 96% for the TLS and 98% for the MLS. These rates decreased, respectively, to 78% and 73% with < 1 cm accuracy. This confirms that TLS e MLS produce comparable results in terms of accuracy, while the latter may result convenient as it reduces the time spent for performing the survey and the post processing phase of point cloud registration. Our results showed that data collected with MLS survey in an dense even-aged black pine plantation, provides acceptable DBH estimations, featuring a 10.8% RMSE respect to ground truth (4.5% RMSE with traditional measurements). The accuracy of DBH estimation with MLS remains sufficiently high at all size classes. The error slightly increases with height measurements, ranging from 13.9% for H and 19.5% for CBH, where traditional hypsometer survey produced 10.2% and 15.8% respectively. It is worth to note that our study confirms the most recent findings in the literature; the accuracy of H estimations decreases when the tree height increases, highlighting some limitation of the proposed approach. Consistently, the RMSE increases from the ground to the top of the tree for two reasons: i) the crown, being more dense, generally occludes the light beam by LiDAR; ii) the distance from the scanner to the stem decreases both measurement accuracy and points resolution. Both of these effects result in a smaller number of good quality arcs [97]. The values achieved in this work are not very different from those recorded in a Finland Boreal forest [97] where the RMSE for total tree height estimation, using a backpack mobile laser scanner, was 8.7%. From the statistical analysis, the authors reported a RMSE of stem Volume computed in two sample plots, ranging from 0.053 m^3 and 0.002 m^3. The tree density in Boreal forests is usually much lower than in scarcely thinned mountain conifer plantations where the standing trees treetops are often hardly detectable. Considering our case with similar characteristics, the RMSE value compared with felled trees is 0.004 m3. A detection accuracy of 90.9% was reached

for the DBH detection from a MLS based point cloud compared with traditional ground data [91]. This is confirmed even in the article by Cabo et al. [30], where TLS e ZEB REVO are compared in Pinus pinea and Platanus hispanica plantations. In those sites, DBH RMSE is 0.011 m and 0.009 m respectively and H RMSE of 1.340 m and 9.440 m. Our approach produces comparable results with those already described in the reviewed literature, despite the authors tested the methodology with trees higher that 15 meters and in sunny conditions that reduce the MLS accuracy. Kaarta Stencil 2 proved to be versatile and featuring higher mobility if compared with TLS. The data processing method proposed in our study provides the most robust denoising method was the Hough transformation, since it maintains stem features up to the tree crown, allowing a better accuracy on the stem modelling phase. It worked out in good combination with the cylinder fit Ransac algorithm for stem modelling. The proposed workflow is linear and replicable to further studies as well the sample used. Dealing with the CBH, the proposed method (Convex Hull) provides a 3D graph showing the differences between the crown and the remaining stem, enabling the CBH visualization. A more efficient approach could be the combination of airborne collected data, for a more realistic detection of the crown shape from the forest canopy top [186]. Finally, an important aspect that needs further studies is the effect of diameter size [99]. In our study we have limited the detection to the dominant and regularly shaped species, the black pine, providing more homogeneous target and facilitating the data processing. The results obtained are encouraging but need to be validated in more heterogeneous structures with mixed species and multi-layer stands.

3.1.6 Conclusion

This study demonstrates the applicability of the hand held MLS with SLAM algorithm for the estimation of metric parameters of individual trees in a black pine (Pinus nigra Arn. plantation). The advantages of the MLS-SLAM application transcend the automatic registration of the scans and the low weight of the device, which favoured a high rate of reliability in retrieving the 3D structure and forest monitoring. Statistical analysis between LiDAR and ground truth data shows an accuracy of about 10% of relative RMSE. The forest environment investigated had very dense and overlapping crowns, and the presence of a consistent number of branches from 8 m height hindered the laser beam in acquiring objects at this height; this limitation reduces the estimate of the maximum tree height and total stem volume calculation. Our method exploited a semi-automatic procedure for the branch-free stem volume estimation, even if few thresholding operations are needed in the loop. Our research paves the way for future experiments, by highlighting limitations that deserve further investigation. Firstly, the sample stand is homogeneous both in terms of tree species and morphology; the same approach should be tested in a more complex contexts. Secondly, the lack of literature benchmarks in the definition of CBH. Indeed, the comparison with ground truth data is left to the operator's subjectivity; a more objective method of CBH extraction should be proposed in future research. Finally, the estimation of H cannot be sufficiently accurate, and integration with aerial data is still mandatory to guarantee a complete mapping of the surveyed area. Nonetheless, remote sensing data will provide new and accurate field data to improve measuring and estimation forest parameters, such as basal area or stand volume.

4.1 Innovation in olive-growing by Proximal sensing LiDAR for tree volume estimation

doi: 10.1109/MetroAgriFor55389.2022.9965016.

Chiappini S., Balestra M., Pierdicca R., Malinverni E.S., Marcheggiani E., Giorgi V. and Neri D.

4.1.1 Introduction

Olive trees are typical Mediterranean landscape elements with significant leverage for more than 16 countries in the Mediterranean area. For most of them, economic wealth also depends on the olive grove's intrinsic and extrinsic value [226]. Olive landscapes result from long-lasting relationships among the local communities, ownership, management, and exploitation [227]. These features are deeply rooted in folks' perceptions of the local traditions. Furthermore, olive products also have become a key Mediterranean Diet component.

The olive landscape has undergone a significant change in Italy after WWII. The process of farm specialization and mechanization, jointly with the productivity requirements, have affected both yield and profitability. The olive production chain has led farmers to commit to high-quality standards [3]. At the same time, the mass migration of householders from marginal and rural areas towards the cities led to the abandonment of traditional wooden crops and the lack of qualified farmhands.

Nowadays, the development of Precision Agriculture (PA) is emerging as an innovation bringer and a game changer. New management strategies based on proximal and remote crop sensing and Information and Communication Technologies (ICT) certainly will help farmers and land managers to withstand, preserve and exploit such delicate landscape settings [228].

Widespread innovation is still limited in olive groves. According to the literature, a few geomatic and spatial data researches have been published yet on this matter. However, we believe laser sensors to extract three-dimensional (3D) tree metrics are a challenging topic. To this goal, Terrestrial laser scanning (TLS) and airborne unmanned aerial vehicle (UAV) solutions could serve the purpose. As a matter of fact, TLS provides high-density point clouds of surveyed trees [26] [229]. So does UAV with quicker surveys, even if part of the tree hidden by the crown cannot be detected [230] [19].

Among the different laser scanning, Light Detection and Ranging (LiDAR) represents an opportunity to develop non-destructive methods for biomass computation which can cost-effectively and more precisely replace current field measurements [228].

In this context, our research aims at estimating olive tree canopy volumes (CV) by Mobile Laser Scanning (MLS), a technique so far mainly for civil engineering. The laser planes produce a cloud of coordinates in 3D space to reconstruct the structure of trees. The triangulation of the outer hull points produces a mesh representing the tree surface [180]. We have texted two different meshing algorithms, convex hull (CH) and alpha shape (AS) [231]. Moreover meshing, previous experiments on tree parameter extraction by 3D data also explored the possibility of slicing the crown into slices 5-10 cm thick [45] [231] [107].

4.1.2 Study area

The study area is in central Italy, in the municipality of Cartoceto, in the Marche region (Fig. 14, 15, 16). The area is a well-known geographical indication (GI) agreed by Italian law by Protected Designation of Origin (PDO) [232]. The studied olive grove has a pattern of 6x6m with 200-250 olive trees per hectare. The study is financed by the support of the regional funds for rural development EFRD "PSR Marche 2014/2020" and the local farmers association "Cartoceto DOP" [233]. The overall research project aims to enhance the association's quality and efficiency while shedding light on the benefits of the olive landscape to the local community and the environment. The history of such a peculiar specialized olive grove land setting spans about 50 years.

Fig. 14 Study area localization in the Marche Region, Italy

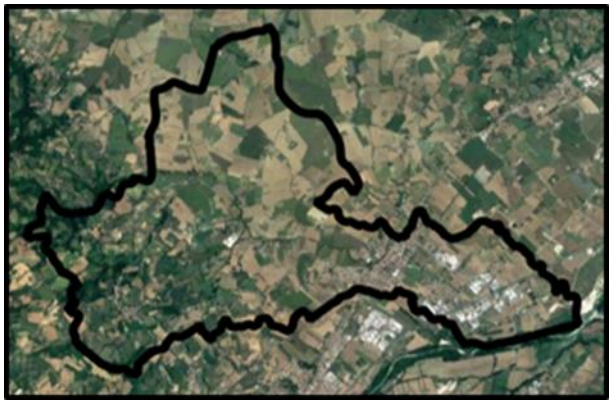

Fig. 15 The administrative limits of the Cartoceto Municipality

Fig. 16 An overview of the analyzed olive grove

4.1.3 Methodology

To collect single tree and crown section point clouds, we used a Kaarta Stencil 2 MLS (Fig. 17). Single olive trees were sampled to extract the canopy volume (CV). We collected 102 million points (Fig. 18 and Fig. 19) in 12-minute fieldwork walking in a closed loop beneath the rows, covering approximately 3665 m2.

Fig. 17 Kaarta Stencil 2 Mobile Laser Scanner

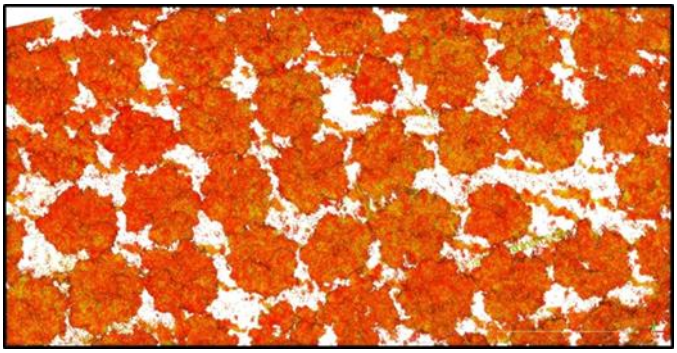

Fig. 18 The top view of the point cloud olive grove

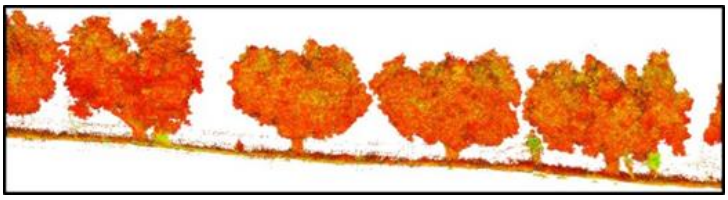

Fig. 19 The side view of point cloud olive grove

The coordinates of five reflective targets, placed at a convenient distance along the pathway, were recorded by a HIPER HR TOPCON GNSS receiver.

Single point clouds have been computed in a semiautomatic way by Cloud Compare (CC) [234], following iterative steps.

The first step is georeferencing the coordinates according to a chosen system of reference, WGS84/UTM33N, in our case, using the CC Align tool. In order to reduce redundancies in the considerable amount of data to be computed, we segmented the off-ground points using the plugin CSF [235]. By Noise Filtering, the filtering operation was repeated once the ground had been split to detect isolated points and low-density aggregated points. At the end of these iterations, 12 trees out of 21 have been reconstructed.

To compute the accuracy of the MLS campaign, we need ground truths (GT) [180] [45] [236] [237]. Different studies on the use of MLS focus on the comparison of measured tree canopy volumes with estimated ones, assuming the tree shape is likewise a geometric primitive. This technique is primarily used in agronomic practice. Two geometric primitives have been used the most: a paraboloid and a toroid.

In this study, we considered both primitives as GTs. In particular, the paraboloid approximates the olive tree shape well, but the toroid matches that of the pruned olive trees. In fact, in experimental conditions, polyconic vase pruning is used mainly in olive groves and creates a hollow zone within the centre of the canopy. We manually clipped the individual tree in CC using the Section tool to the canopy height (H) and the crown width (W) of each single olive tree. These parameters are directly correlated to the olive growth and, among other ecological variables, reflect the fruit yield. Moreover, these canopy metrics help the farmers to batch pesticides [45]. The olive canopy width is estimated using the average measurement of the two crossing axes, while the height is the maximum value along the z-axis.

The single tree canopy volumes to be used as reference GTs have been calculated using the paraboloid primitive (Eq. 1) (Fig. 7) and the toroidal (Eq.2) (Fig. 8).

$$V\ paraboloid = \frac{\pi D^2 H}{6} \quad (1)$$

$$V\ toroidal = 2\,\pi^2 r^2\,R \quad (2)$$

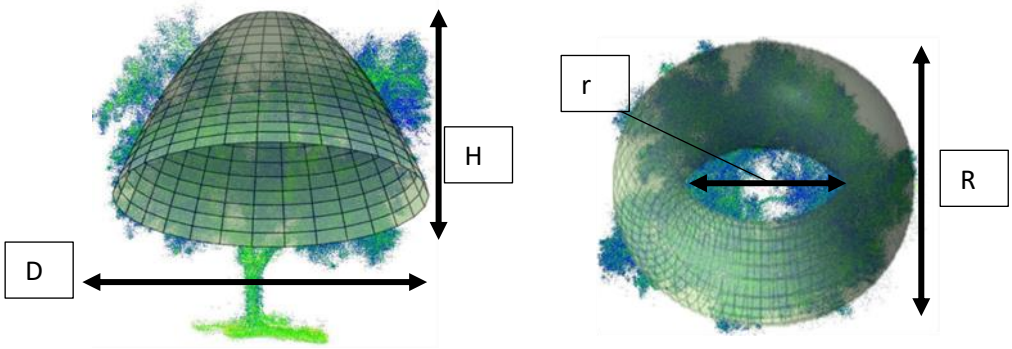

Fig. 20 Geometric primitives shaped like paraboloid (left) , Geometric primitives shaped like toroid (right)

4.1.4 Results

The computed GTs values have been correlated against the volumes measured by MLS LiDAR data. Before doing that, it is necessary to transform the point clouds in a closed surface, e.g. using meshing algorithms. In this work, two different meshing algorithms, CH and AS, have been used to process the crown point clouds by MATLAB version R2020b (Mathworks, Inc.). The CH algorithm reconstructs tree crowns as a 3D convex polyhedron with a triangular surface, removing all outer points. On the other hand, AS performs the geometrical reconstruction from a set of unordered points. Smaller alpha values accurately reconstruct the outer contour of the point cloud. Figure 21 shows crown reconstruction using a CH algorithm, while Figure 22 shows the canopy reconstructed through the AS algorithm (alpha value: 0.5). Thanks to the results, it has been possible to assess the best algorithm performance.

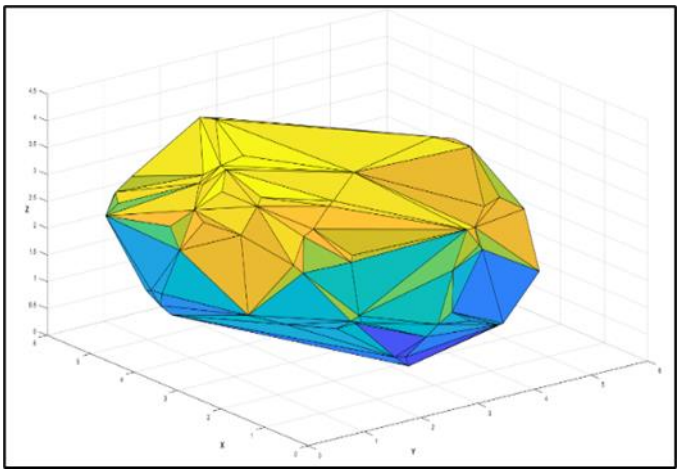

Fig. 21 Convex Hull algorithm's output

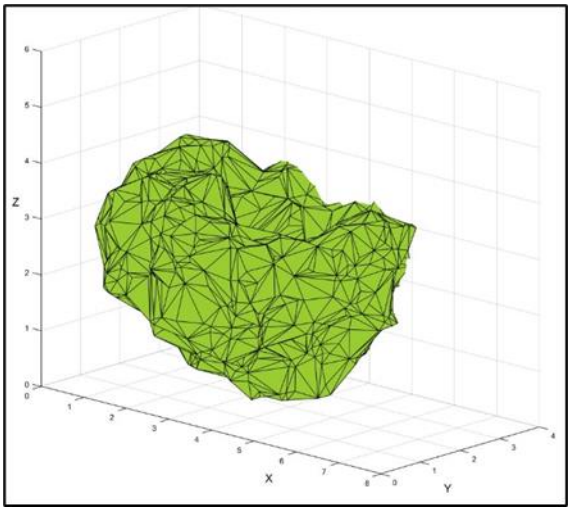

Fig. 22 Alpha Shape algorithm's output (alpha value: 0.5)

Figures 23 and 24 show more correlation between primitives and meshes when we compare the paraboloid with the convex hull (R2= 0.92) and the toroidal with the alpha shape (R2= 0,91). Conversely, the less correlation is for the other pairwise combination, where the values of confidence sharply decrease to R2= 0.55 and R2= 0.78.

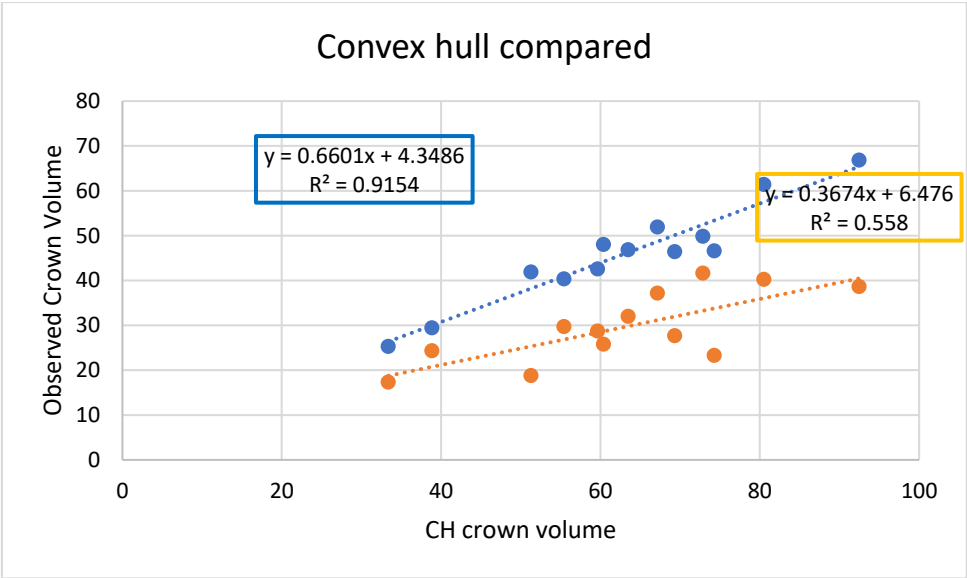

Fig. 23 Correlation R^2 among Convex Hull and Paraboloid (blue) and Toroidal (orange) shape

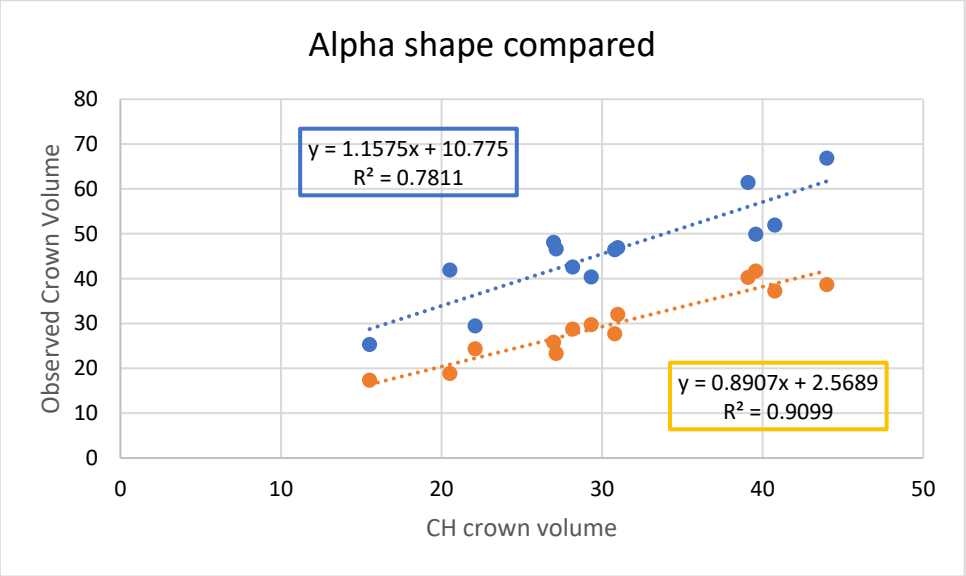

Fig. 24 Correlation coefficient among Alpha Shape and Paraboloid (blu) and Toroidal (orange) shape

4.1.5 Discussion

Conversely, the less correlation is for the other pairwise combination, where the values of confidence sharply decrease to R^2= 0.55 and R^2= 0.78. Finally, the results strongly correlate the ground truths and the measures. These results are in line with what is reported in [45]. Bearing in mind that the strong correlation occurred only when the 3D measurement fits the GT. The Alpha shape algorithm fits the toroidal shapes best, thanks to its more precise reconstruction of the tree structure. ~~It is worth mentioning that the user largely affects the final results since the ground truths are directly taken over the 3D model. That stage is subjective and depends on the user's interpretation.~~ This stage is largely subjective and depends on the user's interpretation based on experience in recognizing the actual shapes of the olive tree canopy, which is never homogeneous due to different species and pruning methods.

4.1.6 Conclusion

In this study, we demonstrated the potential of MLS to estimate tree canopy volume in olive groves. The research should consider agronomic practices (geometric primitives) combined with proximal sensing (meshing and slicing) to obtain higher accuracy. The hope is that future predictive models based on 3D will assist farmers in the best pruning performances [20], selecting the single tree volumes to be cut off in semiautomatic ways. The time-saving and cost-effectiveness of the proposed method will foster the frequency of surveys, making groves monitoring practices more effective. Our future developments will focus on improving the outcomes by comparing pruning techniques and meshing algorithms (i.e. Alpha shape and Voxel-based). Different authors suggest slicing the point clouds representing the crowns along the z-axis with a defined thickness.

5.1 Olive landscape transformation by multi-temporal images and metrics. A study case of Cartoceto municipality, Italy

Chiappini S., Balestra M., khosravi A., Galli A., Marcheggiani E. and Neri D.

Status: ongoing submission

5.1.1 Introduction

Throughout the Mediterranean, the presence of the olive tree (Olea europaea L.) has been an enduring aspect of the landscape for millennia. Thanks to their presence, rural landscapes have been shaped into the form we know today. In addition, traditional cultivars indigenous to the area have become a powerful symbol of identity for local communities. This trend encompasses the territorial extent of our current study in Italy. Beyond being central components of the landscape, olive groves are valuable providers of goods such as oil, table olives, essence, and others and serve as critical providers of ecosystem services [238], [239]. According to Gomez and Bogunovic [240]–[242], the ecosystem services provided by olive groves refer to various ecological functions that result from the agronomic practice of grazing (for example, biodiversity conservation, erosion control, and soil fertility improvement). The latter is vital in low-density olive groves in heterogeneous landscapes with mixed vegetation (agricultural and spontaneous, herbaceous and tree species) [243]–[245].

Besides the environment, other social and cultural aspects have to be considered. In reality, they embody the memories of the past, transmitting centuries-old traditional methods of olive cultivation and processing to future generations [246]. These social implications can aid in combating depopulation and other challenges that have historically plagued marginalised and rural inland regions that are less conducive to intensive crops [247].

Olive-growing landscapes have recently become a new focus for rural tourism, including ecotourism, agritourism, cultural tourism, gastronomic tourism, oleo tourism, etc. [248]. They provide services linked to relaxation, landscapes, traditional culture and escape from mass tourism [249]. Several studies have indicated how olive tourism (especially oleo tourism) could be developed by following what has been happening with so-called food and wine tourism routes in many countries [249], [250] where vineyards significantly contributed to the enhancement of prestigious wine-growing landscapes. Recent research suggested that measurable indexes integrate not only the geographical origin but, in a relevant way, the tradition and expertise involved in producing high-quality products with differentiated personalities [241], [249], which are critical elements of socio-economic development of olive-growing areas. Geographic indications (GI) have been established in the regulation of the European Union to underline the link between food quality and landscape. A form of GI is the Protected Designation of Origin (PDO) [251], [252] or Denominazione di Origine Protetta (DOP) in Italian [253].

Following landscape ecology principles, the landscape is a complex and adaptive system [254], incorporating both socio-economic and ecological functions [255], [256]. A definition that unmistakably is compatible with olive-growing landscapes [257], meant as social-ecological operators or social-ecological landscapes (SEL). Nevertheless, several driving forces, such as demographic dynamics, urban development and market-oriented behaviors of farmers, keep on modifying the landscape characters [59], even within the olive growing landscape. Indeed, the Mediterranean olive SELs have undergone several structural transformations (e.g. increasing density of trees per hectare) over centuries, from cultivations perfectly integrated with the environment to intensive monoculture [258], [259] which could bring to any environmental problems degrading the landscape too. However, there are areas where the persistence of traditional cultivations in olive-growing landscapes has contributed to the vitality of the local community and lifestyles, thereby preserving the quality of historic villages with a medieval character [249], [260].

However, several Authors have highlighted environmental sustainability of intensive and high intensive olive orchards in comparison with traditional ones, including a more water use efficiency, a higher soil organic carbon sequestration, a lower evaporation due to a higher ground cover and a reduction of runoff owing to an increase in root biomass and density [259]. Consequently, the ESs provided by olive growing landscapes have changed or are going to change fast. For these reasons, the primary goals of this study are to describe and comprehend how and where the olive grove landscape changed within the Cartoceto study area during a focal period of transformations for Mediterranean agriculture known as the post-second world war period. Aiming to reach these results we have scheduled to focus on structural/functional characteristics of each olive cultivation models rooted in the Cartoceto municipality, starting from the traditional typology known as "olive trees mixed with crops, at very low density of trees. This cultivation model is defined as a large system with 70-80 trees per hectare [261], [262] lined up in large spaced rows, where the remaining

surface are [263] usually cultivated with other crops (cereals, citrus, grapevine) or meadow-pasture for livestock [257]), particularly sheep (mixed cultivation). This typology was particularly widespread in the study area between the 19th century and the first half of the 20th century [264]. Although these cultivation practices are beneficial for biodiversity [259] the low yield makes them not profitable for harvesting production at competitive prices. To meet the growing global demand [57], [247], [259] farmers have turned to new types of farming practices [261], such as specialized "high intensity" planting patterns per hectare, (1750-2000 on average, with peaks as high as 2500)[261], that require increased mechanization and agrotechnical inputs. The diffusion of intensive grows is only at the beginning in Italy [54] while it is widespread in other Mediterranean areas, such as Spain [261], where this cultivation technique was born in the 90s. Between these two extremes, there is obviously a variety of cultivation types, with a gradual increase in tree density per hectare, including specialised olive orchards (200 to 250 trees per hectare), intensive olive orchards (350 to 700 trees per hectare), and super high-density olive orchards (400 to 2000 trees per hectare) [57], [58], [263], [265], [266].

As a result, studying and quantifying the transformations of olive groves over time becomes critical in order to plan a sustainable rural landscape while also ensuring the preservation of ecological properties [267]–[269]. It is important to remember in this context that the development of a dedicated geographic information system (GIS) allows for the integration of various data sources and methodologies without regard to spatial or temporal constraints [270]–[272]. For example, among geodata we can find many kinds of free remote sensing (RS) images, but they cover about forty years [273], [274] only. Therefore, to reconstruct the historical landscape evolution is needed to make an integration among different data and information, such as historical maps or historical aerial photos, by applying different preprocessing and elaboration techniques. The effects of landscape changes require an appropriate tool for effective management and interpretation of the dynamics of temporal transformation of the spatial pattern. A first method of delimiting the area at Landscape Scale (LS) refers to areas that have not particular shape or size, but whose boundaries are given by natural or man-assigned elements (such as woodland, sea or administrative boundaries) [275]. A second method is based on a geo-ecological territorial approach to demarcate areas with physical-geographical criteria but disregarding the value of landscape and cultural attributes, defined as Landscape Units (LU) [276].

For these reasons, we have developed a methodology that can be replicated using a GIS-based approach in order to identify the primary factors that have led to irreversible changes in the structure of the olive landscape. These changes have had a negative impact on both the outward appearance and the structure of the ecosystem. In these circumstances, the first stage in the process of designing future planning strategies for the conservation of olive areas is to conduct an assessment of the integrity state of olive regions within the landscape structure. Indeed, we want to show that even a simple and quick analysis using land use and land cover (LU/LC) areas intersection at different scale levels of reference allowed us to (i) identify permanent olive groves in the landscape, (ii) identify directions for the study of driving forces of landscape changes, and (iii) establish a landscape diversity metric, which allows for an assessment of the landscape's variety over time and may be useful.

The remainder of this paper is organized as follows: Paragraph 5.1.2 describes the case study, Paragraph 5.1.3 provides the reader with background information on the materials and describes the research method; Paragraph 5.1.4 presents the results and Paragraph 5.1.5 discusses the findings and concludes the paper.

5.1.2 Study area

Cartoceto (Province of Pesaro-Urbino) is in Central Italy, within a traditional olive oil GI area included in the Italian list since 2004 (GU n.291, 13/12/2004). Its traditional Mediterranean landscape was forged during the 16th and 17th centuries by the so called "sharecropping" agricultural system. This system is based on arable land mixed with trees (vine and olive trees) and polyculture, in small farms of a few hectares. Even if simplified, this landscape pattern has been preserved by extreme forms of olive monoculture, which have instead affected several Mediterranean regions in recent decades, including Spain and Portugal. Indeed, a quite high heterogeneity of the landscape pattern is still recognisable today. In other words, specialised olive orchards in this territory more than a widespread practice are coexisting with other land use dynamics (intensification of arable land, expansion of 'urban area, settlement of protected areas of the Natura 2000 network).

The geographical location of Cartoceto is 43° 46' 4" Nord, 12° 52' 54" Est. The population density within the municipality is several points higher than the Marche Region average; at 343,7 inhabitants per km2, it is nearly twice as high as the regional average of 160.1 [277]. The municipality area is 24 km2 and the official census population is 7974 inhabitants (year 2020).

The territory of Cartoceto falls into the Metauro river's hydrographic basin, which flows from Ovest to East to reach Adriatic Sea. Altitude ranges from 27m to 377 m above sea level (Figure 25).

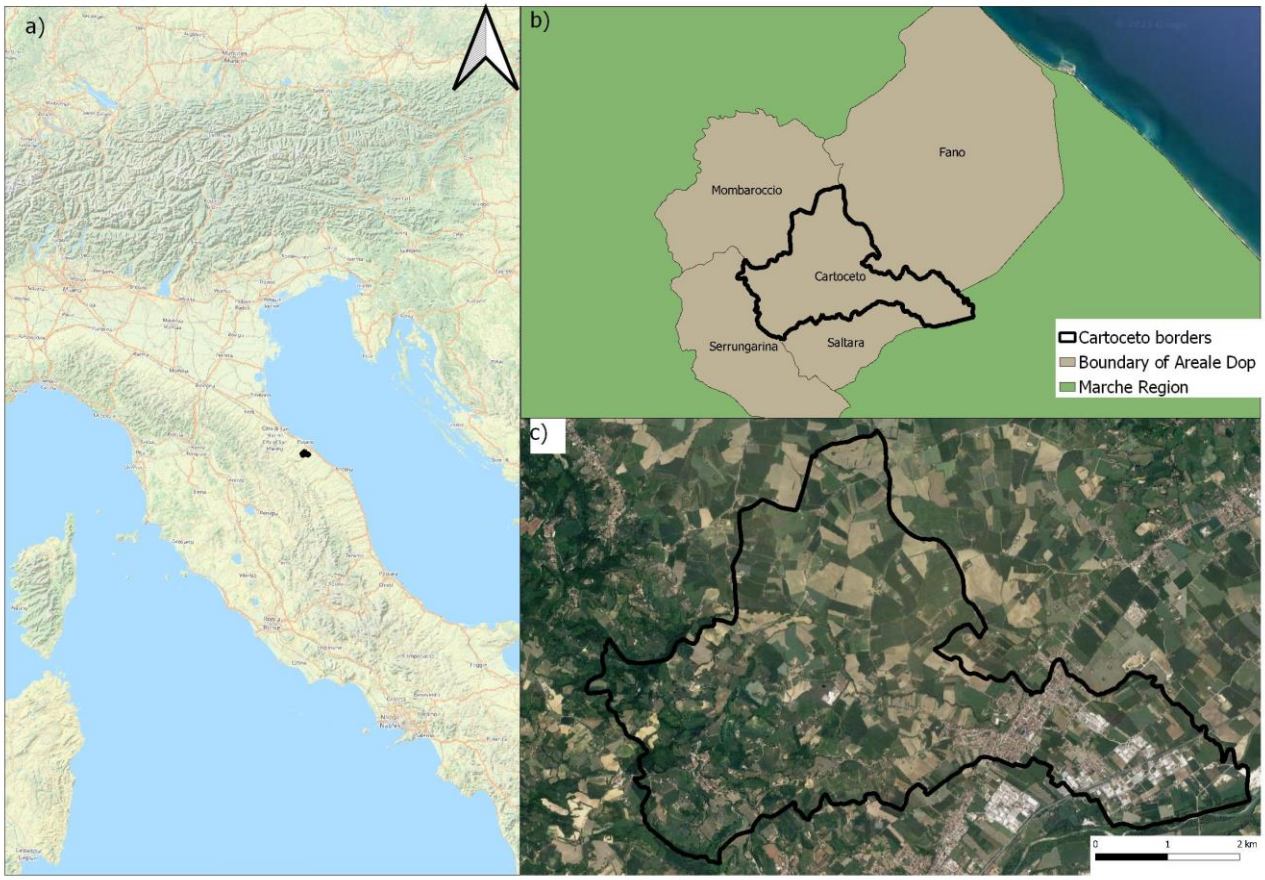

Fig. 25 a) Location of Cartoceto town in the Middle Italy; b) the vision of others neighboring municipalities (in black) inside the area of the Geographical Indication of Cartoceto DOP, c) boundary of Cartoceto

5.1.3 Methodology

Figure 26 depicts the workflow used in this work. which is made up of three sequential steps. The procedure begins with the gathering of data sources (historical maps, land use maps and aerial images), following by thematic mapping of the area was carried out by identifying several LU/LC typologies through photo-interpretation in accordance with the land use scheme specifically tailored for this study by the authors. The second and third steps are data analysis and results, respectively.

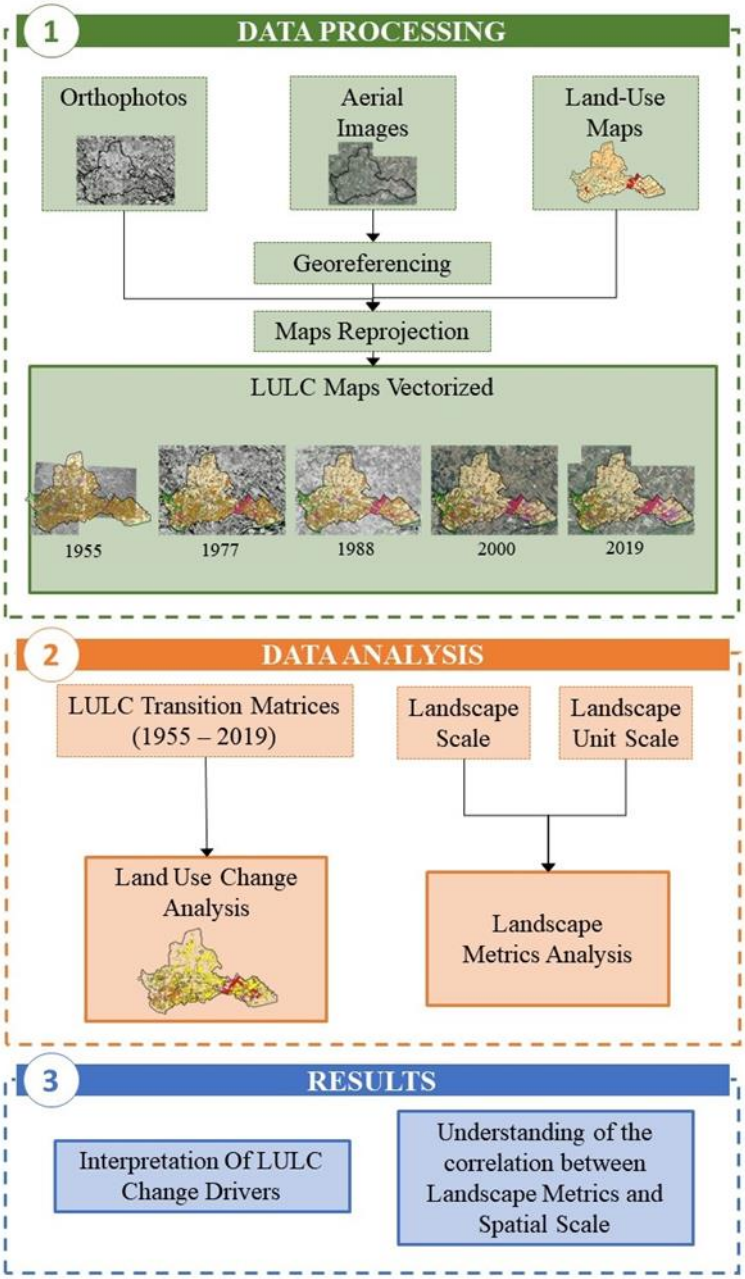

Fig. 26 Flowchart shows the processing steps for Cartoceto's LULC change analysis and landscape metrics.

The process, which consists of three consecutive phases, is shown in Figure 2. In order to create thematic mapping updated to each year under inquiry, the process starts with the acquisition of data sources (land use maps, aerial pictures, and orthophotos). The statistical examination of LU/LC changes made up the second step. The discussion of the findings to comprehend the motivating factors for rural landscape change and landscape metrics at various geographical scales was the third and final part.

Data set

The aerial photographs representing Italy in the year 1955 at the nominal scale of 1:33’000 (programme GAI 55), have been collected from the Italian Military Geographical Institute (IGMI). These are black-and-white aerial photographs were recorded in September 1955 at a flight altitude of approximately 5,000 m using a Fairchild camera (focal length 152 mm). The original printed aerial photos were converted to raster and distributed to customers in digital format (TIFF format) with a resolution of 2400 dpi by the IGM. The whole coverage of the study area consists of three partially overlapped aerial photos have been collected. Likewise, the datasets of aerial photographs for the

years 1977 and 1988 have been downloaded in from the regional cartographic service[278] by web map service (WMS). Thes are georeferenced greyscale digital orthophotos (Monte Mario Projection System / Italy zone 2 - EPSG:3004) acquired with flight altitude of the approximately 5700 m, with a focal length of 153 mm and a resulting in a medium scale of 1:37'000. The flight altitude of the 1988 series was 11'500 m, with a focal length of 153.34 mm and an approximate medium scale of 1:74'000. For the year 2000 a set of colour orthophotos in WMS format (EPSG: 32633-WGS 84/UTM zone 33N) has been acquired from the National Geoportal by the Ministry of Environment [279] with an average size of pixel like .0 meter. The last geospatial dataset available for the study area concerns the year 20 it is composed by a set of nine digital orthophotos from the photogrammetric survey performed from April to September 2019) by the Italian Agricultural Payments Agency (AGEA)[280]. Each orthophoto is composed of four bands, the RGB bands and the NIR band, with an average pixel value of 0.2 m and medium scale of 1:5000. In to assess the integrity of the rural landscape with a dynamic perspective, we also acquired land use maps (LUM) in vector format. The available LUMs refer to two distinct years first LUM was mapped in 1984 by the Marche Region. The LUM is composed by 42 classes, divided into a hierarchical land use classification. First level includes built-up, arable land, woody/agricultural and specialised crops, arboriculture, forest/meadow-grazing and unclassifiable areas. Second and Third level comprise disaggregation of each items at first levels. The second retrieved LUM was made in 2011 and is provided by AGEA by identifying 37 at three level of landscape classification. For the purpose of our research, it is also worth using Landscape Units (LU). In landscape ecology the LU is a homogeneous sub-land with similar characteristics and functions within a larger landscape [281], showing specific characters and functions concerning the entire landscape [282]. LU/LC mapping is very important in metrics analysis because it allows us to better understand the distribution and arrangement of various LC types in a landscape and their impact on ecological processes and biodiversity[283]. This information is critical before calculating landscape metrics to evaluate the impact of land use changes, fragmentation, and other disturbances [282]. To identify the LUs concerning the study case, we referred to a coverage previously realised by the regional agency for Food and agriculture of Marche region (ASSAM) [284] in collaboration with the Joint Research Centre – Institute of the European Commission, in 2007 [285]. The main features of data sources are reported in Table 5. While in Table 6 are described the main features of LUs and in Figure 27 the spatial distribution of the four LUs covering the Cartoceto town.

Table 5 Main features of the datasets used for this work. These are listed in order of publication year.

N.	Title	Year	Source	Detail
1	Aerial photos	1955	Italian military geographical institute (IGMI)	Hard copy scanned at 2500 dpi Scale 1:33,000 Altitude: 5000 m Average image resolution: 0,50 m
2	Aerial photos	1977-1988	Cartographic Office of Marche Region	B/W band, digital GeoTIFF scale 1:10,000 Image resolution:1,50 m
3	Land use map	1984	Cartographic Office of Marche Region	vector data, 42 land cover classes; Three hierarchical levels of landscape classification; Minimum Mapping Unit 0,04 ha
4	Aerial photos	2000	National Geoportal	RGB digital, GeoTIFF scale 1:10,000 Image resolution:1,50 m
5	Land use map	2011	A.G.E.A.	37 land cover classes; Third hierarchical level of landscape classification; Minimum Mapping Unit 0,16 ha i
6	Aerial photos	2019	A.G.E.A.	RGB + NIR digital GeoTIFF scale 1:5,000 Image resolution:0,20 m
7	Soils and Pedo-Landscapes Map	2006	Agri Food Agency of-Marche Region (ASSAM)	Minimum mapping unit of 0,5 haScale 1:250000, three hierarchical levels of Landscape Units (Region, Province, Systems)

Table 6 Landscape Units characteristics from Soil Observatory of Marche Region

Main cover classes	LU Code	Soil Taxonomy Classification
Forests and agricultural activity	5.1.4	Calcaric Cambisols Calcaric Regosols Calcari-Endoleptic Cambisols Endosodi-Vertic Calcisols
Arable land	5.1.5	Calcari-Hyposodic Cambisols Calcaric Cambisols (Endogleyic Endosodi-Vertic Calcisols
Arable land	5.2.1	Calcari-Hyposodic Cambisols Calcaric Cambisols (Endogleyic Eutri-Fluvic Cambisols
Residential and Industrial areas	5.2.2	Hypocalcic Calcisols Cutani-Vertic Luvisols Chromic Luvisols

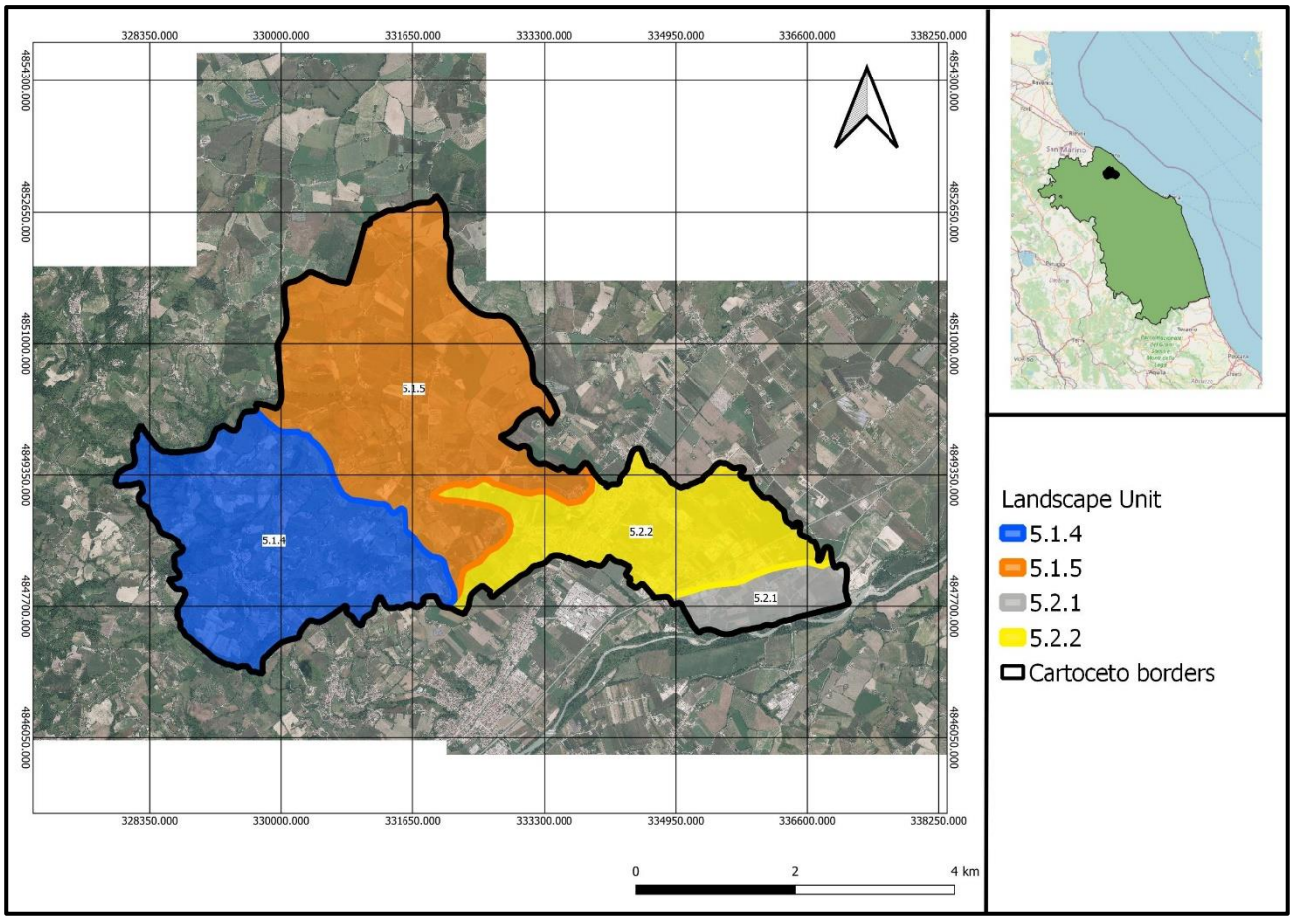

Fig. 27 Landscape unit (LU) in the study area

Land cover processing

To align the multimodal geospatial datasets, both raster and vector, we decided to perform the map reprojection to a planimetric coordinate system unique for all dataset (EPSG: 32633 UTM/WGS84 33N). The only data that needed to be projected to the ground were the aerial photos by IGMI. The latter were georeferenced by taking advantage of orthorectified aerial images generated by AGEA. In this case, a geo-referencing of the entire image was first performed by identifying a series of GCPs at the edges of the image. Once the image was positioned with respect to

the ground points, it was cropped into four parts for each aerial shot. This initiated a refinement of the GCPs toward the center of the image by assigning the various ground control points (GCPs) at rural or religious buildings, or at the intersections of the road and agricultural fields. The transformation was done by using a second-order polynomial, so as to have an average RMS value between 10 - 20 m, employing a sufficient number of ground control points varying between 11-20. In Figure 28 is showed how we have detected the GPC on aerial image among IGMI and AGEA.

Fig. 28 Example of ground control points (GCPs), red targets in the pictures, pairwise. AGEA's false colour orthophoto, year 2019 (left), and b/w IGMI's photographs, year 1955 (right).

LU/LC classification and mapping

To facilitate the interpretation of results, we defined our land scheme of classification by homogenizing different Land Cover (LC) typologies taking the Corine Land Cover project classification as a baseline. We set up the land use classification on three levels, assuming that the identified environmental units (named Landscape Unit) have ecological systems within their boundaries [286]. At the first hierarchical level we find five classes: 1. Artificial surfaces, 2. Permanent crops, 3. Agricultural Areas, 4. Forests and seminatural areas; 5. Water bodies. The second level was defined accordingly with the legend of the thematic maps (LUM) acquired from Marche Region and AGEA. These two hierarchical levels (Table 7) to describe the main land use transformations and land consumption within the study area. Because the focus of our study concerns the different typologies of olive orchards, a specific level for this category has been structured in defining the LUM to adopt in the study. Therefore, a third level for this specific LC has been designed (Table 8). Indeed, each typology of olive orchard included in this level shows unique details, such as the number of trees per hectare and the planting system of trees (Fig. 29). It should be noted that in the panorama of the most widespread international classification schemes, this classification model of different types of olive orchards represents an important semantic innovation that is not easily found in similar studies dedicated to olive growing [287], [288]. The overall number of LCs identified for this work, taking into account the Second Level by Table 7 and the Third Level by Table 8 is 21.

Table 7 Classification scheme of Land Cover (LC): First and Second Level

1° Level	2° Level
1. Artificial surfaces	1.1 Urban fabric
	1.2 Industrial or commercial units
	1.3 Roads and rail networks
	1.4 Mine site
	1.5 Photovoltaic plant
2. Permanent crops	2.1 Vineyard
	2.2 Olive Groves
	2.3 Fruit orchard
3. Agricultural areas land	3.1 Arable land
	3.2 Grasslands
4. Forest and seminatural areas	4.1 Woodland

	4.2 Uncultivated area, transitional woodland-shrub
	4.3 Riparian vegetation
5. Waters bodies	5.1 Rivers
	5.2 Lakes and ponds

Table 8 Classification scheme for Permanent crops: Third level

2° Level	3° Level
2.1 Vineyard	2.1.1 Specialised Vineyard
	2.1.2 Vineyard mixed with trees
2.2 Olive Groves	2.2.1 Isolated olive trees mixed with crops
	2.2.2 Olive rows mixed with crops
	2.2.3 Specialised olive orchards
	2.2.4 Intensive olive orchards
	2.2.5 High-intensity olive orchards
	2.2.6 Garden olive trees

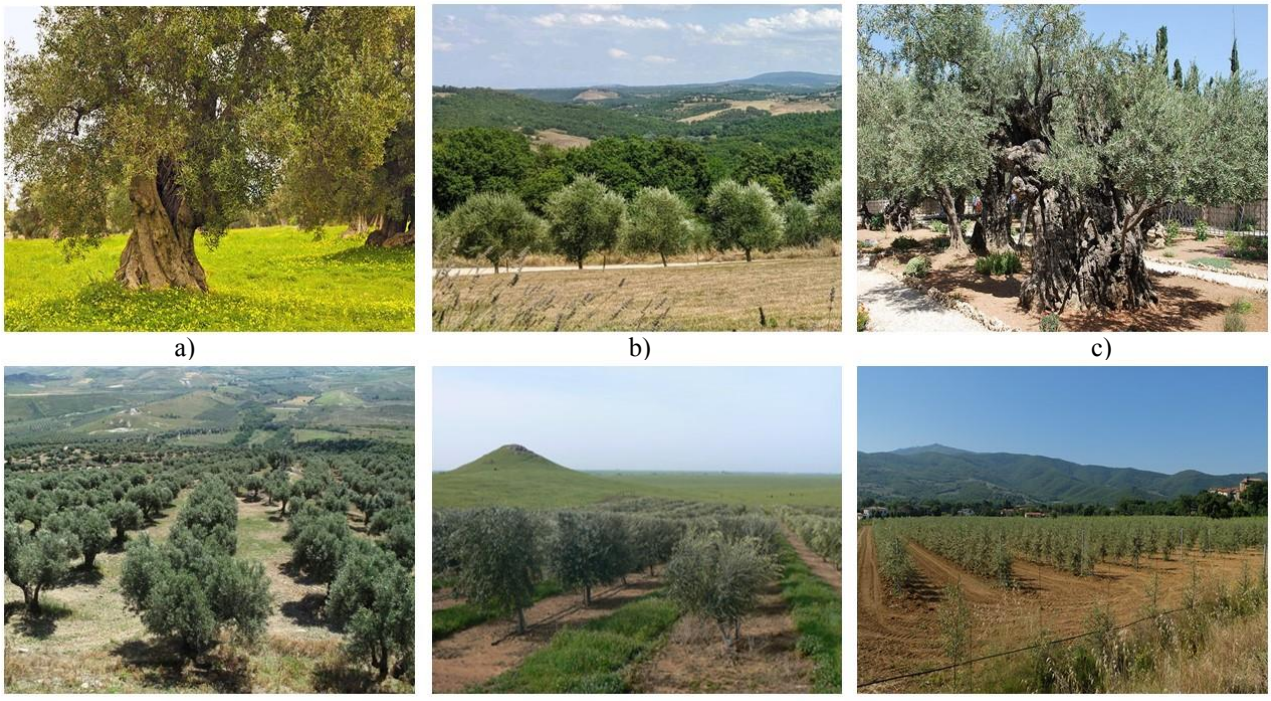

Fig. 29 Example of different olive orchard: a) isolated olive trees mixed with crops, b) Olive trees raws mixed with crops; c) Garden Olive trees; d) Specialised Olive orchards; f) Intensive Olive orchards; g) High-density Olive orchards,

After the legend definition, mapping the LULC for the multitemporal set of aerial photographs was executed by applying the classic method of photo interpretation [80]. A multi-temporal layer in the GIS software was created by checking the information provided by 1984 LUM with the 1955, 1977 and 1988 aerial photographs. While the 2011 LUM was used as the vector basis to support the interpretation of the 2000 and 2019 aerial orthophotos. Therefore, we cross-checked the digitised polygon in the LUMs with the aerial image making changes different land uses appeared, otherwise left unchanged. This LUM generation approach is laborious and time-consuming, but it allows for accurate and up-to-date representation of land use patterns [289]. The LUMs for the years 1955, 1977, 1988, 2000 and 2019 are shown in Figure 30.

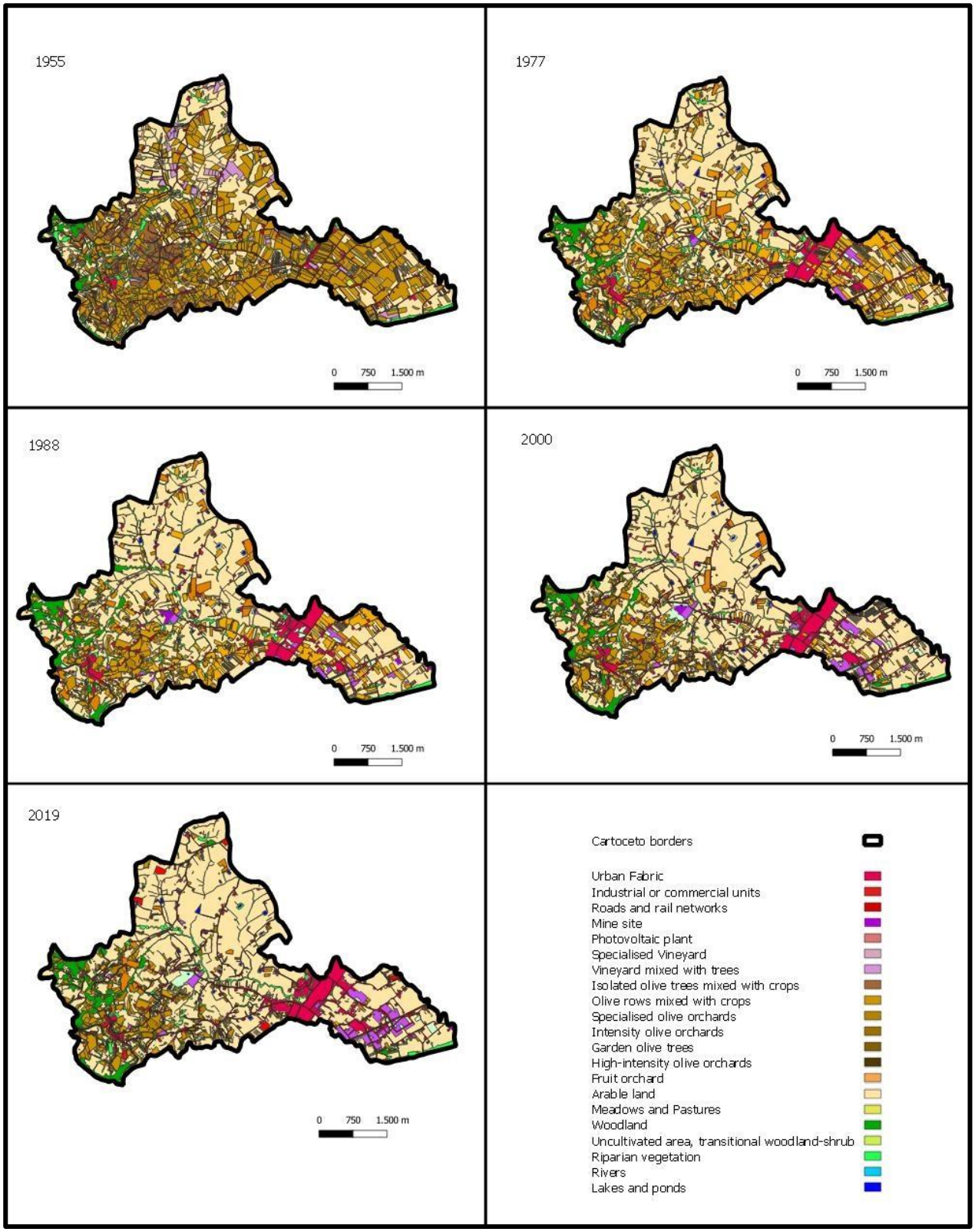

Fig. 30 LUMs for years of analysis

Estimating LU/LC changes and landscape metrics

A spatial comparison of the years 1955 and 2019 LULC vector maps was performed using a post-classification change detection matrix [290]. It is a type of change detection obtained through a cross-tabulation analysis (transition matrix), which allows to highlight the changes that occurred in time both qualitatively (by showing them directly on

the map) and quantitatively (by calculating the total area of land use change that occurred at different times) [291]. Relative and absolute changes for each of the 21 LULC types were calculated from a 21x21 square matrix.. The transition matrices are constructed for the time interval t1 to t2, with rows displaying land classes from time 1 (usually the most recently mapped) and columns displaying land classes from time 2 (the year closest to the current). While row vectors show the evolution of a land use type in the period t1–t2, column vectors show the land use type at time t1, from which another land use type was generated at time t2. The main diagonal line refers to the surface of land-cover types remaining unchanged during the considered time window [292].

As regards the computation of every class variations both net change and annual change rate were processed for each successive pair of year [290]. The net change for each class is calculated by subtracting the total class coverage, expressed as a percentage, from the next and previous year's acreage over the entire period under consideration.

The annual change rate for each LC typology shows how quickly land uses transition to others within the landscape over each time interval considered. According to some Authors [293], [294] we adopted the following formula [295]:

$$r[{}^{0}/_{0}] = \frac{1}{t_2 - t_1} \cdot ln\left(\frac{A_{t_2}}{A_{t_1}}\right) \cdot 100 \quad (1)$$

where At2 and At1 are the surfaces of the same land class at the end and the beginning, respectively, of the time period being evaluated; while t2 and t1 are the end year and the beginning year of the time period, respectively [296].

Finally, the analysis of changes of landscape structure has been performed through the application of spatial metrics. These are used to understand and describe the expansion or the shrinkage of land use classes, for highlighting composition and level of complexity of a landscape. Landscape metrics are computed by referring to the well-known landscape model which is defined as matrix, patches and corridors [297]. Patches in a LULC map are polygons in vectorial format, by definition indicated as a relatively homogeneous area that differs from its surroundings [298], [299].

Landscape metrics provide synthetic, quantitative and aggregate spatial indicators particularly influenced by the LU/LC map scale and resolution [300], [301] and represent one of the key factors in landscape research [302] and landscape planning [303]. The spatial indices used in this work were chosen after a review of [304]–[307] of significant studies extracted from literature and focusing on landscape complexity over different time periods. Aiming to generate a simple and unambiguous set of metrics, a limited number of spatial indices were selected, both at class and landscape level (Table 9) from and for each LULC map of the timeseries number of patches (NP), mean patch size (MPS), edge density (ED) [308] and Shannon diversity index (SHID) [309]. The sum of area and perimeter for each classes, were extracted using the "Statistics Categories" tool of Qgis software [310].

Table 9 Landscape metrics employed in this study

Index	Unit	Equation	Detailed
Number of classes	Number	Data	Total number of classes at landscape or land unit scale
Number of Patches	Number	data	Total number of patches at landscape or land unit scale
Mean Patch Size	ha	$MPS = \sum_{i}^{n} \frac{\sum_{i=1}^{n} a_i}{n} = \frac{A}{n}$	A class level as function of number of patches and the considered landscape area
Edge Density	m/ha	$ED = \sum_{1x=1} \frac{e_{ik}}{A} * 10000$	Sum of all perimeter lengths of class patches divided by the considered landscape area
Shannon's Diversity Index	Number	$SHDI = -\sum_{i=1}^{m} (P_i \cdot ln\, P_1)$	The SHDI is a formula for entropy. The value takes both the number of classes and the abundance of each class into account within the considered landscape

5.1.4 Results

The use of a GIS for a multitemporal analysis of different data has allowed for the harmonisation of all information, making them comparable to each other, and has enabled accurate mapping of olive orchard classes for the year 1955, 1977, 1988, 2000 and 2019. The overlaying LUMs referred to for each year investigated, allow different land use patterns at Landscape Scale (LS) and Landscape Unit scale (LUS).

The Dynamics of Landscape Change

The land use changes and transformation dynamics were analysed over time by GIS approach overlaying the Land Use Maps (LUMs) of year 1955 trand 2019. This allowed to light up all changes in each land use class within the investigated landscape. Through the use of the Sankey diagram [311], the flows of transition among all LC classes over the years investigated is represented in Figure 31. The diagram allows for a more straightforward visual assessment of the transformations and provides an instant view of the magnitude of the change. It is worth noting that thicker lines represent a greater amount of hectares transform. Otherwise, the thickness of the line is smaller.

A second diagram is specifically dedicated to provide a more precise understanding of the transformation dynamics that have influenced the mixed olive-growing typologies, namely 2.2.1 and 2.2.2 LC classes, as shown in Figure 32.

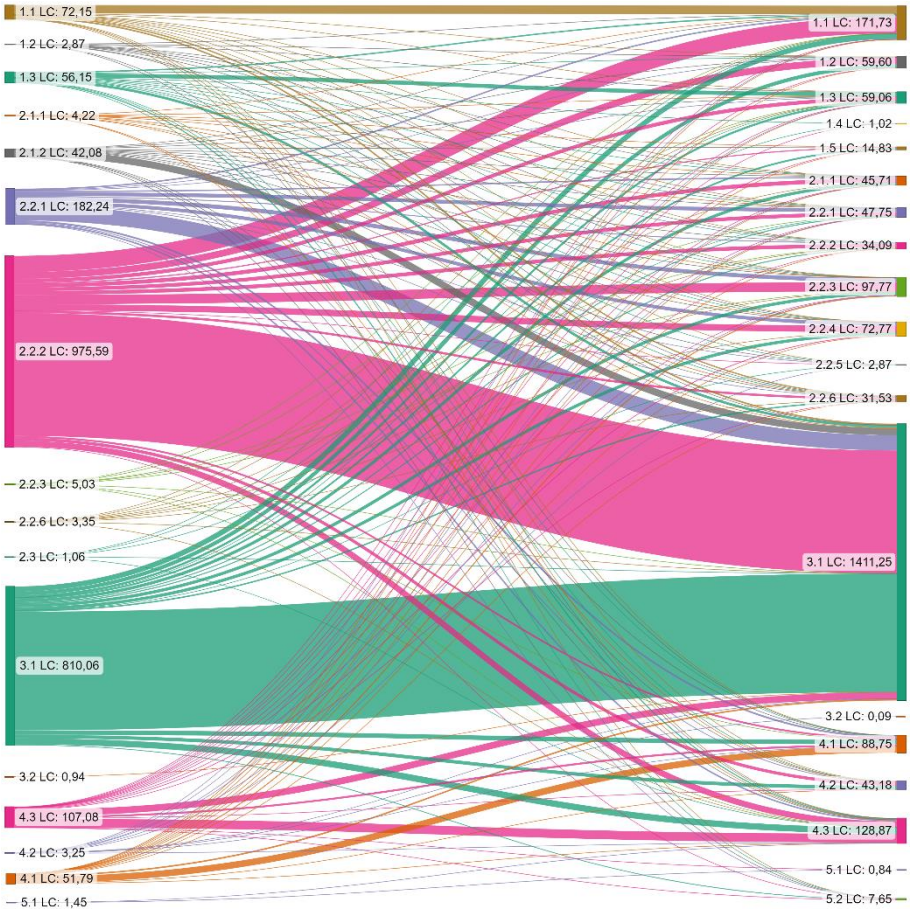

Fig. 31 Flown of transition among LC classes within Cartoceto landscape for the period 1955 – 2019

This dynamics are synthetically described in Table 10. Instead, the Figure 32 maps those transformations highlighting the new land use classes derived from previous mixed olive-growing areas. Upon a simple visual analysis, it is evident that there has been substantial substitution toward areas devoted to arable land (yellow) or increasing urbanization (red). Fragmentation of mixed olive-growing areas into smaller parcels have generated intensification toward new orchards of high-yielding olive trees (orange). Small portions of abandoned areas can be seen close to forested areas (green). Finally , permanent mixed olive-growing areas, named persistent (gray) show the extent and localization of olive-growing unchanged since the 1950s.

Table 10 Persistence of traditional olive cultivations and the four main patterns of change.

Dynamics	Description	
1	Persistence	No changes
2	Intensification	Transition from traditional to intensive growing.
3	Substitution	Substitution with alternative crops, mostly arable land
4	Abandonment	Abandoned and renaturation
5	Urbanization	Soil sealing and urbanisation

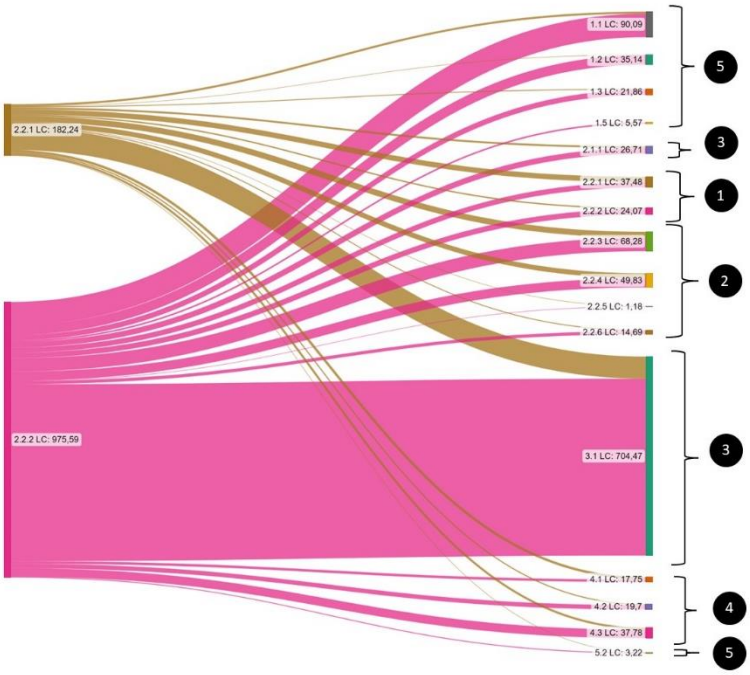

Fig. 32 Dynamics of change in traditional olive cultivation, 1955 – 2019 . Numbered dots pin out the persistency and the four main patterns of change

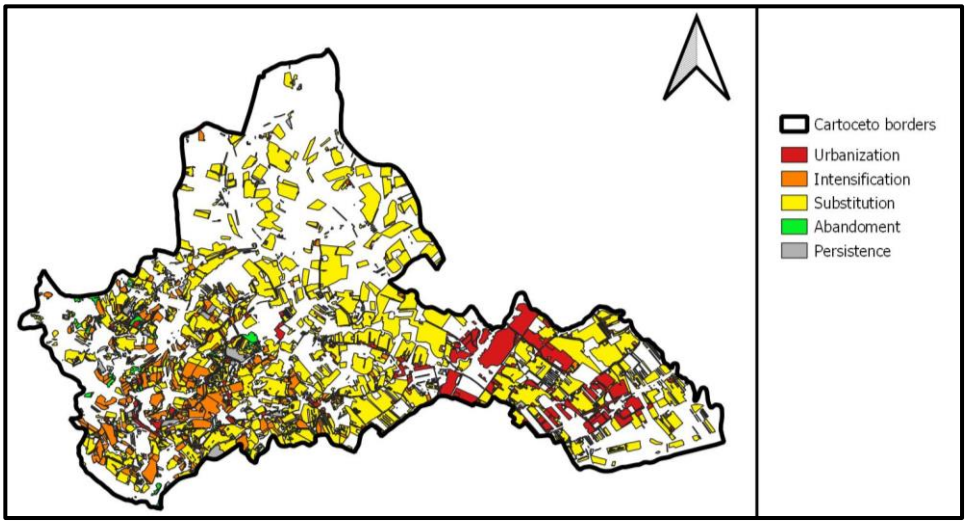

Fig. 33 Map of the dynamic occurring from the 1955 to 2019. It pointed out the persistence of olive mixed orchards

In 1955, the majority of land uses in the study area were dedicated to mixed olive groves with scattered trees (2.2.1 LC) and mixed olive groves with rows of trees (2.2.2 LC), followed by arable land (3.1 LC). The former classes spread over 182.24 ha and 975.59 ha respectively, while the latter was 810.07 ha. As Fig. 31 shows, much of the mixed olive classes were converted to various land uses, generating a completely different landscape in 2019, both

ecologically and visually. However, small portion of traditional mixed olive groves remained unchanged for 64 years. Specifically, these include surfaces of 18.87 ha (2.2.1 LC) and 19.22 ha of 2.2.2 LC demonstrating the significant resilience of this traditional olive-growing method in the study area despite the overall decrease of olive groves.

On the other hand, the most significant transformation affecting the traditional olive groves was the intensification to arable land. This resulted in the conversion of land from the 2.2.1 LU class to arable land (3.1 LC) by subtracting 78.21 ha and, more significantly, the amount of 626.26 ha to 2.2.2. LC classes, as clearly shown in Fig. 32. In terms of evolution within of traditional olive groves, the conversion of 2.2.1 LC class into more intensive olive groves resulted in a transition of 20.80 ha to the specialized olive orchards (2.2.3 LC) , 17.65 ha to the Intensive olive orchards (2.2.4 LU) class, and only 0.03 ha to the High-intensity olive orchards (2.2.5 LC). Additionally, 3.32 ha of the same class were converted to Garden olive trees (2.2.6 LC).

Similar trends were observed in the evolution of 2.2.2 LC, which witnessed the process of olive grove intensification with higher intensity. As shown in Fig. 24, the transformation resulted in 47.47 ha of 2.2.3 LC, 32.18 ha of 2.2.4 LC, and 1.15 ha of 2.2.5 LC. Furthermore, 11.37 ha were converted to Garden olive trees (2.2.6 LC).

Finally, the trend of urban expansion has also affected traditional olive cultivation areas in different ways. New residential settlements (1.1 LC) have occupied 82.75 ha of Olive rows mixed with crops (2.2.2 LC) area. In addition, industrial/commercial settlements (1.2 LC) and transportation infrastructure (1.3 LC) respectively eroded 34.17 ha and 18.76 ha from 2.2.2 LC. Furthermore, in 2019 a new type of urban class for renewable energy production emerged (1.5 LC), occupying an area of 5.57 ha. In contrast, the originally surface of isolated olive trees mixed with crops (2.2.1 LC) have been marginally affected by urbanization. For example, only 7.35 ha have been converted to new residential settlements (1.1 LC).

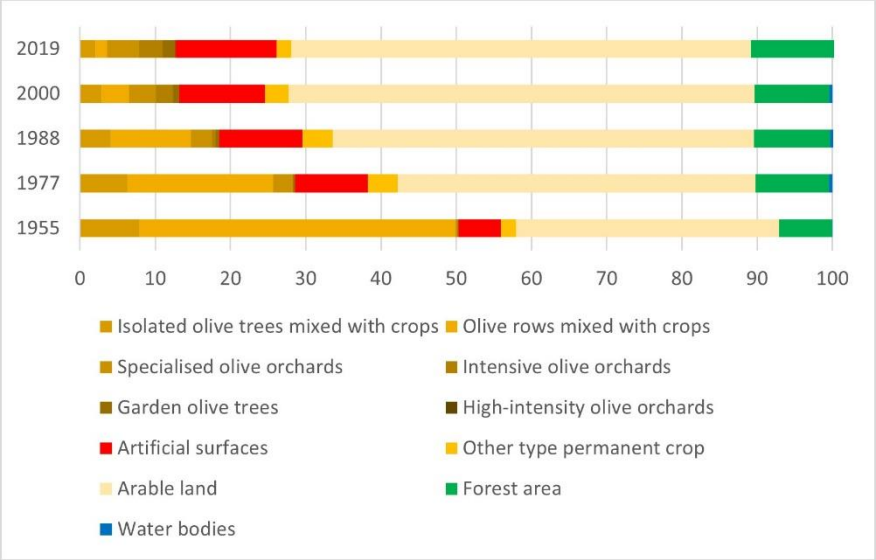

Fig. 34 Percentage of land use classes for 5 time intervals LS

In order to expand the analysis of land use transformations to other land cover and document the trend of such transformations, the percentages of land use for each of the five years considered (1955, 1977, 1988, 2000, 2019) is reported in Figures 34 and 35. This operation was carried out for Landscape Scale (LS) and Landscape Unit Scale (LUS), as they were identified as the two spatial scales of reference for landscape analysis.

Figure 34 shows a constant trend of reduction for isolated olive trees mixed with crops (2.2.1 LC), which covered an area of 8.16% (188.97 ha) in 1955, decreased to 6.27% (145.27 ha) in 1977, and further decreased to 4.03% (93.36 ha) in 1988, 2.88% (66.91 ha) in 2000, and finally 2.04% (47.80 ha) in 2019. A significantly more consistent decline characterizes the olive rows mixed with crops (2.2.2 LC) class, which covered about 40% (935.054 Ha) of the municipal territory in 1955, then halved to an extension of 19.39% (449.27 ha) in 1977, and covered only 10.71% (248.16 ha) in 1988. The negative trend continued, reaching 3.58% (82.83 ha) in 2000 and almost disappearing in 2019 with an area of only 1.5% (35.41 ha).

On the other hand, cereal crops (3.1 LC) marked a progressive increase. The arable land area was 32% (762.16 ha) in 1955, then expanded to 47.56% (1,101.81 ha) in 1977, 55.96% (1,296.73 ha) in 1988, 61.93% (1,434.76 ha) in 2000, finally was 61.10% (1,415.08 ha) in 2019.

To better understand the evolution of the olive growing sector in this territory, it is necessary to take into account the evolution of olive groves inspired by more "modern" cultivation criteria. In 1955, the Specialised olive orchards (2.2.3 LC) showed a completely negligible extension, equal to 0.21% (5.03 ha) then progressively increased over the considered period to reach a current overall area of 4.21% (97.56 ha). The Intensive olive orchards (2.2.4 LC) also spread slowly, starting from 1988 when recorded an area of 0.43%. In 2019, it reached a significant extension of 3.14% (72.83 ha). On the contrary, the most modern and intensive olive cultivation model, High-intensity olive orchards (2.2.5 LC), struggles to establish itself in the study area, appearing only from 2000 and reaching a total area of less than 1% (1.57 ha) in 2019.

The trend observed for garden olive trees (2.2.6 LC) is particularly noteworthy. This type of small-scale olive farming for personal consumption has steadily expanded over the years, growing from 0.14% (3.35 ha) in 1955 to 1.71% (39.59 ha) in 2019, mainly due to the urban area's growth. Notably, the residential area (1.1 LC) has significantly increased in surface area, rising from 3.15% (73.06 ha) in 1955 to 7.44% (172.48 ha) in 2019. Furthermore, the industrial/commercial areas (1.2 LC) have expanded significantly since the ‘80s, reaching a total surface area of 2.57% (59.60 ha) in 2019.

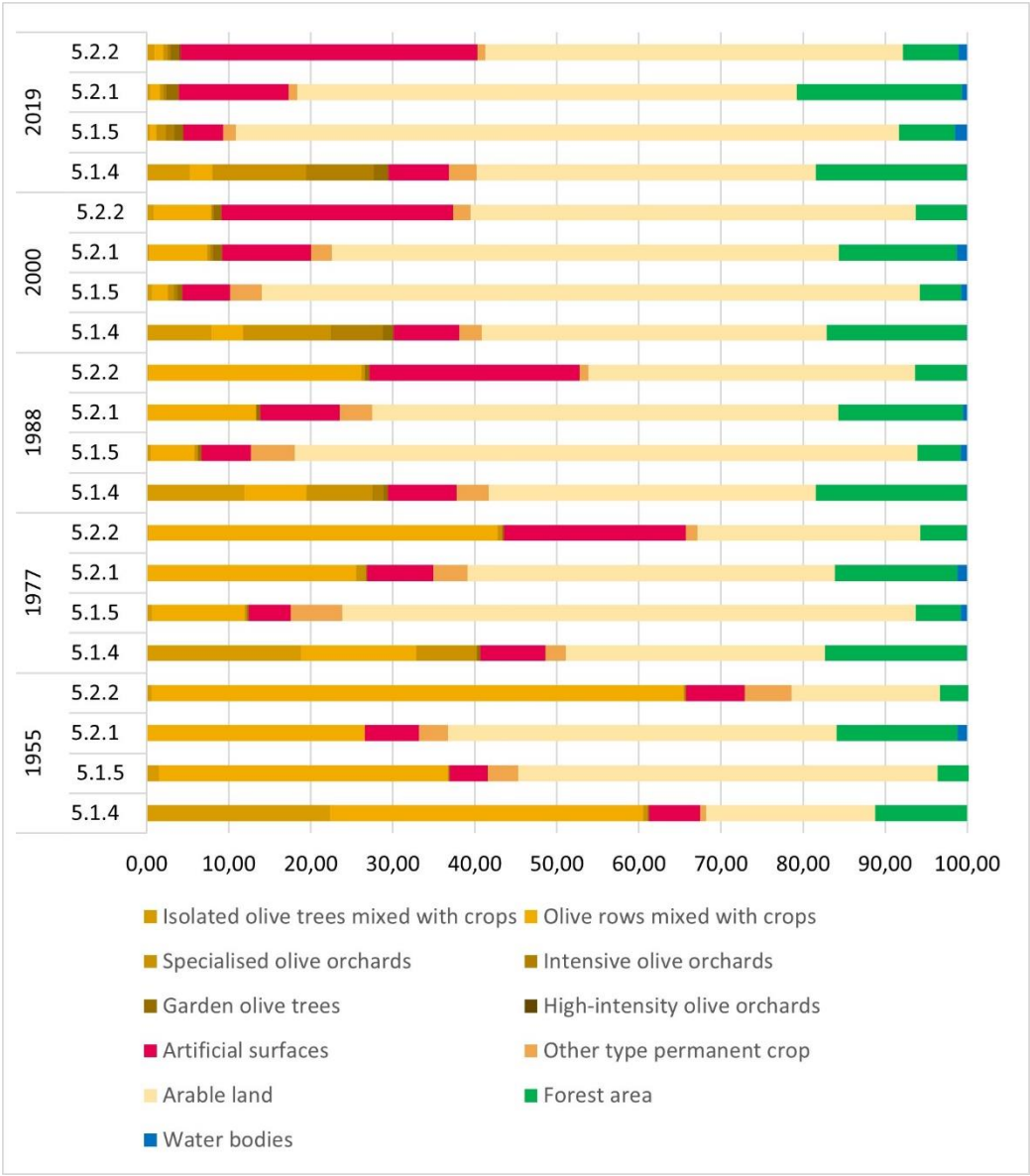

Fig. 35 Percentage of 5.1.4,5.1.5,5.2.1,5.2.2 land use classes for 5 time intervals

The previous description pertains to the land use changes at the Landscape Scale (LS). In contrast, the evolving dynamics at the different Landscape Unit Scale (LUS) appear quite different, as shown in Figure 35. Focusing on the various olive-growing typologies, which represent the central element characterizing the landscape in the considered territory, it can be noted that the olive rows mixed with crops (2.2.2 LC) was present in a heterogeneous but always very significant way in every investigated LUS. Starting from 1955, it covered an area equal to 37.41% (274.77 ha) in the 5.1.4 LUS area around the historic settlement of Cartoceto. In the 5.1.5 LUS it covered 32.34% (316.58 ha), on the less steep eastern hillside of Cartoceto. Finally, it was distributed in the 5.2.1 LUS, covering an area equal to 26.86% (33.01 ha), finally within the 5.2.2 LUS with a surface of to 64.83% (310.67 ha). The latter represents sub-flat areas connecting the alluvial deposits of the Metauro river. This flat morphology was particularly favorable for the expansion of urbanised areas and the intensification of crops cultivation. From 1955 to 2019, the trend of reduction of this type of mixed olive cover provided very high change. A small amount of mixed olive growing with rows persists within the 5.1.4 LUS with an extension equal to 2.72% (28.21 ha), while it almost disappears in adjacent areas. Only 0.77% (7.56 ha) remain in the 5.2.1 LUS (1.4 ha), finally in the 5.2.2 LUS equal to 5.15 ha.

On the other hand the evolution of isolated olive trees mixed with crops (2.2.1 LC) significantly differs by depending on the Landscape Unit Scales (LUS) characteristics. Starting from the 5.1.4 LUS, this traditional olive cultivation type currently maintains a significant coverage share, equal to 5.26% (38.66 ha) of the landscape unit surface, contributing significantly to its traditional character. On the other hand, for the other LUS, values below 1% were recorded in 2019.

The main transformation land use class with a positive trend is represented by the cropland area (3.1 LC). This has increased from 18.26% (134.29 ha) in the 5.1.4 LUS in 1955 to 41.37% (299.93 ha) in 2019, and from 49.27% (483.19 ha) in 1955 to 80.82% (791.07 ha) in 2019 within the 5.1.5 LUS. Furthermore from 47.36% (58.18 ha) in 1955 to 60.91% (75.67 ha) in 2019 in the 5.2.1 LUS, finally from 18.07% (86.43 ha) in 1955 to 50.91% (243.72 ha) in 2019 in the 5.2.2 LUS.

Previous analysis allowed to focus more in deep yearly net change (%) and annual rate of changes (%) for each typology of olive cultivation. Figure 36 shows the temporal evolution of olive classes by referring to LS, while Figure 37,38,39 and 40 respectively refer to LUS. The values of indices were determined by analyzing pairs of subsequent years in order to highlight rates of increase/decrease both in terms of absolute intensity (surface variations) and the speed at which such variations occurred. It is useful to consider that there is not the same number of years between one period and the other. Therefore, all indices must be read carefully.

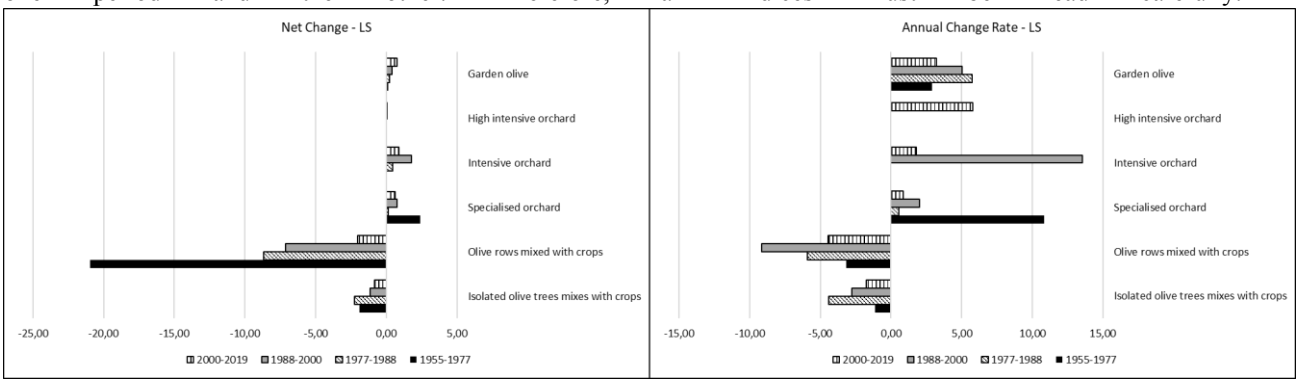

Fig. 36 Net Change (left) and right the Annual Change Rate (right) at LS

Observing the percentages in Figure 36, the isolated olive trees mixed with crops (2.2.1 LC) have had the worst decline rate in the period 1977-1988 with a Net Change of -2.24% and Annual Change Rate of -4.42%, although the value of this decline is insensitive to transformation since 2.2.1 LC has a small land-occupancy rate compared to the spatial scale considered. Instead, the olive rows mixed with crops (2.2.2 C experienced the worst contraction during the pair of years 1955-1977 with a Net Change of -20.96% but with a rather slow decline rate of -3.18% of Annual Change rate, which however increases in the two subsequent periods especially between 1988 and 2000. The specialised olive orchards (2.2.3 LUC marked a high rate of intensification in the period 1955-1977 with an Annual Change Rate of 10.85% and Net Change of +2.41%. In addition, the growth intensity for the most intensive olive grows is rather limited, with Net Change values below 1% and Annual Change Rate below 2%. The only exception is marked by intensive olive orchards (2.2.4 LC) in the period 1988-2000 which results to have a high growth rate of

+13,54%. In contrast to the Garden Olive (2.2.6 LC) Net change is constantly increasing, although with low values, and Annual Change Rates are more intense between 1977 and 2000.

Analysing the Figures 37,38,39,40 it is worth noting that the olive rows mixed with crops (2.2.2 LC) shows a negative Net Change in the period 1955-1977 (-23,40%) within the 5.1.4 LUS, -21,40% within the 5.1.5 LUS and -22,24% within the 5.2.2 LUS, while within the 5.2.1 LUS it records a minor contraction (-1,09%). 2.2.2 LC shows a negative fairly significant speeds of Annual Change Rate up to 2000 both in LUS 5.1.4 and in LUS 5.1.5.. Net Change and the Annual Change Ratio of the isolated olive trees mixed with crops class (2.2.1 LC) show a negative trend for the entire period within the 5.1.4 LUS, where they are more intense, and the 5.1.5 LUS where they appear less intense. On the contrary, positive variations in both the Net Change and the Annual Change Rate were recorded for the specialised olive orchards (2.2.3 LC) and intensive olive Orchards (2.2.4 LC), significantly within the 5.1.4 LUS during the period 1955-1977 and 1988-2000.

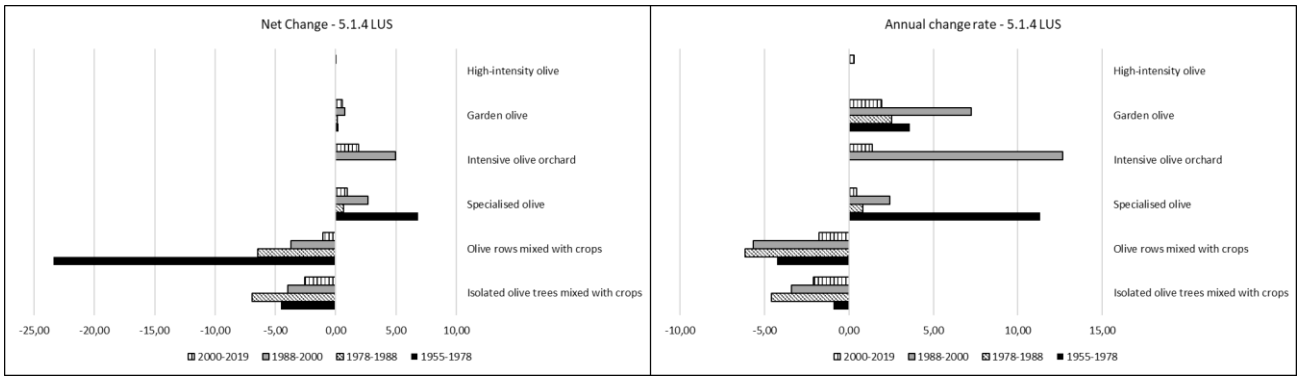

Fig. 37 Net Change (left) and Annual Change Rate (right) at 5.1.4 LUS

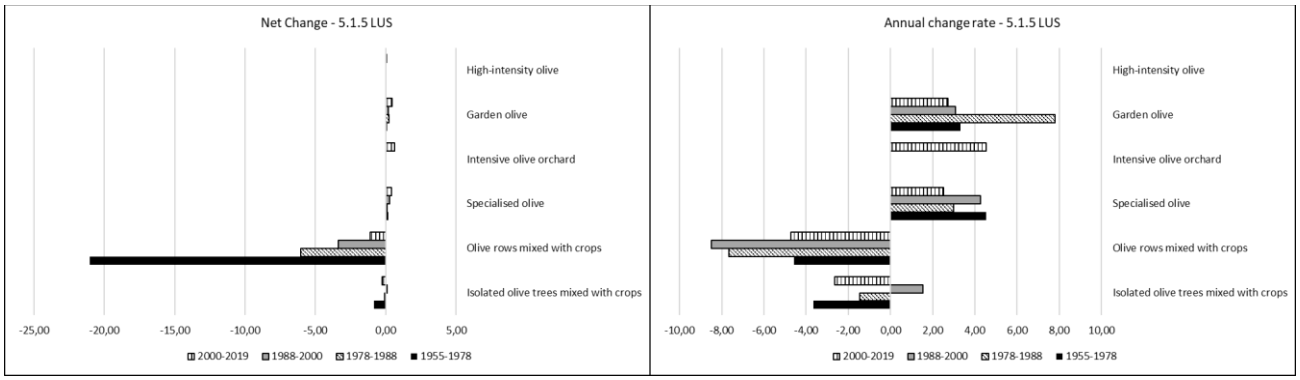

Fig. 38 Net Change (left) and Annual Change Rate (right) at 5.1.5 LUS

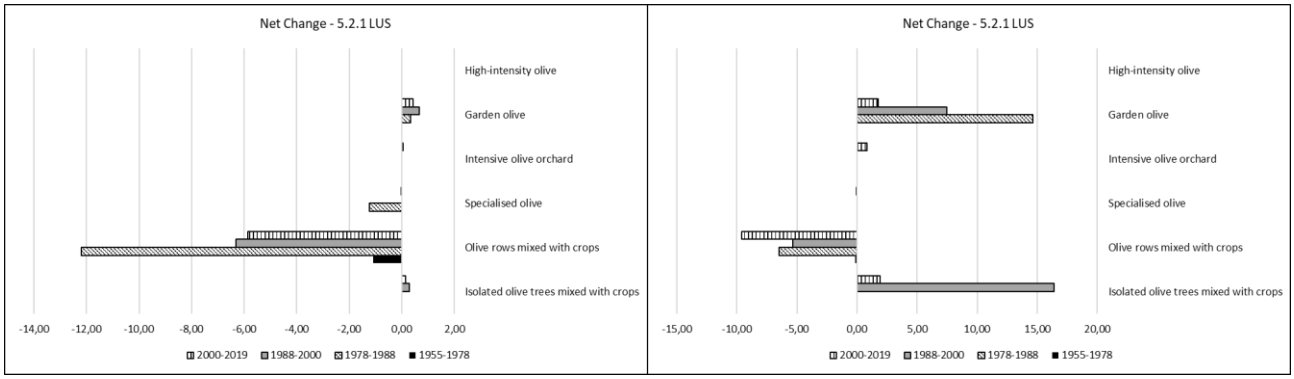

Fig. 39 Net Change (left) and Annual Change Rate (right) at 5.2.1 LUS

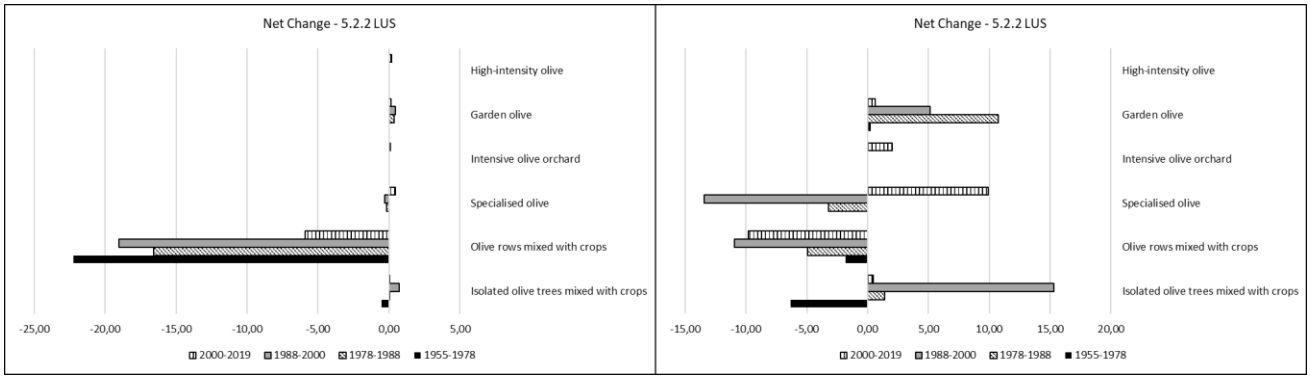

Fig. 40 Net Change (left) and Annual Change Rate (right) at 5.2.2 LUS

Landscape metrics

Landscape changes have been evaluated through landscape metrics on two levels, both LS and LUS, including NC (Number of Classes), NP (Number of Patches), APS (Average Patch Size), ED (Edge Density), SHDI (Shannon's Diversity Index) as described in Table 9. The landscape metrics were calculated for the years 1955, 1977, 1988, 2000 and 2019. In addition, the maximum entropy value in the ideal case (S) was added to these landscape metric classes [312]. This condition is given by taking into account both the maximum number and the uniform distribution of individual land use classes.

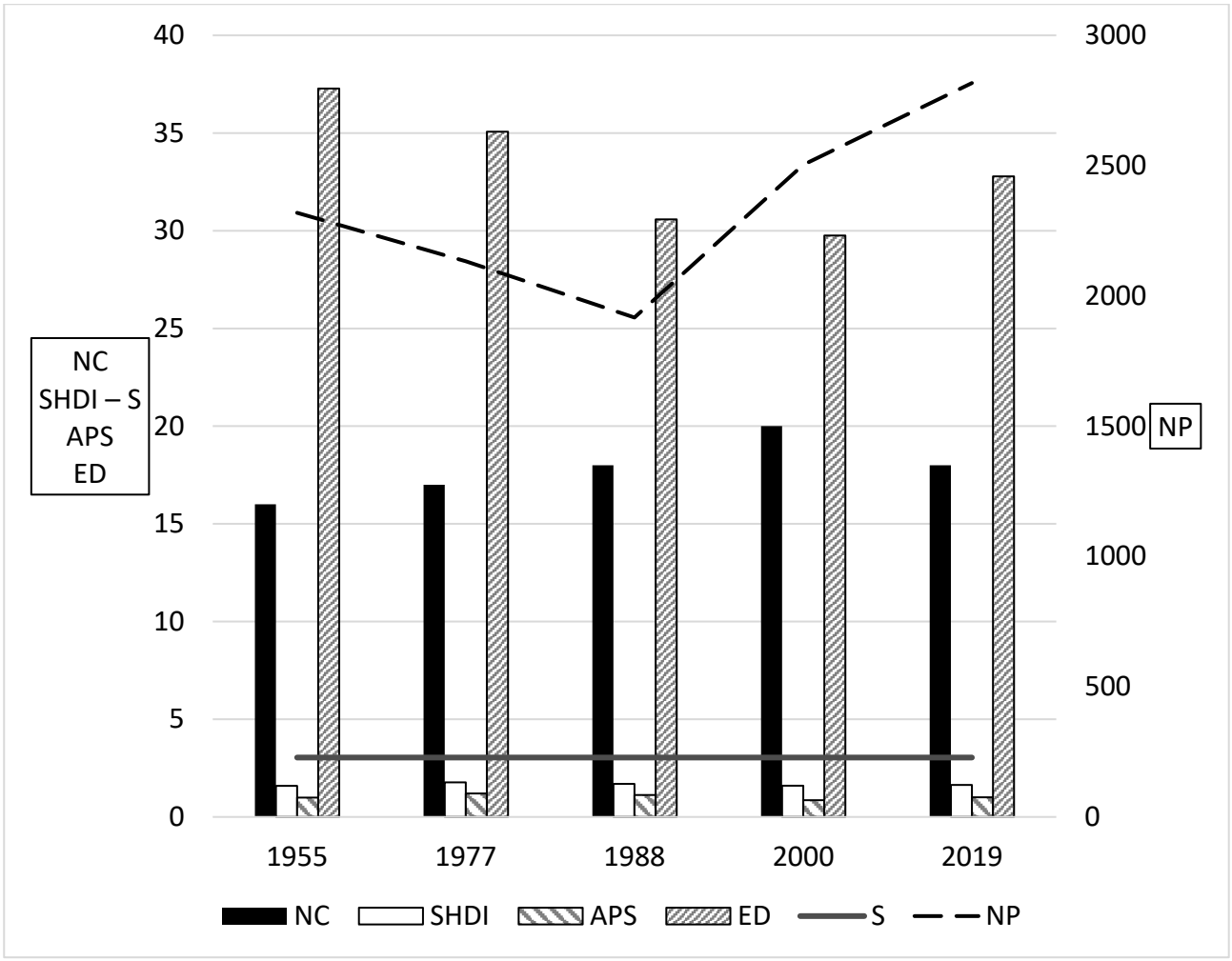

Fig. 41 Landscape Metrics at LS level: a)number of patches (number unit); b)Shannon's Diversity index combined with maximum entropy value in the ideal case (number unit); c) Average patch size (hectares unit); d) Edge density (meter / hectares unit) and e) Number of patches (number of unit)

Figure 41shows the main changes in landscape patterns in the study area from 1955 to 2019. First, it can be observed that the number of classes (NC) is not constant but varies from year to year, reaching a peak in 2000. This results from the fact that in 1955 there was a predominance of agricultural land uses, while from the end of the 1970s new urbanised areas of industrial/commercial type appeared, as well as new small water bodies or ponds to favour the irrigation of crops. New types of "modern" olive groves more intensive than traditional olives also appeared in this period. The increase in NC indicates an overall increase of heterogeneity and fragmentation of the landscape under consideration, confirmed by the parallel increase of the NP metric since 1988, in particular. The following data provides a clear representation of this trend. In 1955 we found 2319 patches (NP) across the territory, an high number as it refers to a period prior to the intense mechanization of agriculture, which will only be established from the 1970s. The spread of mechanization will result, especially for arable land, in an increase of parcels' size in order to make agricultural operations more efficient and will result in a decrease in the number of patches. On the other hand, the trend to increase NP since the late 1980s, reaching a peak in 2019 with 2817 units (Fig. 32). This is another significant indicator of the increased fragmentation of the landscape pattern in the study area, confirmed by the parallel increase of ED and the substantial stability of APS in the indicated period, i.e. from 1988 onwards. In the previous period, between 1955 and 1988, the evolution of ED values was decreasing. It reached its peak in 1955, with a value of 37,274 m/Ha, due to the high parcelling of agricultural areas typical of the share-cropping system in force in those years. Subsequently, it decreased until 1988 as a result of a greater regularization of the parcels' shape induced by mechanisation. It grew again in the subsequent period, reaching a value of 32 m/Ha in 2019, due to the overall increase of landscape heterogeneity in the study area following a sharp increase of patches (NP) and their strong dispersion across the territory. This trend probably causes an overall increase of ecotones between patches.

Furthermore SHDI values, a useful indicator of the overall entropy of the landscape, when it is applied at Landscape Scale (Fig. 42) shows quite limited variations. On the other hand, different trends of this index can appear for more detailed spatial scale models such as Landscape Unit Scale (LUS) by putting in light main driving forces of transformation in the territory which would otherwise be masked. At landscape scale, SHDI scored 1.59 in 1955, peaked in 1977 with 1.77 and then fixed to 1.64 in 2019 far from the maximum entropy theorical value of 3.04. This means that there has been a simplification in the complexity of the landscape, due to land use classes with a notable extent and less fragmentation.

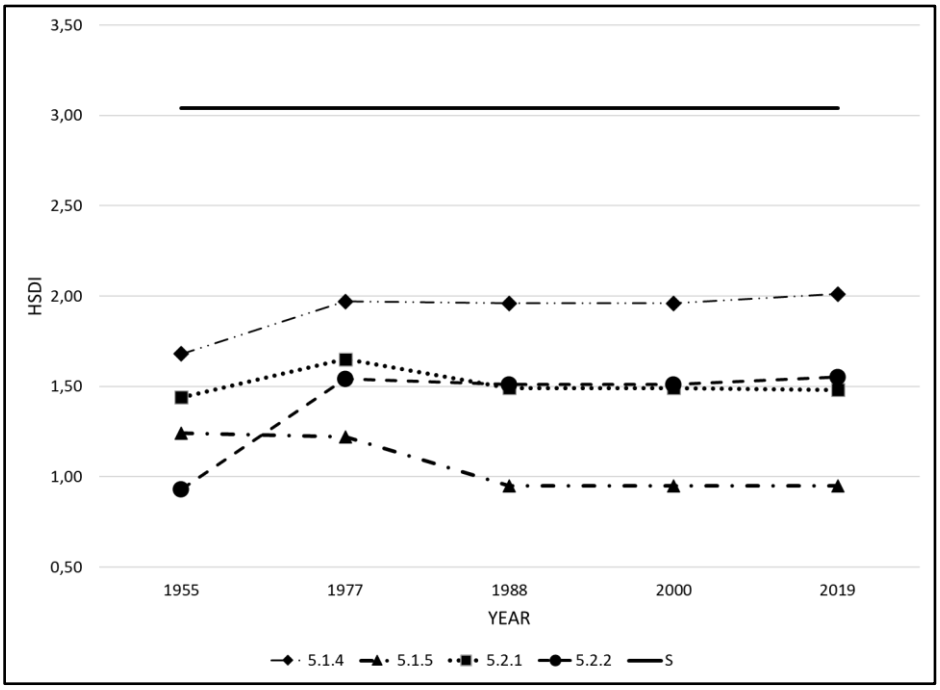

Fig. 42 SHDI fluctuations over investigated years at LUS level

On the contrary, if we analyse (Fig. 42) the trend of SHDI at the Landscape Unit Scale (LUS), we can notice very different behaviours.

In the 5.1.4 LUS, already in 1955, a high degree of fragmentation and heterogeneity of the landscape was recorded, determined by the high number of patches and their complex spatial arrangement, typical of the sharecropping agricultural model, which resulted in an SHDI value of 1.68. In the following years, the SHDI of this LUS further increased until it stabilized in 2019 at a value of 2.01.

This fragmentation and diversity is caused by the high number of land used classes (N), equal to 14 in 1955 and 16 in 2019. In addition, this heterogeneity greatly limited the APS, which remained about 0.85 Ha during all period. The value of ED shows a peak in 1955 (54.72 m/Ha), then decreased in 1988 (42.46 m /Ha) and finally rises to 48.87 m/Ha in 2019. Finally, NP shows an heterogeneous trend. In 1955, 1192 patches were recorded while in 1988 only 852. A new significant increase occurred along following years reaching the amount of 1334 patches in 2019.

Instead, in 5.1.5 LUS the value of SHDI decreases over time, going from 1.24 in 1955 to 0.95 in 2019, denoting a progressive simplification and homogenization of the landscape of this unit following the strong cereal intensification that has characterized the evolution of land use in this unit. Actually, the number of land use classes (N) follows the same trend as in 5.1.4 LUS, with 13 land use classes in 1955 and 16 in 2019. Conversely, the number of patches (NP) decreased from 1112 in 1955 to 928 in 2019. APS has a heterogeneous trend: in 1955 was equal to 0.97 Ha, grew to 1.37 Ha in 2000 then fixed to 0.89 Ha in 2019. Finally, ED values ranged from 47.63 m/Ha in 1955 to 29.50 m/Ha in 2019. These results suggest that over the years the area suffered a kind of homogenisation and orderly trend of conversion of land uses, mainly in favour of low labour intensity crops, hindering ecological diversification. Finally, the trend of SHDI in the 5.2.1 LUS and 5.2.2 LUS during the period considered are quite similar to each other and decidedly different from those of both previous LUS. They essentially show intermediate values compared to the LUS analyzed previously. In 2019, they have an SHDI value of 1.48 and 1.55, respectively, having been characterized by two main drivers of land use transformation, the diffusion of urbanized areas on the one hand and the diffusion of arable land on the other, which have increased their heterogeneity but to a decidedly lesser extent than the 5.1.4 LUS.

To better understand the impact of different drivers of change within the 5.1.4 LUS in comparison to 5.1.5 LUS, is very useful to open a focus on landscape metrics concerning every olive growing typology as shown in Figures 43, 44 and 45.

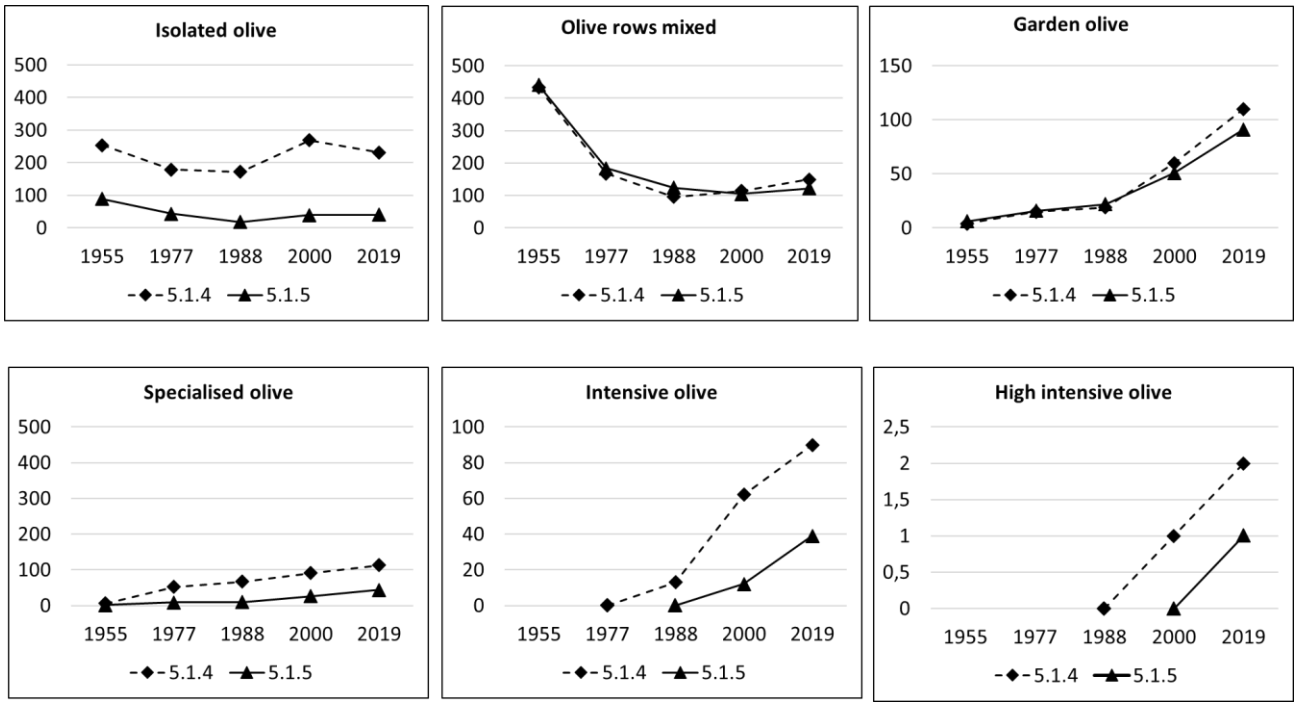

Fig. 43 Number of Patches (NP) for all olive orchard typologies within 5.1.4 LUS and 5.1.5 LUS

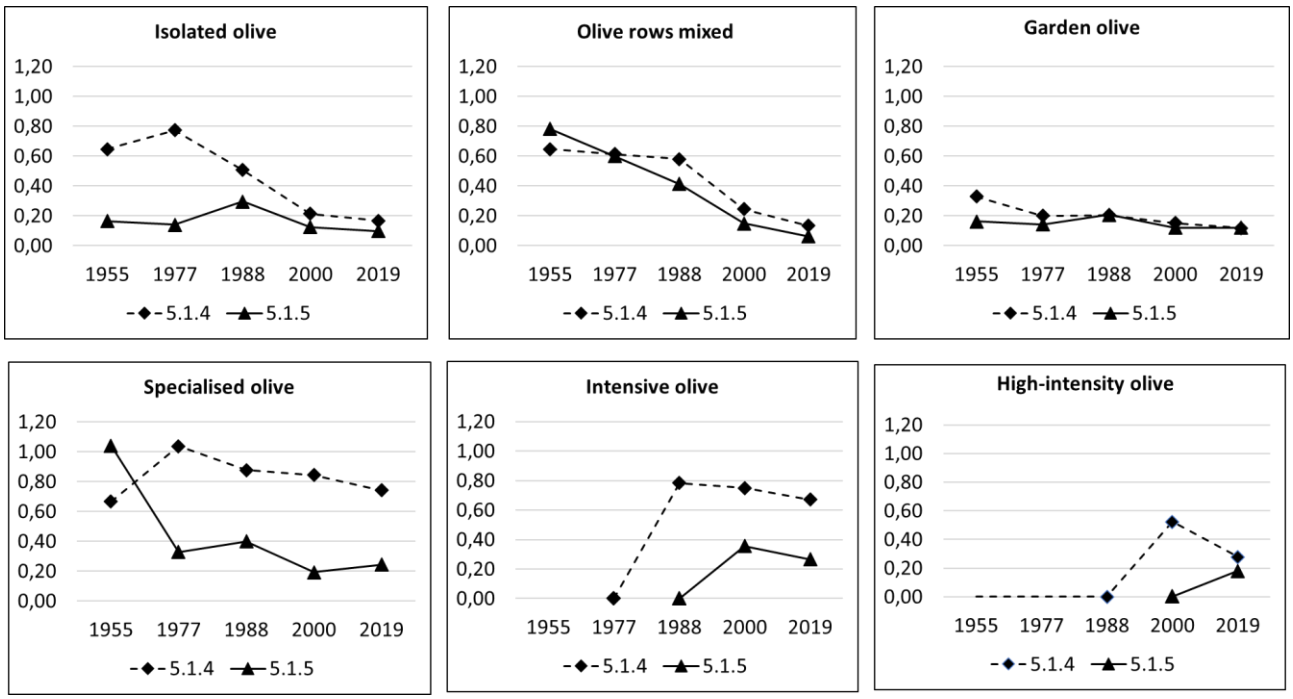

Fig. 44 Number of Average Patches Size (APS) for all olive orchard typologies within 5.1.4 LUS and 5.1.5 LUS

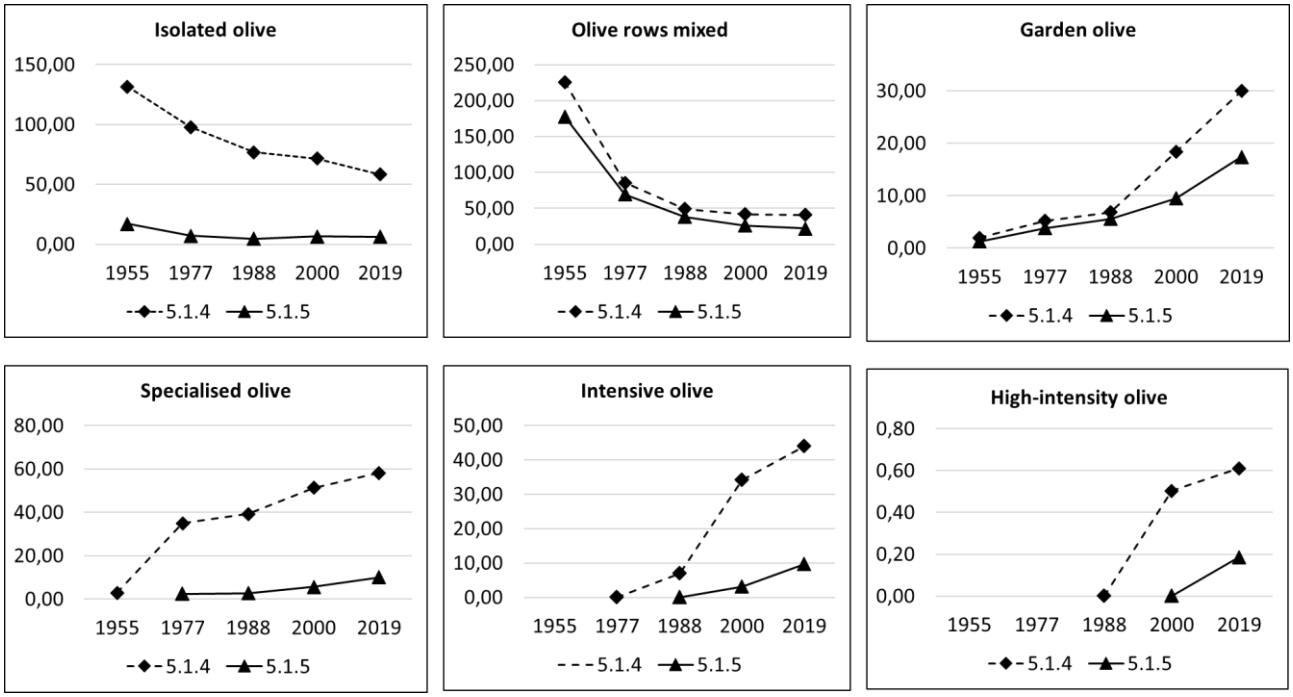

Fig. 45 Edge Density (ED) for all olive orchard typologies within 5.1.4 LUS and 5.1.5 LUS

According to Figure 43, the decrement of NP metric for isolated olive trees mixed with crops (2.2.1 LC) is more evident within 5.1.5 LUS in comparison with 5.1.4 LUS. Actually, in 1955 we find 254 patches within 5.1.4 LUS then dropped to 172 in 1988 and then increased to 231 in 2019. Conversely, NP ranged from 89 in 1955 to 40 in 2019 within 5.1.5 LUS. On the other hand the second typology of traditional olive growing, the olive rows mixed with crops (2.2.2 LC), suffered the highest loss of NP both within 5.1.4 and 5.1.5. In particular, ranging from 433 in 1955 to 149 in 2019 within 5.1.4 LUS and from 441 to 122 within 5.1.5 LUS. On the contrary, the garden olive trees class (2.2.6 LC) shows a constant tendency to grow within both LUS, ranging from 4 to 110 within the 5.1.4 LUS and from 6 to 91 within the 5.1.5 LUS in 1955 and 2019 respectively. Modern and more productive olive orchards have had very different periods of growing. The specialised olive orchards (2.2.3 LC) shows a regular increasing from 1955 to 2019, more evident within 5.1.4 LUS (from 6 to 113 patches) actually. The intensive olive orchards (2.2.4 LC) start to increase from 1977 within 5.1.4 LUS and from 1988 within 5.1.5 LUS. Furthermore, the absolute amount of increasing was stronger for 5.1.4 LUS than for 5.1.5 LUS. Finally, the high intensity olive orchards (2.2.5 LC) were recognised from year 2000 within both LUS, showing a very few number of patches respectively.

As Fig. 44 shows, APS for the isolated olive trees mixed with crops (2.2.1 LC) undergoes a drastic reduction. Within the 5.1.4 LUS there is a shift from 0.65 Ha in 1955 to 0.17 Ha in 2019, while in the 5.1.5 LUS the metric APS ranged from 0.16 Ha in 1955 to 0.10 Ha in 2019. The same declining trend is also recorded for the olive rows mixed with crops (2.2.2 LC) which shows a regular declining tendency. If in 1955 the APS was 0.65 Ha in 5.1.4 LUS, in 2019 it was 0.13 Ha only. Instead, within the 5.1.5 LUS APS moves from 0.78 Ha in 1955 to 0.13 Ha in 2019. Therefore, the traditional olive growing has preserved its presence within both LUS over the investigated 64 years, but the size of residual parcels of these two olive orchards typology has become smaller and smaller. Very similar is the trend of change for garden olive trees (2.2.6 LC) ranging from 0.33 Ha in 1955 to 0.12 Ha in 2019 within the 5.1.4 LUS and from 0.16 Ha to 0,12 Ha within the 5.1.5 LUS.

It is worth of noting the different response for the specialised olive orchards (2.2.3 LC) within the 5.1.4 LUS, where the APS is equal to 0.67 Ha in 1955 and grows to 0.74 Ha in 2019. On the other hand within 5.1.5 LUS, APS in 1955 is equal to 1.04 Ha and decreases to 0.24 Ha showing a quite different evolution of the modern olive growing sector into these two LUS. Also for the intensive olive orchards (2.2.4 LC) we note a decrease of APS. If in 1988 its value was 0.78 Ha, in 2019 it dropped to 0.67 Ha within the 5.1.4 LUS. This trend was less evident within 5.1.5 LUS, with a shift from 0.38 Ha in 2000 to 0.27 Ha in 2019. Finally, the high intensive olive orchards (2.2.5 LC), seem to show a declining trend within the 5.1.4 LUS, ranging from 0.52 Ha to 0.28 Ha, but must be highlighted the exiguity of patches on which APS has been calculated.

According to Figure 45, ED appears clearly influenced by the fragmentation that has affected the olive landscape evolution. For the isolated olive trees mixed with crops (2.2.1 LC), it is evident a sharp declining trend. Within 5.1.4 LUS ED was calculated equal to 131,53 m/ha in 1955 and 58,22 m/Ha in 2019. Instead, within the 5.1.5 LUS the values were lower and equal to 17.24 m/Ha in 1955 and 6.44 m/Ha in 2019. Olive rows mixed with crops (2.2.2 LC) also shows a similar trend. In fact, within the 5.1.4 LUS it was 225,97 m/Ha in 1955, finally it dropped to 41,04 m/Ha in 2019. Within the 5.1.5 LUS it was 177.82 m/Ha in 1955 then dropped to 22.11 m /Ha in 2019. From these results it can be deduced that overall ecologic richness for both landscapes of these LUS has declined hardly over the investigated period, because ED reflects the potential vitality of ecotones of patches. On the other hand, ED values for the Garden Olive Trees (2.2.6 LC) have shown a growing trend. Within the 5.1.4 LUS was equal to 1.99 m/Ha in 1955 and grew to 29.99 m /Ha in 2019. Instead, within the 5.1.5 LUS ranged from 1.29 m/Ha in 1955 to 17.42 m/Ha in 2019. This results open a reflexion about the potential ecological role of this particular kind of olive orchards, which is often connected with urban areas. If we consider the more intensive and productive olive orchards typologies, it can be noted an increasing of ED values probably due to the previous underlined increase of fragmentation of these olive orchards, in particular for the 5.1.4 LUS. Finally, ED values of Specialised Olive Orchards (2.2.3 LC) increased from 2.94 m/Ha in 1955 to 58.10 m/Ha in 2019 within 5.1.4 LUS. Furthermore, within the 5.1.5 LUS the ED values for the same class ranged from 0.44 m/Ha in 1955 to 9.99 m/Ha in 2019. The Intensive Olive Orchards (2.2.4 LC) show an high values of 44.06 m/Ha within the 5.1.4 LUS and a low value of 9.75 m/Ha within the 5.1.5 LUS in the year 2019. Also the High Intensive Olive Orchards (2.2.5 LU) shows a trend of ED increasing, up to 0.61 m/Ha within the 5.1.4 LUS and 0.18m/Ha within the 5.1.5 LUS in 2019, but this cannot be considered very significant due to exiguity of patches belonging to this typology.

5.1.5 Discussion and conclusion

The study, referring to more than 64 years, allowed to identify the main trends of transformation of the Cartoceto landscape Municipality through subsequent comparisons between couples of LUMs specially drafted by the authors for the years 1955-1978-1988-2000-2019. These dates have been selected in relation to the availability of aerial orthophotos at the relevant national and regional public authorities. Therefore, it is useful to make some considerations about the quality of the LUMs produced for the purposes of this study. The first concerns the estimation of the accuracy of the LUMs, a parameter that would be desirable to know for all thematic maps. Unfortunately, it was not possible to determine this parameter for the LUMs generated by the study since there were no repertoires of ground truth available at the date of the orthophotos. This problem always occurs when historical series of remotely sensed data are used, so it can be overcome very hardly. The only available historical information, which was acquired and then used to support the photo-interpretation process, comes from the two LUMs drawn up in 1984 and 2011 by the Marche Region [278] and AGEA [280] respectively.[280]. These thematic maps, however, were deprived of metadata concerning their accuracy, in addition the legends of these two LUMs differed significantly both for number of classes and informative content. In particular, in neither of these two LUMs the "olive" class was articulated into more detailed subclasses. As a consequence, these LUMs were not suitable to identify the different types of olive groves and did not allow to analyze their actual transformations over time. Therefore, the latter was one of the main objectives of the study. Actually, the definition of the third level of the "olive" class in the legend specially developed for this study (Tab. 7) was of fundamental importance. For this purpose, we started to collect ground truths relating to each different type of olive trees considered in the legend, which are all still present today in the study area. This activity allowed to define the main parameters (colour, hue, shape, size, density and spatial distribution of the olive trees) of the "interpretation keys" then used to identify each type of olive in the digital set of orthophotos. However, the definition of these parameters was quite difficult cause of the scale heterogeneity, the different resolution and sensitivity of films (B&W or Colour), which characterized the available digital orthophotos (see Tab. 4). Another significant quality feature of thematic maps is the minimum mapping unit (MMU). In drafting the LUMs, the latter was defined in relation to the possibility of identify an isolated line of olive trees, at least composed of three elements, on the digital orthophoto at the specific scale ratio. This very detailed MMU of the generated LUMs corresponds to 80-100 square meters, therefore much more information than within the LU/LC maps of Marche Region [278] or AGEA [280]. Not only the informative content, but also the spatial delineation of parcels, with particular reference to olive sub-classes, resulted more accurate within the LUMs generated by the study. It must be underlined that this qualitative features of thematic maps are of particular importance when landscape metrics are processed. Indeed, the results of landscape metrics are influenced by the degree of detail of the LUM, as they are correlated with the shape of the patches and the extent of simplification of their spatial representation [313]–[315].

An adequate detail of the LUMs is also important in overlapping operations, in order to highlight and quantify land use changes with greater reliability and identify the speed of such changes over time. Regarding the first aspect, very significant was the overlap of the LUMs relating to the years 1955 and 2019, which allowed to build the Sankey diagram at landscape scale (LS) shown in Figure 23. This chart highlights the extent and final destination of transformations of all types of land use during the investigated period. In particular, it shows very clearly the sharp decrease of promiscuous olive cultivation, above all the olive rows mixed with crops (2.2.2 LC), and the predominant conversion of the latter in the arable land (3.1 LC) and urbanised surfaces (1.1 LC e 1.2 LC).

In addition, the analysis of the change speed over the time intervals considered was useful for interpreting main determinant drivers. For example, the significant surface losses of the two classes of promiscuous olive cultivation (2.2.1 LC and 2.2.2 LC) highlighted by Figure 36 in the periods 1955-1977 and 1978-1988 are probably to be linked to the heavy frosts of 1956 and 1985 that caused the death of millions of olive trees across Italy. To cope with this situation, the Italian government allocated a series of subsidies (Law 839 of 26 July 1956, refinanced several times) that spurred farmers to adopt new, more modern and productive olive orchards, i.e. with a higher trees density per hectare, thus leading to the birth of specialized olive farming. This trend towards a progressive specialization and intensification of olive groves continues, though slowly, in subsequent years. This is evident (Fig. 36, right part) by the high speed of implementation of new intensive olive groves characterizing the 1988-2000 period which follows the frost of 1985. Actually, in the 80s the olive sector are spreading intensive olive orchards, with an higher trees density per hectare than specialized olives of 60s and 70s and more advanced cultivation techniques. This evolution of the Italian olive sector was also supported in this period by subsidies introduced by the Common Agricultural Policy (CAP) of the European Union (at that time European Economic Community, EEC), which supported the realization of new orchards and the acquisition of new machinery in order to increase the mechanization of operations in olive groves.

The transformation trends of land use have also been analysed in more detail at the Landscape Unit Scale (LUS) of Cartoceto territory. It was expected that, within different area for what concerns geo-morphology and anthropization models, the trends of change in land use were, in turn, differentiated. This hypothesis has been fully confirmed by the results obtained, as is evident from what is shown in Figure 35. In particular, the LUS 5.1.4 (middle hills between 88 and 378 m a.s.l. with medium-high slopes on calcarenitic substrate and the presence of the historic village of Cartoceto) still today shows a significant presence of the various typology of olive groves, about 28% of its surface. On the contrary, the LUS 5.1.5 (middle-low hills between 63 and 188 m a.s.l. with medium-low slopes on pelitic substrates and the presence of scattered houses) is predominantly occupied by the intensive arable land today, that insists on about 70% of its surface, while the residual olive trees show a total area of less than 10%. The LUS 5.1.4 also shows the higher persistence, compared to other LUS, of traditional olive groves and, at the same time, denotes a significant presence of specialized, intensive and super intensive olive orchards. The latter have been implemented, both in terms of total surface and speed of spread, from the late 70s to the early 2000s. In summary, the current landscape pattern of these two LUSs is very different today: heterogeneous and with a high rate of diversity in the LUS 5.1.4, uniform and homogenous instead in the LUS 5.1.5. This different reading of the landscape in these two LUSs was also very useful in supporting the following analyses focused on the landscape metrics.

The study carried out in this work, in fact, did not end with the analysis of land use transformations. In order to understand the effects exerted on landscape patterns from the land use transformation discussed earlier, landscape metrics were used with special attention to those relating to the various types of olive trees. By the way, this method is widely used in the context of landscape studies [80], [183], [316].

The landscape metrics considered in this study (N, NP, APS, ED and SHDI) have been selected based on the purpose and scope of the research carried out, as suggested by some authors [182]. The in-depth analysis of metrics and the interpretation of their meaning in terms of landscape patterns were carried out in the relevant paragraph of the results chapter, to which we refer for details. Discussing the study results, it is important to emphasize that, even in the case of metrics, very different results were obtained between computations carried out at landscape scale (LS) than those at Landscape Units Scale. (LUS). This difference especially appears for the SHDI metric, which at the LS level does not show particular variations in the time span of the 64 years investigated (Figure 41). Despite the other metrics, in particular NC, ED and especially NP, show diverse trends. Probably, as also discussed in a recent work [200], the wide territorial scale considered in this case has determined a particular influence in processing SHDI by some classes decisively dominating as total area (arable land and urbanized areas primarily). Probably, as also discussed in a recent work [200], the wide territorial scale considered in this case has determined a particular influence in the calculation of SHDI by some classes decisively dominating on that spatial scale, by total area (arable land and urbanized areas

primarily). This limited the contribution of classes with a smaller total area and greater fragmentation, such as the different types of olive growes, in processing this metric.

On the other hand, metrics calculated at Landscape Units Scale (LUS) show significantly different trends, such as for SHDI as Figure 42 highlights. In particular, we can observe how two distinct clusters of values are formed by comparing the results obtained for the LUS 5.1.4 to those relating to the 5.1.5 through a scatter plot SHDI - ED (Fig. 46) one for each of the two LUSs. This result represents a consistent indication of the fact that in these two different Landscape Units, during the 64 years considered by the study, landscape transformation drivers were significantly different.

.

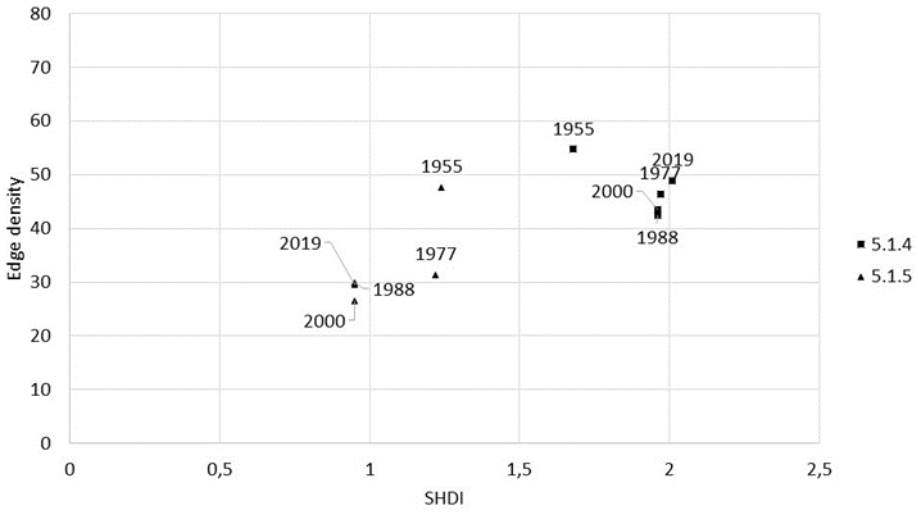

Fig. 46 Scatter plot of SHDI and ED for 5.1.4 and 5.1.5 LUS

The above notes confirm that the analysis of land use change and landscape transformation of a given territory is effectively supported by comparisons between LUMs when an appropriate historical series of data and landscape metrics are set up. However, to a more deeply understanding, it could be said from a socio-cultural point of view, the dynamics impacting the territory and its community over a long time period, such as the considered 64 years, it is useful to directly involve the exponents, especially the older ones, of the local community. Or rather, involve local olive growers. Similar hybrid survey techniques are also detectable in the most recent bibliography [60]. The results of analysis carried out on LUMs of different epochs are combined with the historical survey and interviews of limited but significant number of local farmers who did their business during the survey period. In this direction, during our study, some meetings were organised with highly representative figures of the olive history of the Cartoceto territory and main representatives of the GI consortium (Figure 49 and Table 10). The results of discussions at these meetings are summarised in the following Fig.47 and Tab. 11, which represents a useful summary of the main drivers of change identified and their impacts on land use and olive landscapes transformations within the study area.

In this direction, during the course of this study, some meetings were organized with highly representative figures of the olive history of the Cartoceto land and the current state of this production sector in relation to the establishment of the PDO of the extra virgin olive oil of Cartoceto (Figure 47 and Table 11).

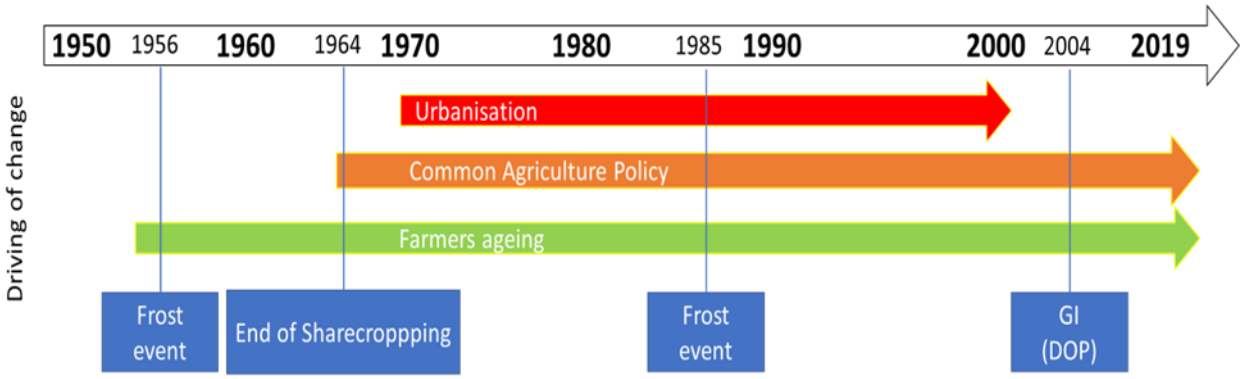

Fig. 47 Basic timeline of historical changes in the agricultural history of olive cultivation in Cartoceto, both at LS and LUS

Table 11 Dynamics of different drivers of changes by exploring the effects on LU/LC and Olive Landscape

Drivers of change	**Event description**	**Impacts on Landscape**
Frost events and new agriculture models	With the frosts of 1956 and 1985, olive grove surfaces drastically reduced, in particular the olive row mixed with crops. Even the trees-line of vines mixed with crops disappeared after 1988. Innovation in agriculture struggled to establish itself, at least until 2000. Farmers only responded to climate-related stress.	Progressive decrease of patches of olive row mixed with crops from 1955 to 2019, but isolated olive mixed with crops increase from 2000 to 2019. However, their average patch size decreases steadily from 1955 to 2019. Specialized and intensive olive groves increase only since the late 1980s, not their average patch size. High-intensity olive groves appear only since 2000 on small patches. Olive-garden increase steadily from 1955 to 2019 in smaller areas. These trends do not occur homogeneously across the landscape. In some landscape units contribute to increase the landscape heterogeneity, in others to decrease it.
More intensive arable land	Abolition of sharecropping (1964) and the reduction of traditional olive orchards push to intensive cereal growing from the mid of 1970s. Between 1955 and 2000, arable land doubles (from 30 percent to 60 percent of the territory). As consequence the average size of fields increases.	In areas where intensive cereal growing is established, mixed olive groves become rare and isolated from late 1980s, losing their ability to visually characterise the rural landscape..
New urbanisation and more infrastructure	Existing residential areas are expanded since the 1970s. In addition, new residential and industrial areas arise in the bottom valleys. Also roads and infrastructure increase, especially after 2000.	Low hill and alluvial areas, starting from late 1970s, held the replacement of traditional olive groves (dominant in 1955) by new urbanized and industrial areas and new intensive cereal growing areas. Closely related to the spread of residential units has been an increase of small olive gardens. In these areas the olive landscape disappears, but the cultural function of witnessing the olive tree as an element of rural tradition is preserved.
Farmers and citizens ageing	Residents double from 1955 to 2021 (about 8000, Istat data) with a progressive aging trend. The average age of farmers has also increased. A generational problem arises in the predominantly family-owned farms. Low propensity for innovation leads farmers to take refuge in traditional crops.	Close to the historic village of Cartoceto is concentrated the most significant permanence of traditional olive-growing patches, if compared to overall territory over the period 1955-2019. Two possible reasons: less damage from the 1956 and 1985 frosts due to the higher average elevation of the hills where the village is located, the emerging of the GI (2004)mainly due to the older olive growers and the Pro-Loco agency of Cartoceto. GI also stimulated the development of more modern models of olive groves.

Geomorphology diversity	The territory of Cartoceto is not homogeneous. Different physiographic units can be distinguished: hilly areas with different substrates and medium to steeply slope are prevalent; sub-flat and alluvial areas have smaller areas. Very different trends of land use evolution has been noted in the different units, especially since the 1980s.	The 5.1.4 LUS, where the village of Cartoceto is located, shows the most significant and mature contemporary olive-growing landscape. This landscape is strongly characterized by traditional olive groves and oil mills , but also by the new types of modern olive groves since the 1980s. All olive orchards are integrated with arable land and woodland vegetation, thus increasing the heterogeneity of this landscape (high SHDI). In contrast in 5.1.5 LUS, the spread of cereal growing gradually erases the olive landscape and results in a progressive homogenization of the landscape (low SHDI) until 2019. .

Starting from these last considerations, the authors are developing a collaboration with the Cartoceto and with the Consortium town of Extra-Virgin Oil of Carroceto PDP aimed at enhancing the olive landscapes of the area in order to develop oil-tourism initiatives.

6 Conclusions and future developments

This chapter will conclude the study by summarising the key research findings of the doctoral study, discussing the value and contribution thereof, and demonstrating the potential of geomatic data acquisition technologies at different levels of detail. In particular, the effectiveness of MLS with the SLAM algorithm has been demonstrated for estimating metric parameters from individual trees in both forestry and specialised olive fields. The advantages of the MLS-SLAM application transcend the automatic registration of the scans and the low weight of the device, which favours a high rate of reliability in retrieving the 3D structure, fast monitoring, and no trees need to be felled.
It is worth noting that Lidar sensors are very suitable for characterising olive canopies to extract metric data in forestry. The best results showed that the data detected by MLS-SLAM in a dense plantation of uniform-aged black pine provided reasonable estimates of DBH, with an RMSE of 10.8% compared to ground truth measurements. At the same time, it is impossible to extract the value of the height of each tree because the leaf density of the canopy prevents the laser pulse from reaching the top of the canopy.
Regarding olive trees, they adapt very well to the three-dimensional study of canopies. The research has been limited to analysing the volume of the canopy by applying two different geometric primitives. From the statistical analysis, it has been demonstrated how the best correlation between the geometric primitive and the mesh is given by the paraboloid-convex hull algorithm with a value of $R2 = 0.92$. In contrast, the analysis pair given by the toroidal-alpha shape has a value of $R2 = 0.91$.
On the other hand, as for analysing the evolutionary dynamics of the rural landscape at a specific spatial scale over time through land use maps, it is well-suited to understand how anthropic or other factors have influenced the dynamics of landscape transformation. In this case, the strong sensitivity between landscape metrics and the spatial scale adopted to describe ecological diversity is worth noting. In fact, spatial models at the landscape scale tend to have a more significant disturbance effect caused by dominant land use classes such as arable land and urban, which tend to conceal the ecological effects of olive groves. The latter being more fragmented and distributed heterogeneously, are easier to identify their influence on reduced spatial scales, as in the case of the Landscape Unit Scale.
With the advancement of technology, several future developments will likely influence both the forestry sector and permanent tree crops and the application of MLS-SLAM in the years to come. Below is a list:

1. Improvement of sensor technology will allow an accurate and detailed representation of forest inventory and tree characteristics. The mobile laser scanner collects exact and complete data on the shape, size, and position of trees and permanent structures. This data can be integrated with that from Airbone Laser Scanner (ALS) and used to create accurate forest inventories and maps of forest cover, density, and biomass.
2. Improvement of forest management: Mobile laser scanner data integrated with GIS allows for better visualisation and analysis of forest structure and tree characteristics. The decision support system created with this information can provide valuable insights and recommendations to forest managers to optimise forest growth, productivity, and sustainability.
3. Real-time data analysis - Future mobile laser scanning technology will be able to process and analyse data on the move during the scanning process. Applying mesh algorithms that adapt well to the characteristics of the canopy based on the tree species will allow green space managers to make real-time decisions, helping them plan interventions based on the activity to be undertaken.
4. Improved forest health monitoring: Mobile laser scanner data can provide information on the conditions of individual trees and help identify any damage or disease outbreaks. This information, integrated with GIS, can be used to create rapid alarm systems and track the spread of diseases, pests or fires.

The second point that we intend to address concerns the integration of high-resolution aerial images and multitemporal land use maps. This union represents a potential future development in the fields of rural landscape conservation, forestry, and urban planning. Possible applications include:

1. Thanks to the combination of visual information and temporal models, aerial images and multitemporal maps can provide accurate and updated information on land cover, allowing for better monitoring of changes over time and distinguishing between different types of land cover.
2. It is possible to develop automatic methods for detecting LU/LC changes, using geospatial data from various sources, such as aerial photos or multispectral satellite images, in order to reduce manual interpretation. This process requires a reliable set of reference data for deep learning or machine learning models.
3. A limitation of the exposed research that cannot be ignored is the absence of parameterization and quantification of landscape changes through spatial patterns at a high level of detail. To overcome this problem, an assumption will

be to resort to the moving window technique by Fragstats software [317]. In this way, it will be possible to produce a series of maps that spatialize the indices, allowing for a more accurate evaluation of the collected information."

4. The integration of aerial images and multitemporal land use maps can lead to significant improvements in land management practices and environmental monitoring, enabling more sustainable and effective use of natural resources, and contributing to the preservation of ecological elements in the landscape.

References

[1] O. Visser, S. R. Sippel, and L. Thiemann, "Imprecision farming? Examining the (in)accuracy and risks of digital agriculture," *J. Rural Stud.*, vol. 86, pp. 623–632, 2021, doi: https://doi.org/10.1016/j.jrurstud.2021.07.024.

[2] EC (European Commision), "EU member states join forces on digitalisation for European agriculture and rural areas." .

[3] M. Shepherd, J. A. Turner, B. Small, and D. Wheeler, "Priorities for science to overcome hurdles thwarting the full promise of the 'digital agriculture'revolution," *J. Sci. Food Agric.*, vol. 100, no. 14, pp. 5083–5092, 2020.

[4] S. Fielke, B. Taylor, and E. Jakku, "Digitalisation of agricultural knowledge and advice networks: A state-of-the-art review," *Agric. Syst.*, vol. 180, p. 102763, 2020.

[5] B. Maestrini and B. Basso, "Drivers of within-field spatial and temporal variability of crop yield across the US Midwest," *Sci. Rep.*, vol. 8, no. 1, p. 14833, 2018, doi: 10.1038/s41598-018-32779-3.

[6] D. J. Mulla, "Twenty five years of remote sensing in precision agriculture: Key advances and remaining knowledge gaps," *Biosyst. Eng.*, vol. 114, no. 4, pp. 358–371, 2013, doi: https://doi.org/10.1016/j.biosystemseng.2012.08.009.

[7] P. Singh *et al.*, "8 - Hyperspectral remote sensing in precision agriculture: present status, challenges, and future trends," in *Earth Observation*, P. C. Pandey, P. K. Srivastava, H. Balzter, B. Bhattacharya, and G. P. B. T.-H. R. S. Petropoulos, Eds. Elsevier, 2020, pp. 121–146.

[8] R. Nigam *et al.*, "Crop type discrimination and health assessment using hyperspectral imaging.," *Curr. Sci.*, vol. 116, no. 7, 2019.

[9] R. Hernández-Clemente, R. M. Navarro-Cerrillo, F. J. R. Ramírez, A. Hornero, and P. J. Zarco-Tejada, "A Novel Methodology to Estimate Single-Tree Biophysical Parameters from 3D Digital Imagery Compared to Aerial Laser Scanner Data," *Remote Sensing*, vol. 6, no. 11. pp. 11627–11648, 2014, doi: 10.3390/rs61111627.

[10] J. R. Rosell *et al.*, "Obtaining the three-dimensional structure of tree orchards from remote 2D terrestrial LIDAR scanning," *Agric. For. Meteorol.*, vol. 149, no. 9, pp. 1505–1515, 2009, doi: https://doi.org/10.1016/j.agrformet.2009.04.008.

[11] R. R. Sola-Guirado, S. Bayano-Tejero, A. Rodríguez-Lizana, J. A. Gil-Ribes, and A. Miranda-Fuentes, "Assessment of the Accuracy of a Multi-Beam LED Scanner Sensor for Measuring Olive Canopies," *Sensors*,

vol. 18, no. 12. 2018, doi: 10.3390/s18124406.

[12] F. Rovira-Más, Q. Zhang, and J. F. Reid, “Creation of Three-dimensional Crop Maps based on Aerial Stereoimages,” *Biosyst. Eng.*, vol. 90, no. 3, pp. 251–259, 2005, doi: https://doi.org/10.1016/j.biosystemseng.2004.11.013.

[13] F. J. Castillo-Ruiz, S. Castro-Garcia, G. L. Blanco-Roldan, R. R. Sola-Guirado, and J. A. Gil-Ribes, “Olive Crown Porosity Measurement Based on Radiation Transmittance: An Assessment of Pruning Effect,” *Sensors*, vol. 16, no. 5. 2016, doi: 10.3390/s16050723.

[14] R. Giuliani, E. Magnanini, C. Fragassa, and F. Nerozzi, “Ground monitoring the light–shadow windows of a tree canopy to yield canopy light interception and morphological traits,” *Plant. Cell Environ.*, vol. 23, no. 8, pp. 783–796, Aug. 2000, doi: https://doi.org/10.1046/j.1365-3040.2000.00600.x.

[15] F. Bongers, “Methods to assess tropical rain forest canopy structure: an overview BT - Tropical Forest Canopies: Ecology and Management: Proceedings of ESF Conference, Oxford University, 12–16 December 1998,” K. E. Linsenmair, A. J. Davis, B. Fiala, and M. R. Speight, Eds. Dordrecht: Springer Netherlands, 2001, pp. 263–277.

[16] W. H. Stuppy, J. A. Maisano, M. W. Colbert, P. J. Rudall, and T. B. Rowe, “Three-dimensional analysis of plant structure using high-resolution X-ray computed tomography,” *Trends Plant Sci.*, vol. 8, no. 1, pp. 2–6, 2003, doi: https://doi.org/10.1016/S1360-1385(02)00004-3.

[17] S. Chiappini *et al.*, “Comparing Mobile Laser Scanner and manual measurements for dendrometric variables estimation in a black pine (Pinus nigra Arn.) plantation,” *Comput. Electron. Agric.*, vol. 198, no. June 2021, p. 107069, 2022, doi: 10.1016/j.compag.2022.107069.

[18] E. Chuvieco, *Fundamentals of satellite remote sensing: An environmental approach*, 2nd ed. FL, USA, 2016.

[19] J. Estornell, L. A. Ruiz, B. Velázquez-Martí, I. López-Cortés, D. Salazar, and A. Fernández-Sarría, “Estimation of pruning biomass of olive trees using airborne discrete-return LiDAR data,” *Biomass and Bioenergy*, vol. 81, pp. 315–321, 2015, doi: 10.1016/j.biombioe.2015.07.015.

[20] Z. Yan, R. Liu, L. Cheng, X. Zhou, X. Ruan, and Y. Xiao, “A Concave Hull Methodology for Calculating the Crown Volume of Individual Trees Based on Vehicle-Borne LiDAR Data,” *Remote Sens.*, vol. 11, no. 6, p. 623, 2019, doi: 10.3390/rs11060623.

[21] V. Luoma *et al.*, “Assessing precision in conventional field measurements of individual tree attributes,” *Forests*,

vol. 8, no. 2, 2017, doi: 10.3390/f8020038.

[22] Y. [1] Y. Wang et al., “Is field-measured tree height as reliable as believed – A comparison study of tree height estimates from field measurement, airborne laser scanning and terrestrial laser scanning in a boreal forest,” ISPRS J. Photogramm. Remote Sens., *et al.*, “Is field-measured tree height as reliable as believed – A comparison study of tree height estimates from field measurement, airborne laser scanning and terrestrial laser scanning in a boreal forest,” *ISPRS J. Photogramm. Remote Sens.*, vol. 147, no. May 2018, pp. 132–145, 2019, doi: 10.1016/j.isprsjprs.2018.11.008.

[23] S. Zhou, G. He, F. Kang, W. Li, J. Kan, and Y. Zheng, “Extracting diameter at breast height with a handheld mobile liDAR system in an outdoor environment,” *Sensors (Switzerland)*, vol. 19, no. 14, 2019, doi: 10.3390/s19143212.

[24] A. E. L. Stovall, A. G. Vorster, R. S. Anderson, P. H. Evangelista, and H. H. Shugart, “Non-destructive aboveground biomass estimation of coniferous trees using terrestrial LiDAR,” *Remote Sens. Environ.*, vol. 200, pp. 31–42, 2017.

[25] S. Momo Takoudjou *et al.*, “Using terrestrial laser scanning data to estimate large tropical trees biomass and calibrate allometric models: A comparison with traditional destructive approach,” *Methods Ecol. Evol.*, vol. 9, no. 4, pp. 905–916, 2018.

[26] B. Brede *et al.*, “Non-destructive tree volume estimation through quantitative structure modelling: Comparing UAV laser scanning with terrestrial LIDAR,” *Remote Sens. Environ.*, vol. 233, no. September, 2019, doi: 10.1016/j.rse.2019.111355.

[27] G. Liu, J. Wang, P. Dong, Y. Chen, and Z. Liu, “Estimating individual tree height and diameter at breast height (DBH) from terrestrial laser scanning (TLS) data at plot level,” *Forests*, vol. 9, no. 7, p. 398, 2018.

[28] M. Dassot, A. Colin, P. Santenoise, M. Fournier, and T. Constant, “Terrestrial laser scanning for measuring the solid wood volume, including branches, of adult standing trees in the forest environment,” *Comput. Electron. Agric.*, vol. 89, pp. 86–93, 2012.

[29] D. Panagiotidis, P. Surový, and K. Kuželka, “Accuracy of Structure from Motion models in comparison with terrestrial laser scanner for the analysis of DBH and height influence on error behaviour,” *J. For. Sci.*, vol. 62, no. 8, pp. 357–365, 2016.

[30] C. Cabo, S. Del Pozo, P. Rodríguez-Gonzálvez, C. Ordóñez, and D. González-Aguilera, “Comparing terrestrial

laser scanning (TLS) and wearable laser scanning (WLS) for individual tree modeling at plot level," *Remote Sens.*, vol. 10, no. 4, 2018, doi: 10.3390/rs10040540.

[31] K. Iizuka, Y. S. Hayakawa, T. Ogura, Y. Nakata, Y. Kosugi, and T. Yonehara, "Integration of multi-sensor data to estimate plot-level stem volume using machine learning algorithms–case study of evergreen conifer planted forests in Japan," *Remote Sens.*, vol. 12, no. 10, p. 1649, 2020.

[32] D. Panagiotidis and A. Abdollahnejad, "Accuracy Assessment of Total Stem Volume Using Close-Range Sensing: Advances in Precision Forestry. Forests 2021, 12, 717." s Note: MDPI stays neu-tral with regard to jurisdictional claims in …, 2021.

[33] D. Panagiotidis and A. Abdollahnejad, "Reliable estimates of merchantable timber volume from terrestrial laser scanning," *Remote Sens.*, vol. 13, no. 18, p. 3610, 2021.

[34] J. G. de Tanago *et al.*, "Estimation of aboveground biomass of large tropical trees with terrestrial LiDAR, Methods Ecol. Evol., 9, 223–234." 2018.

[35] A. Lau *et al.*, "Quantifying branch architecture of tropical trees using terrestrial LiDAR and 3D modelling," *Trees*, vol. 32, pp. 1219–1231, 2018.

[36] M. Kunz, A. Fichtner, W. Härdtle, P. Raumonen, H. Bruelheide, and G. von Oheimb, "Neighbour species richness and local structural variability modulate aboveground allocation patterns and crown morphology of individual trees," *Ecol. Lett.*, vol. 22, no. 12, pp. 2130–2140, 2019, doi: 10.1111/ele.13400.

[37] S. Bauwens, H. Bartholomeus, K. Calders, and P. Lejeune, "Forest inventory with terrestrial LiDAR: A comparison of static and hand-held mobile laser scanning," *Forests*, vol. 7, no. 6, 2016, doi: 10.3390/f7060127.

[38] C. Gollob, T. Ritter, and A. Nothdurft, "Forest inventory with long range and high-speed Personal Laser Scanning (PLS) and Simultaneous Localization and Mapping (SLAM) technology," *Remote Sens.*, vol. 12, no. 9, 2020, doi: 10.3390/RS12091509.

[39] M. Holopainen *et al.*, "Tree mapping using airborne , terrestrial and mobile laser scanning – A case study in a heterogeneous urban forest," *Urban For. Urban Green.*, vol. 12, no. 4, pp. 546–553, 2013, doi: 10.1016/j.ufug.2013.06.002.

[40] M. Mokroš *et al.*, "Novel low-cost mobile mapping systems for forest inventories as terrestrial laser scanning alternatives," *Int. J. Appl. Earth Obs. Geoinf.*, vol. 104, p. 102512, 2021, doi: https://doi.org/10.1016/j.jag.2021.102512.

[41] A. Kukko, H. Kaartinen, J. Hyyppä, and Y. Chen, “Multiplatform mobile laser scanning: Usability and performance,” *Sensors*, vol. 12, no. 9, pp. 11712–11733, 2012.

[42] C. Gollob, T. Ritter, C. Wassermann, and A. Nothdurft, “Influence of scanner position and plot size on the accuracy of tree detection and diameter estimation using terrestrial laser scanning on forest inventory plots,” *Remote Sens.*, vol. 11, no. 13, pp. 1–30, 2019, doi: 10.3390/rs11131602.

[43] A. Nurunnabi, Y. Sadahiro, and R. Lindenbergh, “Robust cylinder fitting in three-dimensional point cloud data,” *Int. Arch. Photogramm. Remote Sens. Spat. Inf. Sci. - ISPRS Arch.*, vol. 42, no. 1W1, pp. 63–70, 2017, doi: 10.5194/isprs-archives-XLII-1-W1-63-2017.

[44] J. Van Brummelen, M. O’Brien, D. Gruyer, and H. Najjaran, “Autonomous vehicle perception: The technology of today and tomorrow,” *Transp. Res. part C Emerg. Technol.*, vol. 89, pp. 384–406, 2018.

[45] A. Fernández-Sarría, I. López-Cortés, J. Estornell, B. Velázquez-Martí, and D. Salazar, “Estimating residual biomass of olive tree crops using terrestrial laser scanning,” *Int. J. Appl. Earth Obs. Geoinf.*, vol. 75, no. August 2018, pp. 163–170, 2019, doi: 10.1016/j.jag.2018.10.019.

[46] C. Zhang *et al.*, “Apple tree branch information extraction from terrestrial laser scanning and backpack-LiDAR,” *Remote Sens.*, vol. 12, no. 21, pp. 1–17, 2020, doi: 10.3390/rs12213592.

[47] Y. Meng, X. Dong, W. Liu, and W. Lin, “Modeling biomass of white birch (Betula platyphylla) in the Lesser Khingan Range of China based on terrestrial 3D laser scanning system,” *Nat. Resour. Model.*, vol. 33, no. 1, p. e12240, 2020.

[48] Y. Jiang, C. Li, F. Takeda, E. A. Kramer, H. Ashrafi, and J. Hunter, “3D point cloud data to quantitatively characterize size and shape of shrub crops,” *Hortic. Res.*, vol. 6, 2019.

[49] R. R. Sola-Guirado, F. J. Castillo-Ruiz, F. Jiménez-Jiménez, G. L. Blanco-Roldan, S. Castro-Garcia, and J. A. Gil-Ribes, “Olive actual ‘on year’ yield forecast tool based on the tree canopy geometry using UAS imagery,” *Sensors*, vol. 17, no. 8, p. 1743, 2017.

[50] K. H. Lee and R. Ehsani, “A Laser Scanner Based Measurement System for Quantification of Citrus Tree Geometric Characteristics,” *Appl. Eng. Agric.*, vol. 25, no. 5, pp. 777–788, 2009, doi: https://doi.org/10.13031/2013.28846.

[51] X. Zhang *et al.*, “Using uav lidar to extract vegetation parameters of inner mongolian grassland,” *Remote Sens.*, vol. 13, no. 4, p. 656, 2021.

[52] F. A. O. Faostat, “Statistics division.Nations, Food and Agriculture Organization of the United,” 2016. .

[53] G. Messina and G. Modica, “Twenty Years of Remote Sensing Applications Targeting Landscape Analysis and Environmental Issues in Olive Growing: A Review,” *Remote Sensing*, vol. 14, no. 21. 2022, doi: 10.3390/rs14215430.

[54] B. De Gennaro, B. Notarnicola, L. Roselli, and G. Tassielli, “Innovative olive-growing models: an environmental and economic assessment,” *J. Clean. Prod.*, vol. 28, pp. 70–80, 2012.

[55] A. Loumou and C. Giourga, “Olive groves: ``The life and identity of the Mediterranean’’,” *Agric. Human Values*, vol. 20, no. 1, pp. 87–95, 2003, doi: 10.1023/A:1022444005336.

[56] ISMEA, “ISMEA Mercati - Trasparenza e conoscenza dei mercati agroalimentari.” https://www.ismeamercati.it/olio-oliva (accessed Dec. 20, 2022).

[57] L. Rallo, D. Barranco, S. Castro-García, D. J. Connor, M. Gómez del Campo, and P. Rallo, “High-density olive plantations,” *Hortic. Rev. Vol. 41*, pp. 303–384, 2013.

[58] and J. F. H. Tous, J., A. Romero, “The hedgerow system for olive growing.,” in *Olea (FAO Olive Network),26*, 2007, pp. 20–26.

[59] A. L. Palazzo and O. Aristone, “Peri-urban matters. changing olive growing patterns in central Italy,” *Sustain.*, vol. 9, no. 4, 2017, doi: 10.3390/su9040638.

[60] T. Dimopoulos and T. Kizos, “Mapping change in the agricultural landscape of Lemnos,” *Landsc. Urban Plan.*, vol. 203, p. 103894, 2020, doi: https://doi.org/10.1016/j.landurbplan.2020.103894.

[61] M. Escribano, P. Gaspar, and F. J. Mesias, “Creating market opportunities in rural areas through the development of a brand that conveys sustainable and environmental values,” *J. Rural Stud.*, vol. 75, pp. 206–215, 2020, doi: https://doi.org/10.1016/j.jrurstud.2020.02.002.

[62] E. Vandecandelaere *et al.*, *Strengthening sustainable food systems through impacts To cite this version : Strengthening sustainable food systems through geographical*. 2020.

[63] L. Flinzberger, Y. Zinngrebe, M. N. Bugalho, and T. Plieninger, “EU-wide mapping of ‘Protected Designations of Origin’ food products (PDOs) reveals correlations with social-ecological landscape values,” *Agron. Sustain. Dev.*, vol. 42, no. 3, p. 43, 2022, doi: 10.1007/s13593-022-00778-4.

[64] “European Council (1992) Council Regulation (EEC) No 2081/92 of 14 July 1992 on the protection of geographical indications and designations of origin for agricultural products and foodstuffs, Brussels.”

[65] G. Belletti, A. Marescotti, J. Sanz-Cañada, and H. Vakoufaris, “Linking protection of geographical indications to the environment: Evidence from the European Union olive-oil sector,” *Land use policy*, vol. 48, pp. 94–106, 2015, doi: 10.1016/j.landusepol.2015.05.003.

[66] H. Vakoufaris, G. Belletti, T. Kizos, and A. Marescotti, *Protected Geographical Indications and the landscape: towards a conceptual framework*. 2014.

[67] G. Cillis and D. Statuto, “Landscape protection and tourist valorisation of the cultural and natural heritage of the UNESCO site of Matera (Italy),” *Proc. Public Recreat. Landsc. Prot. Nat. Hand Hand*, pp. 226–231, 2018.

[68] T. Plieninger, F. Höchtl, and T. Spek, “Traditional land-use and nature conservation in European rural landscapes,” *Environ. Sci. Policy*, vol. 9, no. 4, pp. 317–321, 2006.

[69] G. Scarascia-Mugnozza, C. Sica, and P. Picuno, “The optimisation of the management of agricultural plastic waste in Italy using a geographical information system,” in *International Symposium on High Technology for Greenhouse System Management: Greensys2007 801*, 2007, pp. 219–226.

[70] Q. Fan and S. Ding, “Landscape pattern changes at a county scale: A case study in Fengqiu, Henan Province, China from 1990 to 2013,” *CATENA*, vol. 137, pp. 152–160, 2016, doi: https://doi.org/10.1016/j.catena.2015.09.012.

[71] V. Amici, S. Maccherini, E. Santi, D. Torri, F. Vergari, and M. Del Monte, “Long-term patterns of change in a vanishing cultural landscape: A GIS-based assessment,” *Ecol. Inform.*, vol. 37, pp. 38–51, 2017.

[72] H. M. Badjana, P. Olofsson, C. E. Woodcock, J. Helmschrot, K. Wala, and K. Akpagana, “Mapping and estimating land change between 2001 and 2013 in a heterogeneous landscape in West Africa: Loss of forestlands and capacity building opportunities,” *Int. J. Appl. Earth Obs. Geoinf.*, vol. 63, pp. 15–23, 2017, doi: https://doi.org/10.1016/j.jag.2017.07.006.

[73] R. Fuchs, P. H. Verburg, J. G. P. W. Clevers, and M. Herold, “The potential of old maps and encyclopaedias for reconstructing historic European land cover/use change,” *Appl. Geogr.*, vol. 59, pp. 43–55, 2015, doi: https://doi.org/10.1016/j.apgeog.2015.02.013.

[74] A. Carta, T. Taboada, and J. V Müller, “Diachronic analysis using aerial photographs across fifty years reveals significant land use and vegetation changes on a Mediterranean island,” *Appl. Geogr.*, vol. 98, pp. 78–86, 2018, doi: https://doi.org/10.1016/j.apgeog.2018.07.010.

[75] C. Wohlfart, B. Mack, G. Liu, and C. Kuenzer, “Multi-faceted land cover and land use change analyses in the

Yellow River Basin based on dense Landsat time series: Exemplary analysis in mining, agriculture, forest, and urban areas," *Appl. Geogr.*, vol. 85, pp. 73–88, 2017.

[76] E. Meron, "Pattern-formation approach to modelling spatially extended ecosystems," *Ecol. Modell.*, vol. 234, pp. 70–82, 2012, doi: https://doi.org/10.1016/j.ecolmodel.2011.05.035.

[77] R. Pelorosso, A. Leone, and L. Boccia, "Land cover and land use change in the Italian central Apennines: A comparison of assessment methods," *Appl. Geogr.*, vol. 29, no. 1, pp. 35–48, 2009, doi: https://doi.org/10.1016/j.apgeog.2008.07.003.

[78] M. Agnoletti, "Rural landscape, nature conservation and culture: Some notes on research trends and management approaches from a (southern) European perspective," *Landsc. Urban Plan.*, vol. 126, pp. 66–73, 2014.

[79] D. Statuto, P. Frederiksen, and P. Picuno, "Valorization of Agricultural by-products within the 'Energyscapes': Renewable energy as driving force in modeling rural landscape," *Nat. Resour. Res.*, vol. 28, no. 1, pp. 111–124, 2019.

[80] G. Modica, M. Vizzari, M. Pollino, C. R. Fichera, P. Zoccali, and S. Di Fazio, "Spatio-temporal analysis of the urban-rural gradient structure: An application in a Mediterranean mountainous landscape (Serra San Bruno, Italy)," *Earth Syst. Dyn.*, vol. 3, no. 2, pp. 263–279, 2012, doi: 10.5194/esd-3-263-2012.

[81] "European Commission (2019a) A European Green Deal." https://ec.europa.eu/info/strategy/priorities-2019-2024/european-green-deal_en. (accessed Dec. 20, 2022).

[82] "European Commission (2021b) Farm to Fork Strategy." https://ec.europa.eu/food/horizontal-topics/farm-fork-strategy_en. (accessed Dec. 20, 2022).

[83] H. Schebesta and J. J. L. Candel, "Game-changing potential of the EU's Farm to Fork Strategy," *Nat. Food*, vol. 1, no. 10, pp. 586–588, 2020, doi: 10.1038/s43016-020-00166-9.

[84] A. Sokolovska, "Using satellite remote sensing data to assess the status of urban areas (by example of the city of Kiev)," *Curr. Probl. Rem. Sens. Earth From Sp.*, vol. 1, no. 1, p. 1, 2014.

[85] D. Bailey, R. Billeter, S. Aviron, O. Schweiger, and F. Herzog, "The influence of thematic resolution on metric selection for biodiversity monitoring in agricultural landscapes," *Landsc. Ecol.*, vol. 22, pp. 461–473, 2007.

[86] A. B. Leitão, J. Miller, J. Ahern, and K. McGarigal, *Measuring landscapes: A planner's handbook*. Island press, 2012.

[87] V. Belenok, T. Noszczyk, L. Hebryn-Baidy, and S. Kryachok, “Investigating anthropogenically transformed landscapes with remote sensing,” *Remote Sens. Appl. Soc. Environ.*, vol. 24, p. 100635, 2021, doi: https://doi.org/10.1016/j.rsase.2021.100635.

[88] J. F. Palmer and R. E. Hoffman, “Rating reliability and representation validity in scenic landscape assessments,” *Landsc. Urban Plan.*, vol. 54, no. 1–4, pp. 149–161, 2001.

[89] J. Hyyppä *et al.*, “Algorithms and methods of airborne laser-scanning for forest measurements,” *Int. Arch. Photogramm. Remote Sens.*, vol. 36, p. 8, 2004.

[90] X. Liang *et al.*, “Possibilities of a personal laser scanning system for forest mapping and ecosystem services,” *Sensors*, vol. 14, no. 1, pp. 1228–1248, 2014.

[91] S. Chen, H. Liu, Z. Feng, C. Shen, and P. Chen, “Applicability of personal laser scanning in forestry inventory,” *PLoS One*, vol. 14, no. 2, pp. 1–22, 2019, doi: 10.1371/journal.pone.0211392.

[92] I. Oveland, M. Hauglin, F. Giannetti, N. Schipper Kjørsvik, and T. Gobakken, “Comparing three different ground based laser scanning methods for tree stem detection,” *Remote Sens.*, vol. 10, no. 4, p. 538, 2018.

[93] X. Liang *et al.*, “Possibilities of a personal laser scanning system for forest mapping and ecosystem services,” *Sensors (Switzerland)*, vol. 14, no. 1, pp. 1228–1248, 2014, doi: 10.3390/s140101228.

[94] K. Kanja, U. Karahalil, and B. Çil, “Modeling stand parameters for Pinus brutia (Ten.) using airborne LiDAR data: a case study in Bergama,” *J. Appl. Remote Sens.*, vol. 14, no. 2, p. 22205, 2020.

[95] K. Calders *et al.*, “Terrestrial laser scanning in forest ecology: Expanding the horizon,” *Remote Sens. Environ.*, vol. 251, p. 112102, 2020, doi: https://doi.org/10.1016/j.rse.2020.112102.

[96] J. Ryding, E. Williams, M. J. Smith, and M. P. Eichhorn, “Assessing handheld mobile laser scanners for forest surveys,” *Remote Sens.*, vol. 7, no. 1, pp. 1095–1111, 2015.

[97] E. Hyyppä *et al.*, “Accurate derivation of stem curve and volume using backpack mobile laser scanning,” *ISPRS J. Photogramm. Remote Sens.*, vol. 161, no. November 2019, pp. 246–262, 2020, doi: 10.1016/j.isprsjprs.2020.01.018.

[98] B. Apostol *et al.*, “Data collection methods for forest inventory: a comparison between an integrated conventional equipment and terrestrial laser scanning,” *Ann. For. Res.*, vol. 61, no. 2, pp. 189–202, 2018.

[99] J. Ryding, E. Williams, M. J. Smith, and M. P. Eichhorn, “Assessing handheld mobile laser scanners for forest surveys,” *Remote Sens.*, vol. 7, no. 1, pp. 1095–1111, 2015, doi: 10.3390/rs70101095.

[100] T. L. Potter, “Mobile laser scanning in forests: Mapping beneath the canopy.” University of Leicester, 2019.

[101] I. Balenović, X. Liang, L. Jurjević, J. Hyyppä, A. Seletković, and A. Kukko, “Hand-held personal laser scanning–current status and perspectives for forest inventory application,” *Croat. J. For. Eng. J. Theory Appl. For. Eng.*, vol. 42, no. 1, pp. 165–183, 2021.

[102] F. Giannetti *et al.*, “Integrating terrestrial and airborne laser scanning for the assessment of single-tree attributes in Mediterranean forest stands,” *Eur. J. Remote Sens.*, vol. 51, no. 1, pp. 795–807, 2018.

[103] S. Chen, H. Liu, Z. Feng, C. Shen, and P. Chen, “Applicability of personal laser scanning in forestry inventory,” *PLoS One*, vol. 14, no. 2, pp. 1–22, 2019, doi: 10.1371/journal.pone.0211392.

[104] B. Del Perugia, F. Giannetti, G. Chirici, and D. Travaglini, “Influence of scan density on the estimation of single-tree attributes by hand-held mobile laser scanning,” *Forests*, vol. 10, no. 3, pp. 1–13, 2019, doi: 10.3390/f10030277.

[105] C. Gollob, T. Ritter, and A. Nothdurft, “Forest inventory with long range and high-speed personal laser scanning (PLS) and simultaneous localization and mapping (SLAM) technology,” *Remote Sens.*, vol. 12, no. 9, p. 1509, 2020.

[106] N. Siefen, R. J. McCormick, A. M. Vogel, and K. Biegert, “Effects of laser scanner quality and tractor speed to characterise apple tree canopies,” *Smart Agric. Technol.*, vol. 4, p. 100173, 2023, doi: https://doi.org/10.1016/j.atech.2023.100173.

[107] A. F. Colaço, R. G. Trevisan, J. P. Molin, J. R. Rosell-Polo, and A. Escolà, “A method to obtain orange crop geometry information using a mobile terrestrial laser scanner and 3D modeling,” *Remote Sens.*, vol. 9, no. 8, pp. 10–13, 2017, doi: 10.3390/rs9080763.

[108] N. Tsoulias, S. Fountas, and M. Zude-Sasse, “Estimating the canopy volume using a 2D LiDAR in apple trees,” in *IV International Symposium on Horticulture in Europe-SHE2021 1327*, 2021, pp. 437–444.

[109] K. K. Saha, N. Tsoulias, and M. Zude-Sasse, “Estimation of leaf area of sweet cherry trees trained as spindle using ground based 2D mobile LiDAR system,” in *IV International Symposium on Horticulture in Europe-SHE2021 1327*, 2021, pp. 429–436.

[110] R. Sanz *et al.*, “LIDAR and non-LIDAR-based canopy parameters to estimate the leaf area in fruit trees and vineyard,” *Agric. For. Meteorol.*, vol. 260, pp. 229–239, 2018.

[111] J. Gené-Mola *et al.*, “Fruit detection in an apple orchard using a mobile terrestrial laser scanner,” *Biosyst. Eng.*,

vol. 187, pp. 171–184, 2019.

[112] N. Tsoulias, D. S. Paraforos, G. Xanthopoulos, and M. Zude-Sasse, “Apple shape detection based on geometric and radiometric features using a LiDAR laser scanner,” *Remote Sens.*, vol. 12, no. 15, p. 2481, 2020.

[113] M. Agnoletti, M. Tredici, and A. Santoro, “Biocultural diversity and landscape patterns in three historical rural areas of Morocco, Cuba and Italy,” *Biodivers. Conserv.*, vol. 24, pp. 3387–3404, 2015.

[114] J. Baudry and F. Baudry-Burel, “La mesure de la diversité spatiale. Relations avec la diversité spécifique. Utilisation dans les évaluations d’impact,” *Acta oecologica. Série Oecologia Appl. Montreuil*, vol. 3, no. 2, pp. 177–190, 1982.

[115] R. Cevasco and D. Moreno, “Rural landscapes: the historical roots of biodiversity,” *Ital. Hist. Rural landscapes Cult. values Environ. Rural Dev.*, pp. 141–152, 2013.

[116] Z. Naveh and Z. Naveh, “Culture and Landscape Conservation: A Landscape-Ecological Perspective. In: Gopal BP, Pathak P., Sayena KG (Eds.) Ecology Today: An Anthology of Contemporary Ecological Research International Scientific Publications, New Delhi, pp. 19–48,” *Transdiscipl. Challenges Landsc. Ecol. Restor. Ecol. An Anthol. with Forewords by E. Laszlo M. Antrop Epilogue by E. Allen*, pp. 249–280, 2007.

[117] M. Agnoletti, F. Emanueli, F. Corrieri, M. Venturi, and A. Santoro, “Monitoring traditional rural landscapes. The case of Italy,” *Sustain.*, vol. 11, no. 21, 2019, doi: 10.3390/su11216107.

[118] P. W. Chirwa and W. Mala, “Trees in the landscape: towards the promotion and development of traditional and farm forest management in tropical and subtropical regions,” *Agrofor. Syst.*, vol. 90, pp. 555–561, 2016.

[119] F. Aimar, P. Gullino, and M. Devecchi, “Towards reconstructing rural landscapes: A case study of Italian Mongardino,” *J. Rural Stud.*, vol. 88, pp. 446–461, 2021, doi: https://doi.org/10.1016/j.jrurstud.2021.06.021.

[120] F. Geri, D. Rocchini, and A. Chiarucci, “Landscape metrics and topographical determinants of large-scale forest dynamics in a Mediterranean landscape,” *Landsc. Urban Plan.*, vol. 95, no. 1–2, pp. 46–53, 2010.

[121] W. F. Laurance *et al.*, “Ecosystem decay of Amazonian forest fragments: a 22-year investigation,” *Conserv. Biol.*, vol. 16, no. 3, pp. 605–618, 2002.

[122] M. A. Polyakova *et al.*, “Scale-and taxon-dependent patterns of plant diversity in steppes of Khakassia, South Siberia (Russia),” *Biodivers. Conserv.*, vol. 25, pp. 2251–2273, 2016.

[123] P. D. Turtureanu *et al.*, “Scale-and taxon-dependent biodiversity patterns of dry grassland vegetation in Transylvania,” *Agric. Ecosyst. Environ.*, vol. 182, pp. 15–24, 2014.

[124] T. G. Benton, J. A. Vickery, and J. D. Wilson, “Farmland biodiversity: is habitat heterogeneity the key?,” *Trends Ecol. Evol.*, vol. 18, no. 4, pp. 182–188, 2003.

[125] F. Remondino, I. Toschi, and S. Orlandini, “Mobyle Mapping Systems: recenti sviluppi e caso applicativo,” *GEOmedia*, vol. 19, no. 4, 2015.

[126] F. Westling, K. Mahmud, J. Underwood, and I. Bally, “Replacing traditional light measurement with LiDAR based methods in orchards,” *Comput. Electron. Agric.*, vol. 179, no. July, 2020, doi: 10.1016/j.compag.2020.105798.

[127] S. Kaasalainen, H. Kaartinen, A. Kukko, K. Anttila, and A. Krooks, “Brief communication:" Application of mobile laser scanning in snow cover profiling,” *Cryosph. Discuss.*, vol. 4, no. 4, pp. 2513–2522, 2010.

[128] M. Vaaja, J. Hyyppä, A. Kukko, H. Kaartinen, H. Hyyppä, and P. Alho, “Mapping topography changes and elevation accuracies using a mobile laser scanner,” *Remote Sens.*, vol. 3, no. 3, pp. 587–600, 2011.

[129] L. Chang, X. Niu, T. Liu, J. Tang, and C. Qian, “GNSS/INS/LiDAR-SLAM integrated navigation system based on graph optimization,” *Remote Sens.*, vol. 11, no. 9, p. 1009, 2019.

[130] P. D. Groves, “Principles of GNSS, inertial, and multisensor integrated navigation systems, [Book review],” *IEEE Aerosp. Electron. Syst. Mag.*, vol. 30, no. 2, pp. 26–27, 2015.

[131] W. Liu, Z. Li, S. Sun, R. Malekian, Z. Ma, and W. Li, “Improving positioning accuracy of the mobile laser scanning in GPS-denied environments: An experimental case study,” *IEEE Sens. J.*, vol. 19, no. 22, pp. 10753–10763, 2019.

[132] C. Qian *et al.*, “An integrated GNSS/INS/LiDAR-SLAM positioning method for highly accurate forest stem mapping,” *Remote Sens.*, vol. 9, no. 1, pp. 1–16, 2017, doi: 10.3390/rs9010003.

[133] Q. Mao *et al.*, “A least squares collocation method for accuracy improvement of mobile LiDAR systems,” *Remote Sens.*, vol. 7, no. 6, pp. 7402–7424, 2015.

[134] C. Cabo, S. Del Pozo, P. Rodríguez-Gonzálvez, C. Ordóñez, and D. González-Aguilera, “Comparing terrestrial laser scanning (TLS) and wearable laser scanning (WLS) for individual tree modeling at plot level,” *Remote Sens.*, vol. 10, no. 4, p. 540, 2018.

[135] J. Tang *et al.*, “SLAM-Aided Stem Mapping for Forest Inventory with Small-Footprint Mobile LiDAR,” pp. 4588–4606, 2015, doi: 10.3390/f6124390.

[136] R. Selçuk, R. Nisanci, B. Uzun, A. Yalcin, H. Inan, and T. Yomralioglu, “Monitoring land-use changes by GIS

and remote sensing techniques: case study of Trabzon," in *Proceedings of 2nd FIG Regional Conference, Morocco*, 2003, pp. 1–11.

[137] T. S. Kachhwala, "Temporal monitoring of forest land for change detection and forest cover mapping through satellite remote sensing," in *Proceedings of the 6th Asian Conf. on Remote Sensing. Hyderabad, 1985*, 1985, pp. 77–83.

[138] K. Tansey, I. Chambers, A. Anstee, A. Denniss, and A. Lamb, "Object-oriented classification of very high resolution airborne imagery for the extraction of hedgerows and field margin cover in agricultural areas," *Appl. Geogr.*, vol. 29, no. 2, pp. 145–157, 2009, doi: https://doi.org/10.1016/j.apgeog.2008.08.004.

[139] J. Cihlar, "Land cover mapping of large areas from satellites: status and research priorities," *Int. J. Remote Sens.*, vol. 21, no. 6–7, pp. 1093–1114, 2000.

[140] C. P. Lo and J. Choi, "A hybrid approach to urban land use/cover mapping using Landsat 7 Enhanced Thematic Mapper Plus (ETM+) images," *Int. J. Remote Sens.*, vol. 25, no. 14, pp. 2687–2700, Jul. 2004, doi: 10.1080/01431160310001618428.

[141] C. O. Justice *et al.*, "The Moderate Resolution Imaging Spectroradiometer (MODIS): land remote sensing for global change research," *IEEE Trans. Geosci. Remote Sens.*, vol. 36, no. 4, pp. 1228–1249, 1998, doi: 10.1109/36.701075.

[142] D. P. Roy *et al.*, "Landsat-8: Science and product vision for terrestrial global change research," *Remote Sens. Environ.*, vol. 145, pp. 154–172, 2014, doi: https://doi.org/10.1016/j.rse.2014.02.001.

[143] P. J. Sellers *et al.*, "Remote sensing of the land surface for studies of global change: Models — algorithms — experiments," *Remote Sens. Environ.*, vol. 51, no. 1, pp. 3–26, 1995, doi: https://doi.org/10.1016/0034-4257(94)00061-Q.

[144] A. S. Belward and J. O. Skøien, "Who launched what, when and why; trends in global land-cover observation capacity from civilian earth observation satellites," *ISPRS J. Photogramm. Remote Sens.*, vol. 103, pp. 115–128, 2015.

[145] S. L. Ustin and E. M. Middleton, "Current and near-term advances in Earth observation for ecological applications," *Ecol. Process.*, vol. 10, pp. 1–57, 2021.

[146] C. E. Woodcock *et al.*, "Free access to Landsat imagery," *Science (80-.).*, vol. 320, no. 5879, p. 1011, 2008.

[147] M. A. Wulder, J. G. Masek, W. B. Cohen, T. R. Loveland, and C. E. Woodcock, "Opening the archive: How

free data has enabled the science and monitoring promise of Landsat," *Remote Sens. Environ.*, vol. 122, pp. 2–10, 2012.

[148] Z. Zhu *et al.*, "Benefits of the free and open Landsat data policy," *Remote Sens. Environ.*, vol. 224, pp. 382–385, 2019.

[149] Z. Zhu, "Change detection using landsat time series: A review of frequencies, preprocessing, algorithms, and applications," *ISPRS J. Photogramm. Remote Sens.*, vol. 130, pp. 370–384, 2017.

[150] A. Banskota, N. Kayastha, M. J. Falkowski, M. A. Wulder, R. E. Froese, and J. C. White, "Forest Monitoring Using Landsat Time Series Data: A Review," *Can. J. Remote Sens.*, vol. 40, no. 5, pp. 362–384, Sep. 2014, doi: 10.1080/07038992.2014.987376.

[151] C. E. Woodcock, T. R. Loveland, M. Herold, and M. E. Bauer, "Transitioning from change detection to monitoring with remote sensing: A paradigm shift," *Remote Sens. Environ.*, vol. 238, p. 111558, 2020.

[152] R. Shang *et al.*, "Near-real-time monitoring of land disturbance with harmonized Landsats 7–8 and Sentinel-2 data," *Remote Sens. Environ.*, vol. 278, p. 113073, 2022.

[153] X. Tang, E. L. Bullock, P. Olofsson, and C. E. Woodcock, "Can VIIRS continue the legacy of MODIS for near real-time monitoring of tropical forest disturbance?," *Remote Sens. Environ.*, vol. 249, p. 112024, 2020.

[154] J. Verbesselt, A. Zeileis, and M. Herold, "Near real-time disturbance detection using satellite image time series," *Remote Sens. Environ.*, vol. 123, pp. 98–108, 2012.

[155] Q. Xin, P. Olofsson, Z. Zhu, B. Tan, and C. E. Woodcock, "Toward near real-time monitoring of forest disturbance by fusion of MODIS and Landsat data," *Remote Sens. Environ.*, vol. 135, pp. 234–247, 2013.

[156] S. Ye, J. Rogan, Z. Zhu, and J. R. Eastman, "A near-real-time approach for monitoring forest disturbance using Landsat time series: Stochastic continuous change detection," *Remote Sens. Environ.*, vol. 252, p. 112167, 2021.

[157] M. C. Hansen and T. R. Loveland, "A review of large area monitoring of land cover change using Landsat data," *Remote Sens. Environ.*, vol. 122, pp. 66–74, 2012, doi: https://doi.org/10.1016/j.rse.2011.08.024.

[158] N. G. Pricope, K. L. Mapes, and K. D. Woodward, "Remote Sensing of Human–Environment Interactions in Global Change Research: A Review of Advances, Challenges and Future Directions," *Remote Sensing*, vol. 11, no. 23. 2019, doi: 10.3390/rs11232783.

[159] B. L. Turner, "The sustainability principle in global agendas: implications for understanding land-use/cover

change," *Geogr. J.*, pp. 133–140, 1997.

[160] J. R. Anderson, *A land use and land cover classification system for use with remote sensor data*, vol. 964. US Government Printing Office, 1976.

[161] J. S. Rawat and M. Kumar, "Monitoring land use/cover change using remote sensing and GIS techniques: A case study of Hawalbagh block, district Almora, Uttarakhand, India," *Egypt. J. Remote Sens. Sp. Sci.*, vol. 18, no. 1, pp. 77–84, 2015, doi: https://doi.org/10.1016/j.ejrs.2015.02.002.

[162] C. Homer *et al.*, "Completion of the 2001 national land cover database for the counterminous United States," *Photogramm. Eng. Remote Sensing*, vol. 73, no. 4, p. 337, 2007.

[163] J. G. Masek *et al.*, "North American forest disturbance mapped from a decadal Landsat record," *Remote Sens. Environ.*, vol. 112, no. 6, pp. 2914–2926, 2008.

[164] C. Huang, S. N. Goward, J. G. Masek, N. Thomas, Z. Zhu, and J. E. Vogelmann, "An automated approach for reconstructing recent forest disturbance history using dense Landsat time series stacks," *Remote Sens. Environ.*, vol. 114, no. 1, pp. 183–198, 2010.

[165] R. E. Kennedy, Z. Yang, and W. B. Cohen, "Detecting trends in forest disturbance and recovery using yearly Landsat time series: 1. LandTrendr—Temporal segmentation algorithms," *Remote Sens. Environ.*, vol. 114, no. 12, pp. 2897–2910, 2010.

[166] X. Tang, E. L. Bullock, P. Olofsson, S. Estel, and C. E. Woodcock, "Near real-time monitoring of tropical forest disturbance: New algorithms and assessment framework," *Remote Sens. Environ.*, vol. 224, pp. 202–218, 2019.

[167] M. Drusch *et al.*, "Sentinel-2: ESA's optical high-resolution mission for GMES operational services," *Remote Sens. Environ.*, vol. 120, pp. 25–36, 2012.

[168] J. G. Masek *et al.*, "Landsat 9: Empowering open science and applications through continuity," *Remote Sens. Environ.*, vol. 248, p. 111968, 2020.

[169] H. Huang and D. P. Roy, "Characterization of Planetscope-0 Planetscope-1 surface reflectance and normalized difference vegetation index continuity," *Sci. Remote Sens.*, vol. 3, p. 100014, 2021, doi: https://doi.org/10.1016/j.srs.2021.100014.

[170] J. Li and D. P. Roy, "A Global Analysis of Sentinel-2A, Sentinel-2B and Landsat-8 Data Revisit Intervals and Implications for Terrestrial Monitoring," *Remote Sensing*, vol. 9, no. 9. 2017, doi: 10.3390/rs9090902.

[171] D. P. Roy, H. Huang, R. Houborg, and V. S. Martins, “A global analysis of the temporal availability of PlanetScope high spatial resolution multi-spectral imagery,” *Remote Sens. Environ.*, vol. 264, p. 112586, 2021, doi: https://doi.org/10.1016/j.rse.2021.112586.

[172] G. Iovino, “‘Le fonti informative per il monitoraggio del consumo di suolo.,’” 2014.

[173] K. Rosina, F. Batista e Silva, P. Vizcaino, M. Marín Herrera, S. Freire, and M. Schiavina, “Increasing the detail of European land use/cover data by combining heterogeneous data sets,” *Int. J. Digit. Earth*, vol. 13, no. 5, pp. 602–626, May 2020, doi: 10.1080/17538947.2018.1550119.

[174] T. Langanke, “Copernicus Land Monitoring Service—High Resolution Layer Imperviousness,” 2016. https://land.copernicus.eu/pan-european/high-resolution-layers.

[175] F. Langanke, T., Ramminger, G., Buzzo, G., & Berndt, “Copernicus Land Monitoring Service—High Resolution Layer Forest: Product Specifications Document-European Environmental Agency: Copenhagen, Denmark,” 2017. .

[176] “Istituto Superiore per la Protezione e la Ricerca Ambientale (2014), audizione dell’istituto superiore per la protezione e la ricerca ambientale (ISPRA) presso la commissione agricoltura, congiuntamente con la commissione ambiente, della camera sul consum.” .

[177] F. B. and N. G. and I. M. and A. S. and M. Munafò, “Strumenti del Sistema Nazionale per la Protezione dell’Ambiente per la gestione dei dati sul consumo di suolo.” EUT - Edizioni Università di Trieste, 2014.

[178] S. Bauwens, H. Bartholomeus, K. Calders, and P. Lejeune, “Forest inventory with terrestrial LiDAR: A comparison of static and hand-held mobile laser scanning,” *Forests*, vol. 7, no. 6, p. 127, 2016.

[179] R. J. L. Hartley *et al.*, “Assessing the Potential of Backpack-Mounted Mobile Laser Scanning Systems for Tree Phenotyping,” *Remote Sensing*, vol. 14, no. 14. 2022, doi: 10.3390/rs14143344.

[180] X. Liu, Y. Wang, F. Kang, Y. Yue, and Y. Zheng, “Canopy parameter estimation of citrus grandis var. Longanyou based on lidar 3d point clouds,” *Remote Sens.*, vol. 13, no. 9, 2021, doi: 10.3390/rs13091859.

[181] P. Ettehadi Osgouei, E. Sertel, and M. E. Kabadayı, “Integrated usage of historical geospatial data and modern satellite images reveal long-term land use/cover changes in Bursa/Turkey, 1858-2020.,” *Sci. Rep.*, vol. 12, no. 1, p. 9077, May 2022, doi: 10.1038/s41598-022-11396-1.

[182] S. Barwicka and M. Milecka, “The use of selected landscape metrics to evaluate the transformation of the rural landscape as a result of the development of the mining function—a case study of the puchaczów commune,”

Sustain., vol. 13, no. 21, 2021, doi: 10.3390/su132112279.

[183] P. Picuno, G. Cillis, and D. Statuto, "Investigating the time evolution of a rural landscape: How historical maps may provide environmental information when processed using a GIS," *Ecol. Eng.*, vol. 139, p. 105580, 2019, doi: https://doi.org/10.1016/j.ecoleng.2019.08.010.

[184] A. Müller, R. Olschewski, C. Unterberger, and T. Knoke, "The valuation of forest ecosystem services as a tool for management planning – A choice experiment," *J. Environ. Manage.*, vol. 271, p. 111008, 2020, doi: 10.1016/j.jenvman.2020.111008.

[185] E. Hyyppä *et al.*, "Under-canopy UAV laser scanning for accurate forest field measurements," *ISPRS J. Photogramm. Remote Sens.*, vol. 164, no. April, pp. 41–60, 2020, doi: 10.1016/j.isprsjprs.2020.03.021.

[186] H. Luo, L. Wang, C. Wu, and L. Zhang, "An Improved Method for Impervious Surface Mapping Incorporating LiDAR Data and High-Resolution Imagery at Different Acquisition Times," *Remote Sens.*, vol. 10, 2018, doi: 10.3390/rs10091349.

[187] A. S. Maguya *et al.*, "Moving Voxel Method for Estimating Canopy Base Height from Airborne Laser Scanner Data," *Remote Sens.*, vol. 7, pp. 8950–8972, 2015, doi: 10.3390/rs7078950.

[188] E. Sibona *et al.*, "Direct measurement of tree height provides different results on the assessment of LiDAR accuracy," *Forests*, vol. 8, no. 1, pp. 1–12, 2017, doi: 10.3390/f8010007.

[189] T. de Conto, K. Olofsson, E. B. Görgens, L. C. E. Rodriguez, and G. Almeida, "Performance of stem denoising and stem modelling algorithms on single tree point clouds from terrestrial laser scanning," *Comput. Electron. Agric.*, vol. 143, no. October, pp. 165–176, 2017, doi: 10.1016/j.compag.2017.10.019.

[190] C. Liu, Y. Xing, J. Duanmu, and X. Tian, "Evaluating different methods for estimating diameter at breast height from terrestrial laser scanning," *Remote Sens.*, vol. 10, no. 4, pp. 1–20, 2018, doi: 10.3390/rs10040513.

[191] J. Čerňava, J. Tuček, M. Koreň, and M. Mokroš, "Estimation of diameter at breast height from mobile laser scanning data collected under a heavy forest canopy," *J. For. Sci.*, vol. 63, no. 9, pp. 433–441, 2017, doi: 10.17221/28/2017-JFS.

[192] M. Forsman, J. Holmgren, and K. Olofsson, "Tree stem diameter estimation from mobile laser scanning using line-wise intensity-based clustering," *Forests*, vol. 7, no. 9, 2016, doi: 10.3390/f7090206.

[193] M. Pierzchała, P. Giguère, and R. Astrup, "Mapping forests using an unmanned ground vehicle with 3D LiDAR and graph-SLAM," *Comput. Electron. Agric.*, vol. 145, no. February 2017, pp. 217–225, 2018, doi:

10.1016/j.compag.2017.12.034.

[194] S. Tao *et al.*, “Segmenting tree crowns from terrestrial and mobile LiDAR data by exploring ecological theories,” *ISPRS J. Photogramm. Remote Sens.*, vol. 110, pp. 66–76, 2015, doi: 10.1016/j.isprsjprs.2015.10.007.

[195] D. C. 3D P. C. and M. P. S. O. S. P. 2016. A. online: https://www. danielgm. net/index. ph. (accessed on 9 M. 2019). Daniel Girardeau-Montaut, “No Title.”

[196] Y. K. Karna, T. D. Penman, C. Aponte, and L. T. Bennett, “Assessing legacy effects of wildfires on the crown structure of fire-tolerant eucalypt trees using airborne LiDAR data,” *Remote Sens.*, vol. 11, no. 20, 2019, doi: 10.3390/rs11202433.

[197] K. T. Moe, T. Owari, N. Furuya, and T. Hiroshima, “Comparing individual tree height information derived from field surveys, LiDAR and UAV-DAP for high-value timber species in Northern Japan,” *Forests*, vol. 11, no. 2, pp. 1–16, 2020, doi: 10.3390/f11020223.

[198] J. Trochta, M. Kruček, T. Vrška, and K. Kraâl, “3D Forest: An application for descriptions of three-dimensional forest structures using terrestrial LiDAR,” *PLoS One*, vol. 12, no. 5, 2017, doi: 10.1371/journal.pone.0176871.

[199] K. Itakura and F. Hosoi, “Automatic tree detection from three-dimensional images reconstructed from 360 spherical camera using YOLO v2,” *Remote Sens.*, vol. 12, no. 6, 2020, doi: 10.3390/rs12060988.

[200] W. Zhang *et al.*, “A novel approach for the detection of standing tree stems from plot-level terrestrial laser scanning data,” *Remote Sens.*, vol. 11, no. 2, pp. 1–20, 2019, doi: 10.3390/rs11020211.

[201] J. Holmgren, M. Tulldahl, J. Nordlöf, E. Willén, and H. Olsson, “Mobile laser scanning for estimating tree stem diameter using segmentation and tree spine calibration,” *Remote Sens.*, vol. 11, no. 23, pp. 1–18, 2019, doi: 10.3390/rs11232781.

[202] S. Srinivasan, S. C. Popescu, M. Eriksson, R. D. Sheridan, and N. W. Ku, “Terrestrial laser scanning as an effective tool to retrieve tree level height, crown width, and stem diameter,” *Remote Sens.*, vol. 7, no. 2, pp. 1877–1896, 2015, doi: 10.3390/rs70201877.

[203] P. Tompalski, J. C. White, N. C. Coops, and M. A. Wulder, “Quantifying the contribution of spectral metrics derived from digital aerial photogrammetry to area-based models of forest inventory attributes,” *Remote Sens. Environ.*, vol. 234, no. October, p. 111434, 2019, doi: 10.1016/j.rse.2019.111434.

[204] A. Zaforemska, W. Xiao, and R. Gaulton, “Individual tree detection from uav lidar data in a mixed species woodland,” *Int. Arch. Photogramm. Remote Sens. Spat. Inf. Sci. - ISPRS Arch.*, vol. 42, no. 2/W13, pp. 657–

663, 2019, doi: 10.5194/isprs-archives-XLII-2-W13-657-2019.

[205] A. P. D. Corte *et al.*, “Measuring individual tree diameter and height using gatoreye high-density UAV-lidar in an integrated crop-livestock-forest system,” *Remote Sens.*, vol. 12, no. 5, 2020, doi: 10.3390/rs12050863.

[206] S. Puliti, J. Breidenbach, and R. Astrup, “Estimation of forest growing stock volume with UAV laser scanning data: Can it be done without field data?,” *Remote Sens.*, vol. 12, no. 8, 2020, doi: 10.3390/RS12081245.

[207] M. Mohan *et al.*, “Individual tree detection from unmanned aerial vehicle (UAV) derived canopy height model in an open canopy mixed conifer forest,” *Forests*, vol. 8, no. 9, pp. 1–17, 2017, doi: 10.3390/f8090340.

[208] Y. Wang *et al.*, “Is field-measured tree height as reliable as believed – A comparison study of tree height estimates from field measurement, airborne laser scanning and terrestrial laser scanning in a boreal forest,” *ISPRS J. Photogramm. Remote Sens.*, vol. 147, no. November 2018, pp. 132–145, 2019, doi: 10.1016/j.isprsjprs.2018.11.008.

[209] B. Brede *et al.*, “Non-destructive tree volume estimation through quantitative structure modelling: Comparing UAV laser scanning with terrestrial LIDAR,” *Remote Sens. Environ.*, vol. 233, p. 111355, 2019.

[210] M. Mokroš *et al.*, “Novel low-cost mobile mapping systems for forest inventories as terrestrial laser scanning alternatives,” *Int. J. Appl. Earth Obs. Geoinf.*, vol. 104, 2021, doi: 10.1016/j.jag.2021.102512.

[211] A. Kukko, H. Kaartinen, J. Hyyppä, and Y. Chen, “Multiplatform mobile laser scanning: Usability and performance,” *Sensors (Switzerland)*, vol. 12, no. 9, pp. 11712–11733, 2012, doi: 10.3390/s120911712.

[212] C. Gollob, T. Ritter, C. Wassermann, and A. Nothdurft, “Influence of scanner position and plot size on the accuracy of tree detection and diameter estimation using terrestrial laser scanning on forest inventory plots,” *Remote Sens.*, vol. 11, no. 13, p. 1602, 2019.

[213] K. S. 2, “SLAM Technology.” https://www.kaarta.com/products/stencil-2-for-rapid-long-range-mobile-mapping/ (accessed Mar. 01, 2022).

[214] M. Krůček, K. Král, K. C. Cushman, A. Missarov, and J. R. Kellner, “Supervised segmentation of ultra-high-density drone lidar for large-area mapping of individual trees,” *Remote Sens.*, vol. 12, no. 19, pp. 1–16, 2020, doi: 10.3390/rs12193260.

[215] R. B. Rusu and S. Cousins, “3D is here: Point Cloud Library (PCL),” *Proc. - IEEE Int. Conf. Robot. Autom.*, pp. 1–4, 2011, doi: 10.1109/ICRA.2011.5980567.

[216] T. Hackel, J. D. Wegner, and K. Schindler, “Contour detection in unstructured 3D point clouds,” no. 1610-

1618. 10.1109/CVPR.2016.178., 2016.

[217] R Core Team, “R: A language and environment for statistical computing,” *R Foundation for Statistical Computing*, 2021. .

[218] N. Chernov and C. Lesort, “Fitting circles and lines by least squares: theory and experiment,” *Chernov, Nikolai, Claire Lesort. “Least squares fitting circles.” J. Math. Imaging Vis. 23.3 239-252. DOI10.1007/s10851-005-0482-8*, pp. 1–23, 2008.

[219] B. Lecigne, S. Delagrange, and C. Messier, “Exploring trees in three dimensions: VoxR, a novel voxel-based R package dedicated to analysing the complex arrangement of tree crowns,” *Ann. Bot.*, vol. 121, no. 4, pp. 589–601, 2018, doi: 10.1093/aob/mcx095.

[220] A. Fernández-Sarría, L. Martínez, B. Velázquez-Martí, M. Sajdak, J. Estornell, and J. A. Recio, “Different methodologies for calculating crown volumes of Platanus hispanica trees using terrestrial laser scanner and a comparison with classical dendrometric measurements,” *Comput. Electron. Agric.*, vol. 90, pp. 176–185, 2013, doi: 10.1016/j.compag.2012.09.017.

[221] M. Åkerblom, P. Raumonen, M. Kaasalainen, and E. Casella, “Analysis of geometric primitives in quantitative structure models of tree stems,” *Remote Sens.*, vol. 7, no. 4, pp. 4581–4603, 2015, doi: 10.3390/rs70404581.

[222] J.-R. Roussel *et al.*, “lidR: An R package for analysis of Airborne Laser Scanning (ALS) data,” *Remote Sens. Environ.*, vol. 251, p. 112061, 2020, doi: https://doi.org/10.1016/j.rse.2020.112061.

[223] C. A. Silva *et al.*, “Imputation of individual longleaf pine (Pinus palustris Mill.) tree attributes from field and LiDAR data,” *Can. J. Remote Sens.*, vol. 42, no. 5, pp. 554–573, 2016.

[224] J. Shao *et al.*, “SLAM-aided forest plot mapping combining terrestrial and mobile laser scanning,” *ISPRS J. Photogramm. Remote Sens.*, vol. 163, no. May, pp. 214–230, 2020, doi: 10.1016/j.isprsjprs.2020.03.008.

[225] C. Vatandaşlar and M. Zeybek, “Extraction of forest inventory parameters using handheld mobile laser scanning: A case study from Trabzon, Turkey,” *Meas. J. Int. Meas. Confed.*, vol. 177, no. February, p. 109328, 2021, doi: 10.1016/j.measurement.2021.109328.

[226] I. Volpi, S. Marchi, R. Petacchi, K. Hoxha, and D. Guidotti, “Detecting olive grove abandonment with Sentinel-2 and machine learning: The development of a web-based tool for land management,” *Smart Agric. Technol.*, vol. 3, no. February 2022, p. 100068, 2023, doi: 10.1016/j.atech.2022.100068.

[227] A. L. Palazzo and O. Aristone, “Peri-Urban Matters. Changing Olive Growing Patterns in Central Italy,”

Sustain., vol. 9, no. 4, 2017, doi: 10.3390/su9040638.

[228] E. Belcore, S. Angeli, E. Colucci, M. A. Musci, and I. Aicardi, "Precision agriculture workflow, from data collection to data management using FOSS tools: An application in Northern Italy vineyard," *ISPRS Int. J. Geo-Information*, vol. 10, no. 4, 2021, doi: 10.3390/ijgi10040236.

[229] Y. Malhi *et al.*, "New perspectives on the ecology of tree structure and tree communities through terrestrial laser scanning," *Interface Focus*, vol. 8, no. 2, 2018, doi: 10.1098/rsfs.2017.0052.

[230] D. Panagiotidis, A. Abdollahnejad, and M. Slavík, "3D point cloud fusion from UAV and TLS to assess temperate managed forest structures," *Int. J. Appl. Earth Obs. Geoinf.*, vol. 112, no. July, p. 102917, 2022, doi: 10.1016/j.jag.2022.102917.

[231] Z. Yan *et al.*, "A Concave Hull Methodology for Calculating the Crown Volume of Individual Trees Based on Vehicle-Borne LiDAR Data," *Forestry*, vol. 11, no. 1, pp. 18–35, 2019, doi: 10.3390/rs11060623.

[232] Agriculture and rural development, "Geographical indications and quality schemes explained." https://agriculture.ec.europa.eu/farming/geographical-indications-and-quality-schemes/geographical-indications-and-quality-schemes-explained_en.

[233] https://www.oliocartocetodop.it/, "CONSORZIO OLIO DOP CARTOCETO." .

[234] D. C. 3D P. C. and M. P. S. O. S. P. 2016. A. online: https://www. danielgm. net/index. ph. Daniel Girardeau-Montaut, "No Title." .

[235] W. Zhang *et al.*, "An easy-to-use airborne LiDAR data filtering method based on cloth simulation," *Remote Sens.*, vol. 8, no. 6, pp. 1–22, 2016, doi: 10.3390/rs8060501.

[236] L. Korhonen, J. Vauhkonen, A. Virolainen, A. Hovi, and I. Korpela, "Estimation of tree crown volume from airborne lidar data using computational geometry," *Int. J. Remote Sens.*, vol. 34, no. 20, pp. 7236–7248, 2013, doi: 10.1080/01431161.2013.817715.

[237] W. Lin, Y. Meng, Z. Qiu, S. Zhang, and J. Wu, "Measurement and calculation of crown projection area and crown volume of individual trees based on 3D laser-scanned point-cloud data," *Int. J. Remote Sens.*, vol. 38, no. 4, pp. 1083–1100, 2017, doi: 10.1080/01431161.2016.1265690.

[238] J. Wu and R. Hobbs, "Key issues and research priorities in landscape ecology: an idiosyncratic synthesis," *Landsc. Ecol.*, vol. 17, no. 4, pp. 355–365, 2002.

[239] Z. Mao, J. Centanni, F. Pommereau, A. Stokes, and C. Gaucherel, "Maintaining biodiversity promotes the

multifunctionality of social-ecological systems: holistic modelling of a mountain system," *Ecosyst. Serv.*, vol. 47, p. 101220, 2021.

[240] J. A. Gómez, T. A. Sobrinho, J. V Giráldez, and E. Fereres, "Soil management effects on runoff, erosion and soil properties in an olive grove of Southern Spain," *Soil Tillage Res.*, vol. 102, no. 1, pp. 5–13, 2009.

[241] J. A. Gómez, J. Infante-Amate, M. González de Molina, T. Vanwalleghem, E. V Taguas, and I. Lorite, "Olive cultivation, its impact on soil erosion and its progression into yield impacts in Southern Spain in the past as a key to a future of increasing climate uncertainty," *Agriculture*, vol. 4, no. 2, pp. 170–198, 2014.

[242] I. Bogunovic *et al.*, "Land management impacts on soil properties and initial soil erosion processes in olives and vegetable crops," *J. Hydrol. Hydromechanics*, vol. 68, no. 4, pp. 328–337, 2020.

[243] E. Brunori, L. Salvati, A. Antogiovanni, and R. Biasi, "Worrying about 'vertical landscapes': Terraced olive groves and ecosystem services in marginal land in central Italy," *Sustain.*, vol. 10, no. 4, pp. 10–13, 2018, doi: 10.3390/su10041164.

[244] A. J. Carpio, J. Castro, V. Mingo, and F. S. Tortosa, "Herbaceous cover enhances the squamate reptile community in woody crops," *J. Nat. Conserv.*, vol. 37, pp. 31–38, 2017.

[245] R. Pizzolotto, A. Mazzei, T. Bonacci, S. Scalercio, N. Iannotta, and P. Brandmayr, "Ground beetles in Mediterranean olive agroecosystems: Their significance and functional role as bioindicators (Coleoptera, Carabidae)," *PLoS One*, vol. 13, no. 3, p. e0194551, Mar. 2018, [Online]. Available: https://doi.org/10.1371/journal.pone.0194551.

[246] H. Y. and B. O. V. and Y. Hürol, "The conservation of traditional olive oil mills in Cyprus," *J. Archit. Conserv.*, vol. 24,2, no. Routledge, pp. 105–133, 2018, doi: 10.1080/13556207.2018.1483551.

[247] F. Duarte, N. Jones, and L. Fleskens, "Traditional olive orchards on sloping land: sustainability or abandonment?," *J. Environ. Manage.*, vol. 89, no. 2, pp. 86–98, 2008.

[248] J. I. Pulido-Fernández, J. Casado-Montilla, and I. Carrillo-Hidalgo, "Introducing olive-oil tourism as a special interest tourism," *Heliyon*, vol. 5, no. 12, p. e02975, 2019, doi: https://doi.org/10.1016/j.heliyon.2019.e02975.

[249] M. G. Millán, M. del P. Pablo-Romero, and J. Sánchez-Rivas, "Oleotourism as a sustainable product: An analysis of its demand in the south of Spain (Andalusia)," *Sustainability*, vol. 10, no. 1, p. 101, 2018.

[250] V. M. Moreno, J. M. Q. Rubio, and I. R. Guerra, "Potencial del oleoturismo como diversificación económica del sector cooperativo agrario: el caso español," *Rev. Ciencias Soc.*, vol. 17, no. 3, pp. 533–541, 2011.

[251] G. Di Vita, M. D'Amico, G. La Via, and E. Caniglia, "Quality Perception of PDO extra-virgin Olive Oil: Which attributes most influence Italian consumers?," *Agric. Econ. Rev.*, vol. 14, no. 389-2016–23498, pp. 46–58, 2013.

[252] Y. Erraach, S. Sayadi, A. C. Gomez, and C. Parra-Lopez, "Consumer-stated preferences towards Protected Designation of Origin (PDO) labels in a traditional olive-oil-producing country: The case of Spain," *New Medit*, vol. 13, no. 4, pp. 11–19, 2014.

[253] A. W. Hegnes, "The map and the terroir: Adapting geographical boundaries for PDO and PGI in Norway," *Br. Food J.*, 2019.

[254] N. Zaccarelli, I. Petrosillo, G. Zurlini, and K. H. Riitters, "Source/sink patterns of disturbance and cross-scale mismatches in a panarchy of social-ecological landscapes," *Ecol. Soc.*, vol. 13, no. 1, 2008.

[255] L. Ponti, A. P. Gutierrez, P. M. Ruti, and A. Dell'Aquila, "Fine-scale ecological and economic assessment of climate change on olive in the Mediterranean Basin reveals winners and losers," *Proc. Natl. Acad. Sci.*, vol. 111, no. 15, pp. 5598–5603, 2014.

[256] J. Berkes, Fikret and Folke, Carl and Colding, "Linking social and ecological systems: management practices and social mechanisms for building resilience," *Cambridge Univ. Press*, 2000.

[257] E. Brunori, M. Maesano, F. V. Moresi, G. Matteucci, R. Biasi, and G. Scarascia Mugnozza, "The hidden land conservation benefits of olive-based (Olea europaea L.) landscapes: An agroforestry investigation in the southern Mediterranean (Calabria region, Italy)," *L. Degrad. Dev.*, vol. 31, no. 7, pp. 801–815, 2020.

[258] J. Infante-Amate *et al.*, "The making of olive landscapes in the south of Spain. A history of continuous expansion and intensification," in *Biocultural diversity in Europe*, Springer, 2016, pp. 157–179.

[259] J. Guerrero-Casado, A. J. Carpio, F. S. Tortosa, and A. J. Villanueva, "Environmental challenges of intensive woody crops: The case of super high-density olive groves," *Sci. Total Environ.*, vol. 798, p. 149212, 2021.

[260] M. Borrello, L. Cecchini, R. Vecchio, F. Caracciolo, L. Cembalo, and B. Torquati, "Agricultural landscape certification as a market-driven tool to reward the provisioning of cultural ecosystem services," *Ecol. Econ.*, vol. 193, p. 107286, 2022.

[261] C. M. Díez, J. Moral, D. Cabello, P. Morello, L. Rallo, and D. Barranco, "Cultivar and tree density as key factors in the long-term performance of super high-density olive orchards," *Front. Plant Sci.*, vol. 7, p. 1226, 2016.

[262] M. A, *Olivicoltura*, Ramo Edito. Rome, 1972.

[263] H. Mairech *et al.*, "Is new olive farming sustainable? A spatial comparison of productive and environmental performances between traditional and new olive orchards with the model OliveCan," *Agric. Syst.*, vol. 181, p. 102816, 2020.

[264] M. Orciani, V. Frazzica, L. Colosi, and F. Galletti, "Gregoriano Cadastre : transformation of old maps into Geographical Information System and their contribution in terms of acquisition , processing and communication of historical data," vol. 2, no. 2, pp. 92–104, 2007.

[265] L. Rallo, "The olive industry in Spain," *Proc. Olivebioteq*, pp. 5–10, 2006.

[266] E. V Taguas *et al.*, "Opportunities of super high-density olive orchard to improve soil quality: Management guidelines for application of pruning residues," *J. Environ. Manage.*, vol. 293, p. 112785, 2021, doi: https://doi.org/10.1016/j.jenvman.2021.112785.

[267] P. G. Angold *et al.*, "Biodiversity in urban habitat patches," *Sci. Total Environ.*, vol. 360, no. 1–3, pp. 196–204, 2006, doi: 10.1016/j.scitotenv.2005.08.035.

[268] I. De la Hera, I and Unanue, A and Aguirre, "Effects of area, age and vegetation cover on breeding avian species richness in urban parks from Vitoria-Gasteiz," *Munibe (Ciencias Nat.*, vol. 57, pp. 195-206, 2009.

[269] M. Luck and J. Wu, "A gradient analysis of urban landscape pattern: A case study from the Phoenix metropolitan region, Arizona, USA," *Landsc. Ecol.*, vol. 17, no. 4, pp. 327–339, 2002, doi: 10.1023/A:1020512723753.

[270] F. Malandra, A. Vitali, C. Urbinati, and M. Garbarino, "70 Years of Land Use / Land Cover Changes in the Apennines (Italy): A Meta-Analysis," pp. 1–15, 2018, doi: 10.3390/f9090551.

[271] M. A. K. Gillespie *et al.*, "A method for the objective selection of landscape-scale study regions and sites at the national level," *Methods Ecol. Evol.*, vol. 8, no. 11, pp. 1468–1476, 2017, doi: 10.1111/2041-210X.12779.

[272] E. Bielecka, "Gis spatial analysis modeling for land use change. A bibliometric analysis of the intellectual base and trends," *Geosci.*, vol. 10, no. 11, pp. 1–21, 2020, doi: 10.3390/geosciences10110421.

[273] J. G. Garden, C. A. Mcalpine, H. P. Possingham, and D. N. Jones, "Habitat structure is more important than vegetation composition for local-level management of native terrestrial reptile and small mammal species living in urban remnants: A case study from Brisbane, Australia," *Austral Ecol.*, vol. 32, no. 6, pp. 669–685, 2007, doi: 10.1111/j.1442-9993.2007.01750.x.

[274] M. Alberti, J. M. Marzluff, E. Shulenberger, G. Bradley, C. Ryan, and C. Zumbrunnen, “Integrating humans into ecology: Opportunities and challenges for studying urban ecosystems,” *Urban Ecol. An Int. Perspect. Interact. Between Humans Nat.*, vol. 53, no. 12, pp. 143–158, 2008, doi: 10.1007/978-0-387-73412-5_9.

[275] R. L. Pressey and M. C. Bottrill, “Approaches to landscape-and seascape-scale conservation planning: convergence, contrasts and challenges,” *Oryx*, vol. 43, no. 4, pp. 464–475, 2009.

[276] S. Zielinski *et al.*, “An Integrated Method for Landscape Assessment: Application to Santiago de Cuba Bay, Cuba,” *Sustainability*, vol. 13, no. 9, p. 4773, 2021.

[277] Adminstat ITALIA, “Adminstat ITALIA.” https://ugeo.urbistat.com/AdminStat/it/it/demografia/dati-sintesi/cartoceto/41010/4 (accessed Oct. 10, 2022).

[278] Marche Region, “Land Department of Marche Region.” https://www.regione.marche.it/Regione-Utile/Paesaggio-Territorio-Urbanistica/Cartografia/Repertorio/Cartausosuolo10000_78-84.

[279] G. Nazionale, “Available online: http://www. pcn. minambiente. it,” *GN (accessed 17 March 2009)*.

[280] AGEA, “Italian Agricultural Payments Agency.” www.agea.gov.it.

[281] R. T. T. Forman and M. Godron, “Patches and structural components for a landscape ecology,” *Bioscience*, vol. 31, no. 10, pp. 733–740, 1981.

[282] V. Ingegnoli, *Landscape Bionomics Biological-Integrated Landscape Ecology*. .

[283] S. Br and M. Kubacka, “Landscape Diversity and the Directions of Its Protection in Poland Illustrated with an Example of Wielkopolskie Voivodeship,” 2021.

[284] A. Marche, “Agenzia Servizi Settore Agroalimentare delle Marche.” http://www.assam.marche.it/en/ http://www.meteo.marche.it/blogmeteoassam.aspx?postid=5843b211-9043-4aaa-929e-ef0da7ec0b2b (accessed Oct. 01, 2022).

[285] S. Gay *et al.*, “Final report on the project’Sustainable Agriculture and Soil Conservation (SoCo)’,” Joint Research Centre (Seville site), 2009.

[286] T. Bernhardsen, *Geographic information systems: an introduction*. John Wiley & Sons, 2002.

[287] S. Landi *et al.*, “Impact of Super-High Density Olive Orchard Management System on Soil Free-Living and Plant-Parasitic Nematodes in Central and South Italy,” *Animals*, vol. 12, no. 12, p. 1551, 2022.

[288] M. Vieri and D. Sarri, “Criteria for introducing mechanical harvesting of oil olives : results of a five-year

project in Central Italy," no. November 2014, 2010.

[289] P. Szarek-Iwaniuk, A. Dawidowicz, and A. Senetra, "Methodology for Precision Land Use Mapping towards Sustainable Urbanized Land Development," *Int. J. Environ. Res. Public Health*, vol. 19, no. 6, p. 3633, 2022.

[290] D. Lu, P. Mausel, E. Brondízio, and E. Moran, "Change detection techniques," *Int. J. Remote Sens.*, vol. 25, no. 12, pp. 2365–2401, Jun. 2004, doi: 10.1080/0143116031000139863.

[291] M. Vizzari, "Spatio-temporal analysis using urban-rural gradient modelling and landscape metrics," *Lect. Notes Comput. Sci. (including Subser. Lect. Notes Artif. Intell. Lect. Notes Bioinformatics)*, vol. 6782 LNCS, no. PART 1, pp. 103–118, 2011, doi: 10.1007/978-3-642-21928-3_8.

[292] G. Maggiore, T. Semeraro, R. Aretano, L. De Bellis, and A. Luvisi, "GIS Analysis of Land-Use Change in Threatened Landscapes by Xylella fastidiosa," pp. 1–24, doi: 10.3390/su11010253.

[293] E. Andrieu, S. Ladet, W. Heintz, and M. Deconchat, "History and spatial complexity of deforestation and logging in small private forests," *Landsc. Urban Plan.*, vol. 103, no. 2, pp. 109–117, 2011, doi: https://doi.org/10.1016/j.landurbplan.2011.06.005.

[294] S. Di Fazio, G. Modica, and P. Zoccali, "Evolution trends of land use/land cover in a Mediterranean forest landscape in Italy," *Lect. Notes Comput. Sci. (including Subser. Lect. Notes Artif. Intell. Lect. Notes Bioinformatics)*, vol. 6782 LNCS, no. PART 1, pp. 284–299, 2011, doi: 10.1007/978-3-642-21928-3_20.

[295] J.-P. Puyravaud, "Standardizing the calculation of the annual rate of deforestation," *For. Ecol. Manage.*, vol. 177, no. 1, pp. 593–596, 2003, doi: https://doi.org/10.1016/S0378-1127(02)00335-3.

[296] G. Modica, S. Praticò, and S. Di Fazio, "Abandonment of traditional terraced landscape: A change detection approach (a case study in Costa Viola, Calabria, Italy)," *L. Degrad. Dev.*, vol. 28, no. 8, pp. 2608–2622, 2017, doi: 10.1002/ldr.2824.

[297] U. Walz, "Indicators to monitor the structural diversity of landscapes," *Ecol. Modell.*, vol. 295, pp. 88–106, 2015.

[298] A. Lausch *et al.*, "Understanding and quantifying landscape structure – A review on relevant process characteristics, data models and landscape metrics," *Ecol. Modell.*, vol. 295, pp. 31–41, 2015, doi: https://doi.org/10.1016/j.ecolmodel.2014.08.018.

[299] D. Moser, H. G. Zechmeister, C. Plutzar, N. Sauberer, T. Wrbka, and G. Grabherr, "Landscape patch shape complexity as an effective measure for plant species richness in rural landscapes," *Landsc. Ecol.*, vol. 17, no. 7,

pp. 657–669, 2002, doi: 10.1023/A:1021513729205.

[300] M. Herold, N. C. Goldstein, and K. C. Clarke, “The spatiotemporal form of urban growth: measurement, analysis and modeling,” *Remote Sens. Environ.*, vol. 86, no. 3, pp. 286–302, 2003.

[301] M. Herold, H. Couclelis, and K. C. Clarke, “The role of spatial metrics in the analysis and modeling of urban land use change,” *Comput. Environ. Urban Syst.*, vol. 29, no. 4, pp. 369–399, 2005.

[302] E. Uuemaa, M. Antrop, J. Roosaare, R. Marja, and Ü. Mander, “Landscape metrics and indices: an overview of their use in landscape research,” *Living Rev. Landsc. Res.*, vol. 3, no. 1, pp. 1–28, 2009.

[303] F. Orlandi, J. Rojo, A. Picornell, J. Oteros, R. Pérez-Badia, and M. Fornaciari, “Impact of climate change on olive crop production in Italy,” *Atmosphere (Basel).*, vol. 11, no. 6, p. 595, 2020.

[304] F. Aguilera, L. M. Valenzuela, and A. Botequilha-Leitão, “Landscape metrics in the analysis of urban land use patterns: A case study in a Spanish metropolitan area,” *Landsc. Urban Plan.*, vol. 99, no. 3, pp. 226–238, 2011, doi: https://doi.org/10.1016/j.landurbplan.2010.10.004.

[305] H. Alphan, E. Karamanli, M. A. Derse, and C. Uslu, “Analyzing pattern features of urban/rural residential land use change: The case of the southern coast of Turkey,” *Land use policy*, vol. 122, p. 106348, 2022, doi: https://doi.org/10.1016/j.landusepol.2022.106348.

[306] M. Usman and J. E. Nichol, “Changes in agricultural and grazing land, and insights for mitigating farmer-herder conflict in West Africa,” *Landsc. Urban Plan.*, vol. 222, p. 104383, 2022, doi: https://doi.org/10.1016/j.landurbplan.2022.104383.

[307] M. H. K. Hesselbarth, J. Nowosad, J. Signer, and L. J. Graham, “Open-source Tools in R for Landscape Ecology,” pp. 97–111, 2021.

[308] K. McGarigal and B. J. Marks, “FRAGSTATS: spatial pattern analysis program for quantifying landscape structure,” *Gen. Tech. Rep. - US Dep. Agric. For. Serv.*, no. PNW-GTR-351, 1995.

[309] C. E. Shannon and W. Weaver, “The mathematical theory of communication. Urbana, IL: University fo Illinois Press. cited in Magurran, AE, 2004, Measuring biological diversity.” Blackwell Publishing: Oxford, UK, 1949.

[310] QGIS Development Team., “QGIS Geographic Information System. Open Source Geospatial Foundation Project.” 2022, [Online]. Available: http://qgis.osgeo.org.

[311] N. Cuba, “Research note: Sankey diagrams for visualizing land cover dynamics,” *Landsc. Urban Plan.*, vol. 139, pp. 163–167, 2015, doi: https://doi.org/10.1016/j.landurbplan.2015.03.010.

[312] A. Bitner, “Entropy of the Land Parcel Mosaic as a Measure of the Degree of Urbanization,” pp. 1–16, 2021.

[313] K. Pukowiec-Kurda and M. Sobala, “Nowa metoda oceny stopnia antropogienczego przekształcenia krajobrazu na podstawie metryk krajobrazowych,” *Pr. Kom. Kraj. Kult.*, no. 31, pp. 71–84, 2016.

[314] J. Wu, W. Shen, W. Sun, and P. T. Tueller, “Empirical patterns of the effects of changing scale on landscape metrics,” *Landsc. Ecol.*, vol. 17, pp. 761–782, 2002.

[315] J. Wu, “Effects of changing scale on landscape pattern analysis: scaling relations,” *Landsc. Ecol.*, vol. 19, pp. 125–138, 2004.

[316] A. Medeiros, C. Fernandes, J. F. Gonçalves, and P. Farinha-Marques, “A diagnostic framework for assessing land-use change impacts on landscape pattern and character – A case-study from the Douro region, Portugal,” *Landsc. Urban Plan.*, vol. 228, no. October 2021, 2022, doi: 10.1016/j.landurbplan.2022.104580.

[317] K. McGarigal, S. A. Cushman, M. C. Neel, and E. Ene, “FRAGSTATS: spatial pattern analysis program for categorical maps,” *Comput. Softw. Progr. Prod. by authors Univ. Massachusetts, Amherst. Available Follow. web site www. umass. edu/landeco/research/fragstats/fragstats. html*, vol. 6, 2002.

Acknowledgements

Concludendo questo percorso che ho intrapreso inaspettatamente, mi sento in dovere di esprimere la mia gratitudine a coloro che mi hanno sostenuto e accompagnato più da vicino. Desidero iniziare ringraziando il Prof. Andrea Galli che mi ha accolto nel suo mondo non solo come dottorando, ma come un familiare. Senza ombra di dubbi è stata tra le persone più paziente che ho conosciuto in vita, aspettando i miei tempi per comprendere i vari argomenti trattati dal settore scientifico AGR10, di cui io, avendo una formazione da Ingegnere Edile, ero completamente ignaro. Un enorme ringraziamento anche ad Ernesto, Professore e amico, il mio personalissimo madrelingua inglese e consigliere dei progetti svolti insieme. Non posso dimenticare di menzionare il mio primo collega a Agr10, il mio super amico Mattia, con cui ho condiviso le esperienze di ricerca durante il dottorato facendoci conoscere dentro e fuori dal D3A, sia per le doti tecniche che umane. Nonostante le innumerevoli discussioni, ci siamo dati forza vicendevolmente per portare avanti tutti i progetti e i corsi di laurea. Voglio poi ringraziare vivamente la Prof.ssa Eva Savina Malinverni, che mi ha introdotto nel mondo della ricerca con il mio primo assegno di ricerca, insegnandomi le basi della geomatica. Infine, ma non meno importante, voglio ringraziare tutti i miei colleghi del gruppo GAP, in particolare Rob che è stato non solo un collega, ma un amico che mi ha ascoltato e supportato anche nei momenti di incomprensione in questo settore. Un ringraziamento speciale anche a Fra, che è stato il mio primo collega nel mondo della ricerca e poi amico. Inoltre, voglio ringraziare tutti i colleghi che hanno contribuito ad accrescere le mie competenze.

Infine, un immenso grazie ai miei genitori, ai quali dedico il titolo di PhD La loro presenza e pazienza durante questi anni di fatica sono stati un faro e una base sicura quando lo stress e le delusioni prendevano il sopravvento. Un grande ringraziamento va anche a tutte le persone che mi hanno sostenuto e spronato a portare a termine questo percorso di crescita della mia vita, che ha segnato indelebilmente la mia esistenza.

A tutti voi, grazie!